Science and Technology Facilities Council

Central Laser Facility Annual Report

2019–2020

Central Laser Facility
Science & Technology Facilities Council
Rutherford Appleton Laboratory
Harwell Campus
Didcot, Oxfordshire OX11 0QX
T: +44 (0)1235 445647
E: clfannrep@stfc.ac.uk
W: www.clf.stfc.ac.uk

The production team for this Annual Report was as follows:

Editor: Raoul Trines

Production: Tracey Burge, Lizzie Henderson and Raoul Trines

Section Editors: David Carroll, Richard Chapman, Ian Clark, Dave Clarke, Rob Clarke, James Green, Chris Hooker, Ian Musgrave, Rajeev Pattathil, Jonathan Phillips, Alex Robinson, Dan Symes, Martin Tolley, Christopher Tynan, Adam Wyatt

This report is available on the CLF website at www.clf.stfc.ac.uk

Design, layout and production: UKRI Creative Services (JRS)

Thanks to all of the above for their contribution towards producing this report and, of course, to all of the authors for their submissions.

Cover image: A miniature snow globe complete with snow and trees perches upon a single pine needle. Created by Chris Spindloe from Scitech, this miniature creation demonstrates the incredible abilities of our Scitech and Target Fabrication department. Photo taken using an Octopus Imaging Facility Microscope.

Contents

Foreword 4

Overview 6

Industry engagement and innovation 10

Communication and outreach activities within the CLF 13

High energy density and high intensity physics 18

Laser science and development 29

Artemis update 38

Plasma diagnostics 40

Imaging and dynamics for physical and life sciences 43

Appendices 60

- Operational statistics 60
- Publications 68
- Panel membership and CLF structure 77

Foreword

Professor John Collier
Director, Central Laser Facility, STFC Rutherford Appleton Laboratory, Harwell Campus, Didcot, UK
Email address: **john.collier@stfc.ac.uk** Website: **www.clf.stfc.ac.uk**

For over forty years, our team of Central Laser Facility (CLF) scientists, engineers and researchers have been developing laser technologies and techniques that have proven instrumental in opening up new areas of study and research. Based at the STFC Rutherford Appleton Laboratory in Oxfordshire, we operate several of the most advanced laser systems in the world, and have a rich history of innovation and development, empowering an international community of scientists in their efforts to solve major economic and societal challenges. Moreover, we continue to listen to our many collaborator organisations – in academia and in the commercial sector – and are constantly evolving to help meet their needs, as well as the ever growing and changing demands of science.

Our five major laser facilities enable scientists to investigate a broad range of science areas, spanning physics, chemistry and biology, and research topics ranging from the investigation of complex biological reactions within cells to new ideas for future energy production:

- The **Vulcan** facility, one of the most intense lasers in the world, has broken records on several occasions for producing the highest optical intensity ever on a target. It is based on versatile Nd:glass chirped-pulse-amplification technology delivering beams into two target areas, and is used in fusion energy, electron- and ion-acceleration research, laboratory astrophysics and plasma physics research. Work this year on a new short-pulse beamline for the Vulcan TAP area will deliver a PW level pulse (30 J in 30 fs and enable new areas of imaging and combined proton/ electron interactions to take place.

- The **Gemini** facility is a high-power laser based on titanium-sapphire chirped-pulse-amplification technology, with capabilities that balance and complement those of Vulcan. The energy contained in the pulses from the front end are delivered to a very small target extremely quickly, allowing experimenters to study the way matter behaves under extreme conditions of temperature and pressure. Recent experiments have demonstrated that Gemini's laser-driven x-ray sources are suitable for advanced imaging techniques suited to scientific studies and industrial inspection.

- **Artemis** is a high-repetition-rate titanium-sapphire laser system providing a unique combination of ultrafast and XUV pulses for studies of ultrafast dynamics in atomic, molecular, and condensed-matter systems. Artemis has just had a major upgrade, adding a new laser system and a third XUV beamline, making more energy available for XUV generation.

- **Ultra** is a world-class time-resolved (pump-probe) spectroscopy facility that combines laser, detector and sample manipulation technology to probe ultrafast molecular dynamics, facilitating innovative research in the physical and life sciences in academia and industry. Work carried out in Ultra provided fundamental insights into the mechanisms of charge transport, useful in guiding the design of better organic semiconductors and molecular wires and therefore improved devices in emerging applications, such as display devices in mobile phones and photovoltaic solar cells.

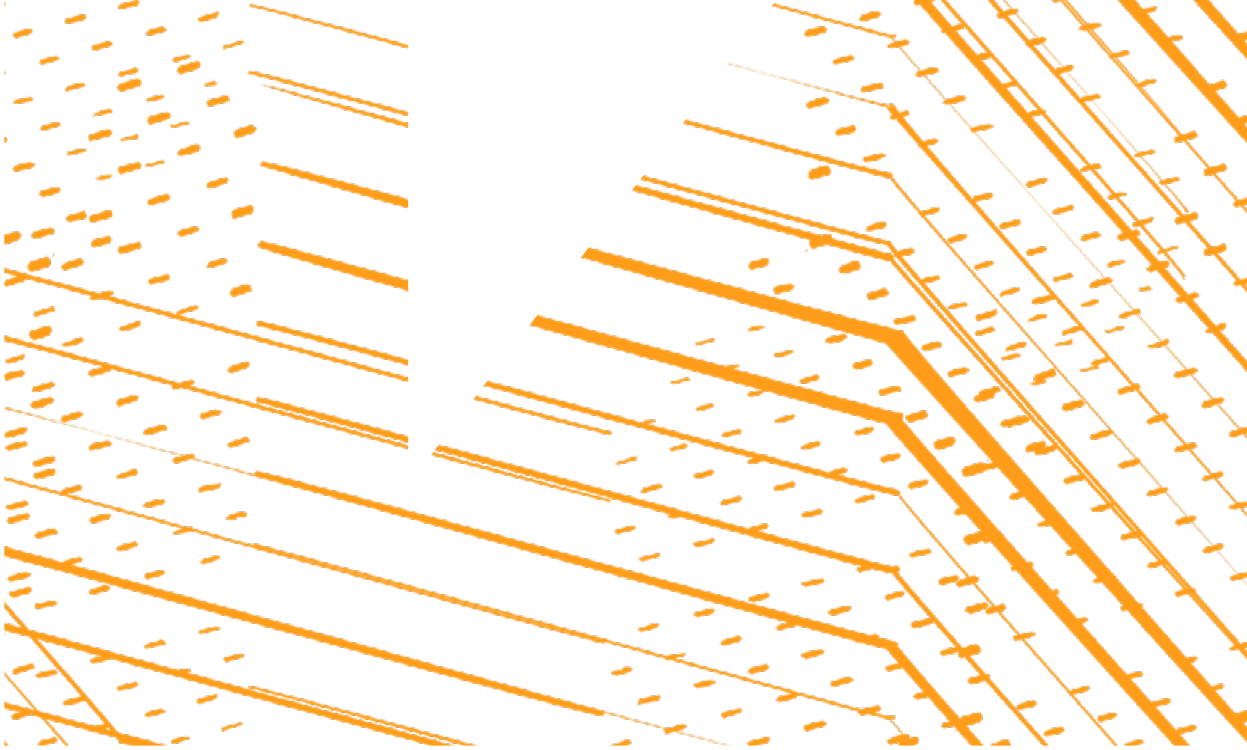

- **Octopus** is a unique user facility with a suite of advanced laser-based imaging and laser trapping capabilities. Advanced image processing algorithms are used to image real systems in real environments in real time, often well below the diffraction limit, with the modular nature of the facility allowing the development and exploitation of new advanced imaging techniques as they become available, to address grand challenges in the life sciences area. When the COVID-19 pandemic hit at the start of this reporting year, the Octopus facility remained open for CLF scientists to carry out collaborative work to increase understanding of the SARS-CoV-2 virus at the centre of the pandemic, and in particular how exactly it attacks cells.

Underpinning our laser facilities are enabling capabilities, from computational plasma physics to target micro-fabrication and engineering, which are helping our users to push the boundaries of science and research.

I remain tremendously proud of the CLF's expert staff, who are at the heart of our success, and who work hard to deliver scientific output and technical development of the highest order. When COVID-19 prevented most staff and users from coming to site, a huge amount of effort was put into enabling people to work from home, and providing remote access to our facilities. Staff were prepared to come to site to manufacture ventilators, demonstrating their willingness to apply their skills and expertise to help others. There is so much we can be proud of.

This annual report for the CLF provides a snapshot of some of the scientific and technical research that has been carried out by users of the CLF and its staff over the financial year 2019-20. I do hope that you enjoy reading this selection of abstracts, and feel inspired by the achievements of all those involved.

Professor John Collier FLSW
Director, Central Laser Facility

Overview of the Central Laser Facility (CLF)

Cristina Hernandez-Gomez
Central Laser Facility, STFC Rutherford Appleton Laboratory, Harwell Campus, Didcot, UK
Email address: **cristina.hernandez-gomez@stfc.ac.uk** Website: **www.clf.stfc.ac.uk**

The CLF is a world leading centre for research using lasers in a wide range of scientific disciplines. This section provides an overview of the capabilities offered to our international academic and industrial community.

VULCAN

Vulcan is a versatile high power laser system that is composed of Nd:glass amplifier chains capable of delivering up to 2.6 kJ of laser energy in long pulses (nanosecond duration) and up to 1 PW peak power in a short pulse (500 fs duration) at 1053 nm.

It currently has eight beam lines. Two of these beam lines can operate in either short pulse mode or long pulse mode, while the remaining six normally operate in a long pulse mode. The short-pulse and long-pulse systems operating jointly can be directed to two different target areas, enabling sophisticated interaction and probing experiments.

We have continued the design of a new short-pulse beamline for the Vulcan TAP area based on the technique of OPCPA which the CLF has pioneered. The upgrade will deliver a PW level pulse (30 J in 30 fs) in addition to the existing PW (500 J, 500 fs) and long pulse (250 J) capabilities. This will enable new areas of imaging and combined proton/ electron interactions to take place. Designs for the main compressor and turning chambers are complete and in the process of procurement. At the same time, the refurbishment of the old Target Area East is nearing completion – transforming the area into a new laser bay for the new beamline front end and main amplifiers.

GEMINI

Gemini is a Titanium-Sapphire based dual-beam high power laser system with two synchronised Petawatt-class beams, enabling pump-probe studies at extreme light intensities (>10^{21} Wcm^{-2}). Many experiments focus on the study and development of laser-driven plasma accelerators with a view to employing these unique sources in a wide range of applications. This year, control of a plasma accelerator using active feedback optimisation strategies was demonstrated in Target Area 2. These methods are critical to producing reliable and flexible secondary source facilities in the future. Progress continued towards using x-rays generated with Gemini for imaging applications. Control of the Target Area 3 pulses for x-ray scanning was automated, allowing several tomographic datasets to be acquired. The betatron x-ray source generated within the laser wakefield accelerator was also used to conduct single-shot x-ray absorption spectroscopy. This important result proves that these laser-driven x-ray sources are suitable for advanced imaging techniques that provide a wealth of information for scientific studies and industrial inspection.

The performance of Gemini was enhanced by the replacement of the pump laser for the kHz front-end. This resulted in a significant improvement in both energy and stability, and has proved reliable over the past year of operations. The transmission grating in the pulse stretcher was also replaced, improving the picosecond timescale contrast by a factor of 10. In Target Area 3 an independent probe beam has been installed, greatly simplifying experimental layouts inside the target vacuum chamber. The beam has a compressor separate to the main beams allowing variations in the pump beam properties while maintaining a short pulse probe. Manual and motorised delay stages enable time resolved optical imaging of the plasma.

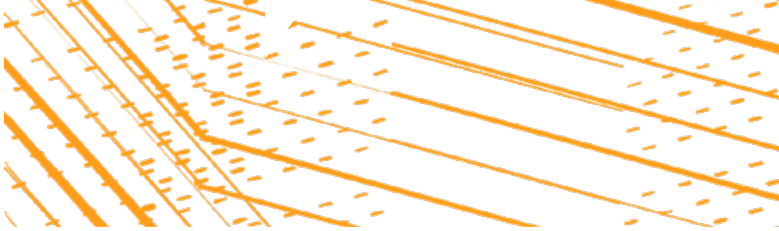

ARTEMIS

Artemis is the CLF's facility for ultrafast laser and XUV science. It offers ultrashort pulses at high repetition-rate, spanning the spectral range from the XUV to the far-infrared. The facility is configured flexibly for pump-probe experiments. Tuneable or few-cycle pulses can be used as pump and probe pulses, or to generate ultrafast, coherent XUV pulses through high harmonic generation. XUV beamlines lead to end-stations for time-resolved photoelectron spectroscopy (for both gas-phase and condensed matter experiments) and coherent lensless XUV imaging.

Artemis has just had a major upgrade, and has re-located across campus to newly refurbished labs in the Research Complex at Harwell (RCaH), adding a new laser system and a third XUV beamline. The new laser system produces 1700 nm and 3000 nm pulses at 100 kHz repetition rate, and is a joint purchase with Ultra. It will complement the existing 1 kHz Ti:Sapphire system, which has been updated with a new amplifier to increase the energy available for XUV generation. Over 2019-20, the laboratory infrastructure has been completed and all equipment installed in the new labs.

TARGET FABRICATION

The Target Fabrication Group makes the majority of the solid targets shot on the CLF's high-power lasers and also supports micro-assembly and characterisation in the wider CLF. The Group is also responsible for the production of targets for academic access shots on the Orion Facility at AWE. Commercial access to target fabrication capabilities is available to external laboratories and experimentalists via the spin-out company Scitech Precision Ltd.

A wide variety of microtarget types are produced to enable the exploration of many experimental regimes. Fabrication techniques include thin film coating, precision micro assembly, laser micromachining, and chemistry processes, all verified by sophisticated characterisation. STFC's advanced capabilities in both high precision micro machining and MEMS microfabrication are also utilised. The Group is ISO9001 accredited, providing a high level of traceability for all supplied microtargets.

In collaboration with Scitech Precision, a high stability, high rep-rate (HRR) tape drive has been tested, to deliver targets to the Gemini laser and other HRR facilities at up to 10Hz. Through the EPIC project there has been a rapidly developing collaboration with several institutions across India to produce complex tapes which will enable new applications and experiments. Work has continued to implement robotic assembly for simple target geometries facilitating the production of array targets for HRR experiments.

The Group remains at the leading edge of target fabrication technology, collaborating with universities in areas such as nanowire growth, thin diamond production, and advanced micro machining. Work with the LSF on the assembly of advanced micro optics has enabled a number of high profile publications.

THEORY AND MODELLING

The Plasma Physics Group supports scheduled experiments throughout the design, analysis and interpretation phases, as well as users who need theoretical support in matters relating to CLF science. We support principal investigators using radiation hydrodynamics, particle-in-cell, hybrid and Vlasov-Fokker-Planck codes, as well as by providing access to large-scale computing. Access to the PRISM suite has been renewed, as endorsed by the CLF User Forum. This is part of a rolling 3 year agreement with PRISM CS, which comes up for renewal after 2021. Support for student training in plasma physics, computational methods and opportunities for networking with colleagues will continue to be provided. Extended collaborative placements within the group are particularly encouraged.

In 2019, SCARF-Magnete has become operational.

ULTRA AND OCTOPUS

(Research Complex at Harwell)

The CLF operates two facilities in the RCaH: Ultra, for ultrafast molecular dynamics measurements in chemistry and biology, and Octopus, a cluster of advanced laser microscopes for life science research.

ULTRA

In the molecular and materials dynamics area Ultra offers a state-of-the-art high power high repetition rate fs / ps systems to generate pulses for a range of highly sensitive pump and probe vibrational spectroscopy techniques. These capture 'movies' of the atomic and molecular dynamics used to study processes ranging from reactions in nature, energy capture and storage, catalysis and fundamental quantum level research on molecular and bio-molecular electronics, probes, therapeutics, enzymes and DNA. Kerr gated time resolved resonance Raman (TR^3) is unique in enabling highly fluorescent samples to be studied. Time-Resolved Multiple-Probe Spectroscopy (TR^MPS) captures reactions from their earliest beginning on femtosecond timescales to completion on milliseconds timescales. Fast scanning ultrafast 2DIR spectroscopies capture intra- and inter-molecular vibrational coupling and energy transport applied in fundamental molecular dynamics research and in pharmaceutical analytical research. Broad spectral band surface sum frequency generation provides insights into the chemical changes that occur at interfaces and surfaces where many reactions in nature and industry occur.

OCTOPUS

In the imaging area, the Octopus cluster offers a range of microscopy stations linked to a central core of pulsed and CW lasers offering “tailor-made” illumination for imaging. Microscopy techniques offered include total internal reflection (TIRF) and multi-wavelength single-molecule imaging, confocal microscopy (including multiphoton), fluorescence energy transfer (FRET) and fluorescence lifetime imaging (FLIM). Super-resolution techniques available are Stochastic Optical Reconstruction Microscopy (STORM) with adaptive optics, Photoactivated Localization Microscopy (PALM), Structured Illumination Microscopy (SIM) and Stimulated Emission Depletion Microscopy (STED), Light Sheet Microscopy, and super-resolution cryo-microscopy. Laser tweezers are available for combined manipulation/trapping and imaging with other Octopus stations, and can also be used to study Raman spectra and pico-Newton forces between particles in solution for bioscience and environmental research. A cryo focused ion beam scanning electron microscope (FIB-SEM) is also available for volume imaging. This will form part of a correlative light and electron microscopy (CLEM) workflow currently under development.

Chemistry, biology, and spectroscopy laboratories support the laser facilities, and the CLF offers access to a multidisciplinary team providing advice to users on all aspects of imaging and spectroscopy, including specialised biological sample preparation, data acquisition, and advanced data analysis techniques. Access is also available to shared facilities in the Research Complex, including cell culture, scanning and transmission electron microscopy, NMR, and x-ray diffraction.

ENGINEERING SERVICES

Engineering is fundamental to all the operations and developments in the CLF. The engineering team operates across all of the CLF’s facilities, and endeavours to continually improve and expand the capabilities and reliability of the CLF. Mechanical, electrical and software support is provided for the operation of the laser facilities, for the experimental programmes on these facilities, and for the CLF’s research and development activities.

These developments can range from small-scale modifications to existing equipment to improve its performance, through to larger scale projects, such as the design and development of commercial projects. In addition, we have active engineering collaborations with regional and international partners such as, HiLASE (Prague, Czech Republic), XFEL (Hamburg, Germany) and TIFR (Hyderabad, India).

Over the last year the Mechanical Engineering Section has seen significant growth. The mechanical workshop is now fully staffed, and new machinery is in place to expand its capabilities. The workshop and storage area for the Experimental Support Technicians has also been regenerated to provide a purpose-built assembly area.

CENTRE FOR ADVANCED LASER TECHNOLOGY AND APPLICATIONS (CALTA)

The mission of CLF's Centre for Advanced Laser Technology and Applications (CALTA) is to develop a new class of efficient, high power laser capable of operating for extended periods at 10Hz. Such a laser is essential in order to transform single shot, proof of principle demonstrations of effects into real world applications.

The technology pursued within CALTA is based on the DiPOLE architecture, first demonstrated at the CLF some years before the establishment of CALTA. Initially, DiPOLE was developed as a potential driver of inertial fusion energy schemes. This has now broadened to include advanced imaging, materials processing, non-destructive testing, medical diagnostics, security and defence, and fundamental science.

The DiPOLE architecture is based on laser diode pumped Ytterbium-YAG in the form of a transparent ceramic slabs, cooled by a high speed flow of cryogenic Helium. DiPOLE has demonstrated stable, 1 kW operation for extended periods (>12 hours) in 100 J, 10 ns pulses delivered at 10 Hz. With an overall optical efficiency of >20%.

In the period covered by this report, DiPOLE systems have demonstrated >70% energy conversion to the second harmonic, making it well suited to pumping of a Titanium Sapphire amplification stage for the generation of ultra-short pulses. Recent results also include preliminary operation at 150 J per pulse at 1 Hz for a period of 30 minutes; no damage was observed.

The first 1 kW DiPOLE system, developed under a commercial contract for the HiLASE facility in the Czech Republic, has been in operation since December 2016. To date it has delivered ~50 Million pulses to a number of applications laboratories including laser induced damage threshold (LIDT) measurements and aerospace component surface treatment studies.

DiPOLE technology will be used at the heart of the new EPAC facility to pump a PW/10 Hz Titanium Sapphire amplifier for the generation of secondary radiation. This will be used by a diverse user community for industrial, scientific and defence applications.

Economic impact

This year's industrial contract-access projects amount to 22 facility access weeks delivering experimental access to Gemini, Ultra and Octopus, and access to CLF scientific expertise.

Internationally, the CLF's commissioning of the D-100X laser for the European X-FEL exceeded expectations; extending the world-leading reputation of the DiPOLE systems. Extreme Photonics Innovation Centre (EPIC) in India was inaugurated as a jointly funded hub for innovation and CLF IPI industrial scientists collaborated with HiLASE on an international aerospace and laser shock peening workshop.

Ongoing and new innovation proof-of-concept projects include exploitation of microwave plasma produced VUV, successful automation of proprietary FLImP single molecule imaging and award-winning publications on Shifted Excitation Raman Difference Spectroscopy (SERDS). The CLF filed two new patent families this year, giving a current total of 21 active patent families.

Access to facilities

Calls for access are made twice annually, with applications peer reviewed by external Facility Access Panels.

The CLF operates 'free at the point of access', available to any UK academic or industrial group engaged in open scientific research, subject to external peer review. European collaboration is fully open for the high power lasers, whilst European and International collaborations are also encouraged across the CLF suite for significant fractions of the time. Dedicated access to CLF facilities is awarded to European researchers via the LaserLab-Europe initiative (**www.laserlab-europe.net**) funded by the European Commission.

Hiring of the facilities and access to CLF expertise is also available on a commercial basis for proprietary or urgent industrial research and development.

Please visit **www.clf.stfc.ac.uk** for more details on all aspects of the CLF.

Industry engagement and innovation

Kathryn Welsby
Central Laser Facility, STFC Rutherford Appleton Laboratory, Harwell Campus, Didcot, UK
Email address: **kathryn.welsby@stfc.ac.uk** Website: **www.clf.stfc.ac.uk**

This article highlights the industrial user engagement, industry partnerships, and innovation activities of the Central Laser Facility for the reporting period April 2019 to March 2020.

Industrial users and engagement

This year saw the ground-breaking ceremony for the CLF's Extreme Photonics Application Centre (EPAC), a new national facility to support UK science, technology, innovation and industry. EPAC was successfully funded due to its strong partnership between UKRI, industry, MoD, and academia. EPAC will generate scientific breakthroughs and stimulate new solutions to challenging problems, to help advance UK science and technology, with emphasis on industrial applications helping to keep us safer, improve our healthcare and support a cleaner, more productive economy.

The CLF delivered 10 commercial contracts, amounting to 22 facility access weeks with industrial users this year, delivering experimental access to Gemini, Ultra and Octopus, and access to CLF scientific expertise. Work ranged from pharmaceutical applications of advanced spectroscopy, novel use of fluorescence lifetime microscopy in catalytic science, to providing data on technology readiness of laser driven MeV X-rays. Through utilisation of CLF's expertise in combination with its world-class facilities, the CLF continues to drive impact across a wide variety of industrial sectors and contribute advanced characterisation in industrial R&D.

The CLF is an active partner in the STFC Bridging For Innovators (B4I) programme – an ISCF funded scheme that has been introduced to boost industrial collaboration with national facilities. This year's B4I projects include optimisation of laser technology in commercial spectrometers, investigating the effect of oil pick-up on crisp structures, analysing novel sources of myosin production from invasive limpet species for biomedical applications, and characterising new catalysts for reduced CO_2 emissions.

A team of catalytic experts from SME Finden used their B4I funding for industry-led access to CLF's ultrafast Kerr-gate Raman spectroscopy technique. The B4I experiment studied new catalytic pathways in the production of dimethyl ether (DME) from methanol. Producing DME using methanol has the potential to reduce CO_2 emissions by 95% when compared to conventional fuels.

Collaborating with CLF scientists, PepsiCo Research Fellows and academic partners from Chalmers University of Technology in Sweden and Liverpool University utilised their matched B4I funding to access a number of advanced fluorescence imaging techniques, to determine their suitability for food manufacturing research. This year, further growth across agriculture and food manufacturing industrial sectors has taken place, opening a new collaborative community applying the facility's advanced microscopy and spectroscopy techniques. The CLF has actively supported STFC Food Network+ and the Food Standard Agency (FSA) in supporting SME scoping projects, assisting the STFC community in making a meaningful contribution to the UK food system.

Industry partnerships

The CLF's long-standing partnership with Johnson Matthey (JM) continues, with CLF-JM research fellow Dr Kathryn Welsby leading the research programme for STFC-JM fellows. The team of fellows have been working to encourage multi-facility collaborations

to solve industrial challenges and add insight into fundamental R&D for JM business units. JM is striving to lead on clean energy solutions and sustainability of resources, and JM's scientific interests at Harwell this year have included advanced characterisation of next generation battery technology, fuel cell characterisation, catalysis and clean air applications.

UKRI-EPSRC Innovation Fellow Dr Chris Thornton, in partnership with JM, Manufacturing Technology Centre and Warwick Manufacturing Group, has delivered a second imaging experiment focussing on soft X-ray generation. The experiment allowed for the successful collection of X-ray images that can be used for tomographic reconstruction of samples supplied by WMG and JM, contributing to an MTC report for a potential laser-plasma accelerator to be used for industrial imaging. The work highlighted the potential of the technology, and reaffirmed the importance of the work that the CLF does as a knowledge transfer body for technology innovation.

CLF scientist Dr Paul Donaldson has been awarded a UKRI Future Leaders Fellowship on molecular stopwatch measurements of dynamics in catalysts, battery electrolytes and ionic liquids in situ. The Fellowship has close links to industry, including JM and the UK Catalysis Hub, and will work towards future industrial applications of the advanced techniques being developed, looking to improve the science of catalysts and batteries, in the hopes of creating a greener future in transport.

International impact

The Tata Institute of Fundamental Research (TIFR) and the CLF have developed a strong collaboration on the science of laser-driven accelerators. This year saw the inauguration of the new jointly-funded hub for innovation, called the Extreme Photonics Innovation Centre (EPIC), that will drive innovation through development of cutting-edge technology.

CLF scientists from the newly established CLF Industrial Partnership and Innovation (IPI) group were collaborators on the HiLASE international workshop entitled *Trends and challenges in laser processing – aerospace*. This event in Prague brought together senior industry experts across the aerospace sector and scientific expertise in micro-machining, laser shock peening and 3D printing, to discuss technology readiness and advancements required for industrial deployment in aerospace manufacturing and inspection.

In collaboration with CLF scientist Dr Kathryn Welsby, industrial access at the CLF, for the first time, housed visiting scientists from the University of South Australia. The facility access utilised UoSA's Dr Craig Priest's research teams' expertise in working with industrial partners on minerals, water quality, health, and advanced manufacturing applications of microfluidic devices.

The D-100X laser for the European X-FEL was test commissioned during the autumn of 2019, meeting, and exceeding, its specification. The demonstrated performance underpins and extends the reputation of DiPOLE as the world leading technology for high efficiency, high repetition rate and high power lasers. D-100X was shipped to Hamburg in January 2020, and a joint HZDR/CLF team began the task of unpacking, reassembling and recommissioning.

Innovation

CLF's IPI group continues to scan for innovative concepts and technology transfer opportunities, to capture and drive forward the most impactful ideas and inventions.

This year, the CLF filed two new patent families, giving a current total of 21 active patent families, and eight invention disclosure forms were submitted for consideration for future patent filing. Additionally, three proof-of-concept projects were funded or ongoing, and two CLASP projects have been advanced. An ongoing CLASP-funded project to produce and exploit VUV from microwave plasma has successfully developed a device capable of both controlled ignition and subsequent stabilisation of a microwave plasma discharge at atmospheric pressure.

In conjunction with industrial (AstraZeneca, Oxford Nanoimaging (ONI)) and clinical (King's College London) collaborators, Professor Marisa Martin-Fernandez and her team at the CLF have successfully automated the STFC proprietary single molecule imaging method (Fluorescence localisation imaging with Photobleaching, FLImP), including using AI approaches to automatically recognise cells of interest and to extract the most useful information to characterise biological structures at the nanometre scale. Working with IRIS, SCD and STFC Innovations, a prototype, fully-automated, cloud-based FLImP data analysis pipeline has also been developed, to allow the rapid distribution of this exciting technique to academic and industrial partners.

CLF's POCF project on Shifted Excitation Raman Difference Spectroscopy (SERDS) with Charge-Shifting Charge-Coupled Device (CCD) was awarded the 2020 William F. Meggers Award from the Society for Applied Spectroscopy (SAS), for their outstanding paper published in the journal Applied Spectroscopy. This recognition goes to the CLF and Ferdinand-Braun-Institut team, Kay Sowoidnich, Michael Towrie, Martin Maiwald, Bernd Sumpf and Pavel Matousek. Their technique enables superior performance for application with handheld scanning devices in outdoor or variable lighting conditions. This new innovation can potentially be used for discriminating healthy cells from cancerous cells in non-invasive tissue scanning, and can deliver sub-surface inspection.

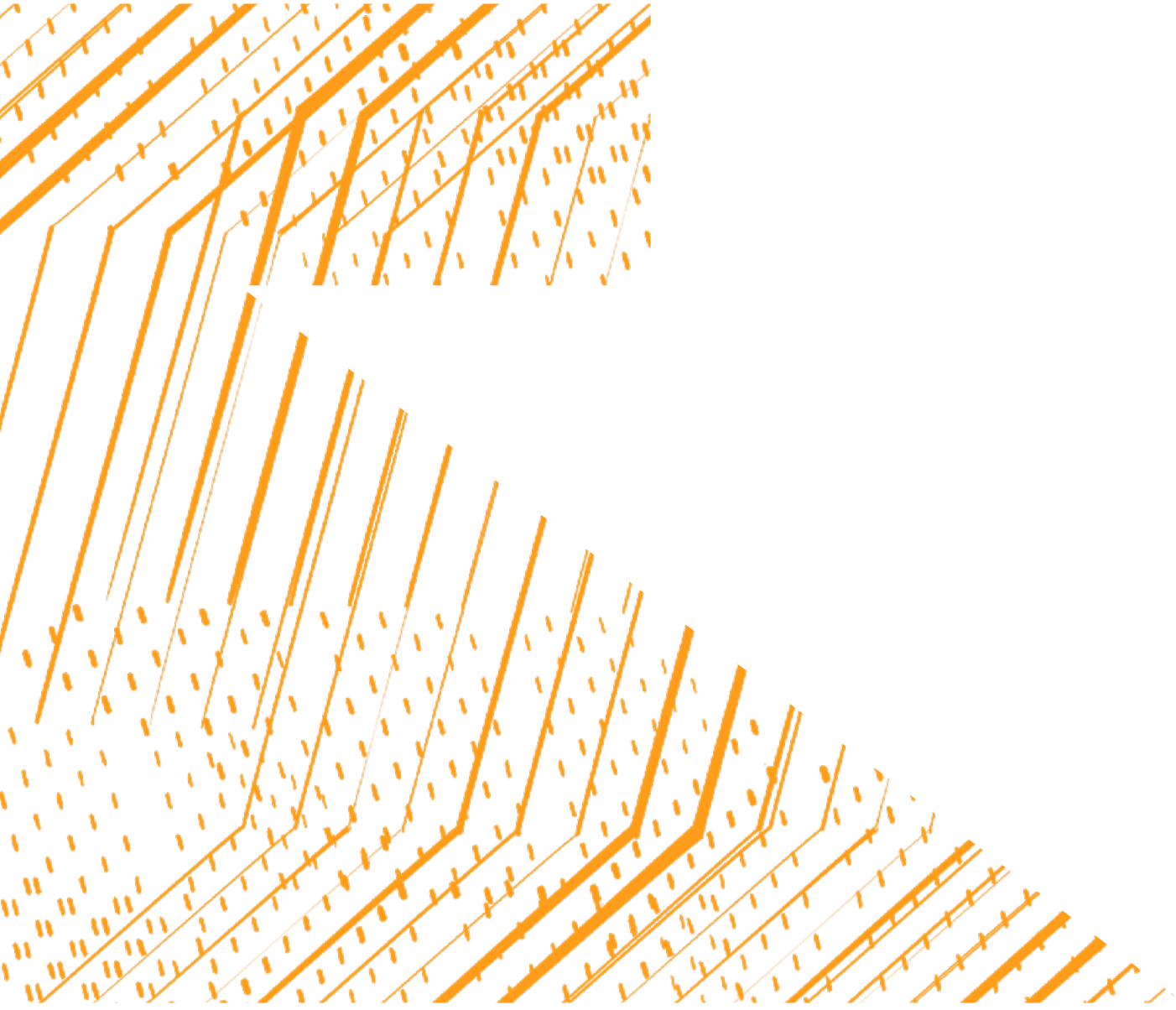

Communication and outreach activities within the CLF

Helen Towrie, Emma Springate
Central Laser Facility, STFC Rutherford Appleton Laboratory, Harwell Campus, Didcot, UK
Email address: **helen.towrie@stfc.ac.uk, emma.springate@stfc.ac.uk** Website: **www.clf.stfc.ac.uk**

CLF's Communication Strategies

The CLF recognises the importance of communication with our current and potential users, STFC, UKRI and other funders, new industry partners, the wider scientific community, and the general public. Outreach activities raise the profile of our world-class research and may inspire the next generation, while communication activities help to publicise the high-impact and inspiring science that the CLF delivers.

Over the past year, the CLF has embarked on several exciting projects to help achieve its strategy of finding new and innovative ways to communicate what we do. This has involved working directly with STFC communications team members, hosting and involving ourselves in events that increase our visibility, and exploring new media as a vessel for communication.

Most notably in 2019/2020, we have helped with public engagement and communication surrounding our new science lab, the Extreme Photonics Applications Centre (EPAC), the details of which are outlined in the EPAC section of this article.

Exploiting social media

Social media continues to play a key role in how we share our stories directly with users and the public. The CLF Twitter, which was created in 2018, now has 587 followers (187 more than last year) and we regularly use it to interact with Principal Investigators, users and staff.

We continue to keep in close contact with the STFC Twitter and Instagram team, where we can reach a more general public audience as opposed to the more scientific audience that the CLF Twitter aims to attract. More recently, we have started looking into LinkedIn, which could allow us to reach an audience of professionals who may be looking to work at a place like the CLF. To aid these discussions and others, a CLF representative attends a monthly Social Media meeting where all the departments communicate new ideas, campaigns and best practices.

Over the past 12 months, the CLF website has attracted over 32,000 users, with almost 100,000 unique page views. Excluding approximately 3,000 users based at Harwell, this corresponds to 80 external users per day. This is 9,000 more users than last year and 24 more users a day. Out of the 32,000 users, 935 came from Twitter, 257 from Facebook, 9 from YouTube, 83 from LinkedIn and 5 from Instagram.

In the previous year, we had just under 23,000 users, with almost 102,000 unique page views. Excluding approximately 2,500 users based at Harwell, this corresponded to 56 external users per day. Out of the 23,000 users, 693 came from Twitter, 214 from Facebook, 53 from YouTube and 20 from LinkedIn.

Established YouTuber Primrose Kitten on her visit to the CLF.

We are pleased to see that our daily users are up, and that our efforts on Twitter are gaining tangible traction. Our speculation as to why there were so many total users in 2019/2020, but slightly fewer unique page views than in 2018/2019, is that perhaps more people may have come to the website to look only at the new, single pages related to EPAC and the UK XFEL. This supposition is backed up by the fact that there were 2,216 unique views of the UK XFEL Science Case page, and 1,504 of the EPAC introduction page – a high number of views for single pages on the CLF website.

Attracting a wider audience

We have continued to explore the idea of working with established YouTubers to get our science out to new audiences. In January 2020, we invited Primrose Kitten (Jen) to visit the CLF. Jen is a YouTuber with 144k subscribers who are mostly GSCE-student age. This is the age at which children are deciding on what they would like their future career to be, and is often the pivotal moment for young girls to decide for or against science as their future career. As we know, the decision is unfortunately more often against.

During Jen's visit in January, she interviewed and had lab tours from three female scientists and technicians who shared their interesting and relatable journeys. The videos she created were designed to show girls that labs are not intimidating places, and that you can carve out a life very happily at a place like the CLF. The videos, although gaining a lower view count than most of her other videos (which is unsurprising due to the fact that most other videos are about GCSE revision, a priority for most viewers), generated upliftingly positive comments: "*Wow. That is some professional work you guys are doing*", "*She's clearly extremely intelligent and very passionate. Great interview!!*", "*Omg she came for a lecture in our school.*"

Primrose Kitten (left) visit with Simon Clark and Ceri Brenner.

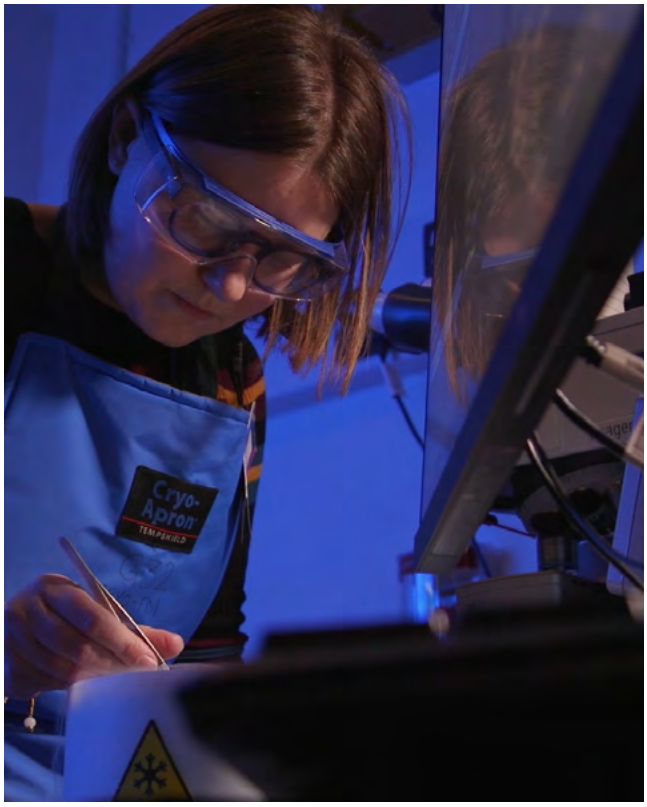

Octopus still from the professional videographer footage.

Additionally, our work with videographer Raquel Taylor continued; a highlight being a big update to our B roll footage. This was conducted by an external professional videographer and organised by Raquel, and we are very thankful to the staff who put up with the disruption caused by this video shoot. After visiting in March 2019, we have now received the footage and stills, which have been used throughout the year for social media, the CLF website, various presentations, and by RAL and STFC. We expect to continue to be able to use this fantastic footage for years to come for the benefit of the labs.

Finally, in March 2019, one of our target fabricators, Donna Wyatt, went on BBC Radio Oxford to talk about her job. We were very excited by this opportunity, because it not only showed off the incredible work Donna can and does do, but also her relatable background story showed young people that a science degree and PhD is not the only way to get into science. BBC Radio Oxford had 84,000 listeners per week from July 2019 to December 2019, many of whom would be people the CLF could never normally reach.

Ultra still from the professional videographer footage.

DiPOLE still from the professional videographer footage.

Organising user events

A highlight of 2019 was the Event for UNESCO's International Day of Light. Organised by Prof Bob Bingham, talks were given by CLF director Prof John Collier, CLF Impact and Engagement Officer Helen Towrie and closing with Prof Sir Jim Hough (University of Glasgow), whose research focusses on gravitational wave detection. Opening remarks were by a representative of UNESCO. The event not only aimed to show the science surrounding light, but also light from an artistic perspective, and how the two may seem like opposite ends of a scale but are actually closely intertwined.

This year, the annual Target Area Operator (TAO) training weeks ran for their 20th year! Organised by Dr David Carroll, the latest session took place in the summer of 2019. To celebrate the 20th Anniversary, the Communications Team shared the news on the CLF Twitter.

TAO training weeks celebrated their 20th year in 2019.

Given that many laser and plasma scientists from the UK and around the world will be users of our facility during their careers, we conduct training weeks on various techniques and safety aspects to ensure experiments will be as successful as possible. Although these courses are tailored to meet the needs of the CLF's High Power Laser (HPL) facilities, they help to develop skills and knowledge that are applicable to experiments at other laser facilities, and also provide an opportunity for the attending scientists to network with each other.

In December 2019, the CLF once again ran the annual HPL Christmas Conference. This was a brilliant opportunity for the high power laser community to come together to share new ideas, and to hear talks from scientists both senior and at the beginning of their careers. One of the highlights of the three-day conference is always the PhD and University student poster competition. This event gives young scientists with budding careers a chance to share their ideas, be involved in new discussions, and make valuable connections.

This year, CLF Director Prof John Collier opened the conference with exciting announcements about EPAC, EPIC and a celebration of two decades of cooperation with 33 European laser infrastructures from 16 countries.

International Day of Light 2019.

Maintaining all avenues of communication

While we are always looking for new ways to engage the public, we also work to maintain our usual avenues of communication. This includes tours, newsletters, events, and articles.

Over the past 12 months, 25 articles have been shared on the CLF news section of the website, averaging around two per month. These articles have covered a wide range of topics, from recent papers, to events, to staff achievements.

We also continue to give tours in collaboration with the efforts of the RAL Public Engagement Team. Here are some headline stats from 2019/2020 for the CLF:

- 11 events held, plus work experience students placed in the CLF, and tours for work experience students
- Total people engaged via public engagement programme: 1247, of which:
  - 1063 public (family audiences, so estimate ~30% were age 8-14, a key target)
  - 175 secondary school (teachers and students) at school events and as work experience students
  - 9 teachers at teacher-training events
- 17 CLF staff volunteered at least once

The biggest events this year were Stargazing and Black Panther. The CLF once again hosted the RAL Stargazing event in its Visitor Centre, as it is a great indoor space for families with inquisitive children.

Feedback collected by the RAL Public Engagement Team showed that 42% of the audience at Stargazing was 'new-to-RAL'.

The Black Panther event was attended by CLF Impact and Engagement Officer Helen Towrie and Communications student Vynn Chander, where they showed off RAL's interactive displays and demos. The event was held in a part of the county that is considered an area of higher deprivation.

Finally, just as this financial year drew to a close, we made a major change to our e-newsletter in response to the lockdown brought on by the COVID-19 pandemic and lockdown. Instead of a bi-monthly CLF in.brief, we shared a weekly newsletter that has been short, punchy and filled with personal touches to help staff feel connected to each other and the facility. New features have included a Director's Message – a message from John Collier about current happenings – and a 'Sweet of the Week' – a play on our 'Tweet of the Week'– in which we have featured a cute staff baby or pet with a short caption. We hope this newsletter has added a light-hearted and perhaps comical touch to the weekly updates during the 'new normal'.

EPAC

This year, there has been a particular effort to create content ready for the announcement and Ground Breaking Ceremony of the Extreme Photonics Applications Centre (EPAC). For the CLF Communications Team, this project required both careful foreplaning and spontaneity when needed.

Recruitment: Recruitment efforts for EPAC have involved creating a bespoke leaflet to engage new recruits, designing a collection of images, gifs and videos for social media and the website, supporting HR with EPAC recruitment drives, and constructing a set of webpages with sections designed to appeal to a general audience, as well as more knowledgeable science and industry readers.

General Support: One of the first jobs our team needed to do was to create 'elevator pitches' for EPAC – these are short, punchy captions to summarise EPAC.

Since their creation, these have been used countless times to describe EPAC in presentations, on social media and on the website. We also produced multiple EPAC posters aimed at different audiences. We provided a poster for the local community evening, an event in Parliament, and for an STFC staff drop-in session co-ordinated with the construction company, Mace.

The most important moment for EPAC (and arguably the highlight of the year) was the Ground Breaking Ceremony in February. Nobel Prize winner Prof Donna Strickland and the Science Minister at the time Chris Skidmore were our guests for the day. The CLF Communications Team was present throughout and ready to help if needed, and in the meantime we took photos and live tweeted. Post event, we shared a summary of the EPAC Ground Breaking Ceremony on the CLF website.

This event was extremely exciting for the CLF for many reasons. Not only were we able to formally announce the Extreme Photonics Applications Centre, but we were able to do it with two important and influential people. During her visit, Prof Donna Strickland also attended a RAL WiSTEM meeting, which meant a lot as she is such an influential woman in STEM. She then finished off the day with a fantastic talk on the invention that advanced lasers worldwide and won her a Nobel Prize alongside Prof Gérard Mourou.

CLF Comms COVID-19 Response

As we all know, the end of this financial year marked the beginning of the worldwide lockdowns due to the novel virus COVID-19. In the early days, the CLF Communications Team worked with senior staff to make sure that key information was shared with the staff and users who needed it. This included a rapid call to access from Octopus, inviting users to utilise the imaging facility in the fight against COVID, and updating the website to reflect site shut-downs and new policies. As the pandemic continues, we plan to prioritise getting information of this nature out to our audiences quickly and efficiently. All the Communications Team have been able to work from home efficiently. With the suspension of tours and face-to-face events, we have focussed our efforts on connecting with the public digitally, and continue to keep up a dialogue with RAL Public Engagement as they assess what types of digital interactions would be effective in lieu of tours.

As mentioned earlier in this article, we have started a weekly CLF in.brief, replacing our old bi-monthly in.brief. This e-newsletter intends to keep staff up to date with happenings and inject a light-hearted feel to the end of the week.

Extreme Photonics Applications Centre: Ground Breaking Ceremony.

High energy density and high intensity physics

Computer tomography with laser-generated X-rays at Gemini

S.J.D. Dann, C. Thornton, C.D. Armstrong, C.D. Baird, C.M. Brenner, D.R. Symes *(Central Laser Facility, STFC Rutherford Appleton Laboratory, Harwell Campus, Didcot, UK)*
M.J.V. Streeter, J-N. Gruse, J.C. Wood, N.C. Lopes, S.P.D. Mangles, Z. Najmudin *(John Adams Institute for Accelerator Science, Imperial College London, UK)*
C.D. Murphy, C.I.D. Underwood *(York Plasma Institute, Department of Physics, University of York, UK)*
L.R. Pickard *(National Composites Centre, Bristol and Bath Science Park, Feynman Way Central, Bristol, UK)*
K.D. Potter *(Advanced Composites Collaboration for Science and Innovation (ACCIS), University of Bristol, UK)*

We describe recent CT imaging work at Gemini. We focus on aspects of the scanning and reconstruction processes that are needed to deal with the poor repeatability of current laser-driven x-ray sources. In particular, we describe golden ratio scanning, a useful technique employed with sources of degrading quality, and a custom beam profile correction step, applied to correct for the pulse-to-pulse changes in the x-ray beam profile and direction. The beam profile is inferred by fitting a polynomial function based on the border regions of the image. A regularisation method ensures that this fit accurately represents the beam, as shown in the figure. After image processing has been performed, standard CT reconstruction techniques can be applied to the data-set to produce a 3D visualisation of the object. Integrating these processing steps into a standardised software package used by other imaging facilities is a key objective for developing CT capability for the EPAC facility.

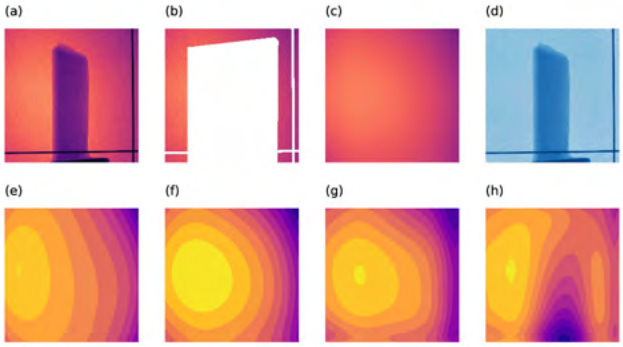

An example of the beam profile correction process applied to x-ray images obtained using Gemini: (a) the original image; (b) the image after removing the sample and alignment wires; (c) the reconstructed x-ray beam profile; (d) the transmission map, obtained by dividing (a) by (c). The second row shows how the regularisation parameter ∝ affects the fitting process: (e) ∝ =10^{-3} is too large failing to fit to the beam profile correctly; (f) ∝=10^{-4} provides a good fit and is used for (c-d); (g) ∝=10^{-5} and (h) ∝=10^{-6} overfit the data.

Contact: S.J.D. Dann (stephen.dann@stfc.ac.uk)

Laser wakefield acceleration with active feedback at 5Hz

S.J.D. Dann *(Physics Department, Lancaster University, UK; Central Laser Facility, STFC Rutherford Appleton Laboratory, Harwell Campus, Didcot, UK)*
C.D. Baird, C.D. Murphy *(York Plasma Institute, University of York, UK)*
N. Bourgeois, O. Chekhlov, C.D. Gregory, S.J. Hawkes, C.J. Hooker, V.A. Marshall, B. Parry, P.P. Rajeev, E. Springate, Y. Tang, C. Thornton, D.R. Symes *(Central Laser Facility, STFC Rutherford Appleton Laboratory, Harwell Campus, Didcot, UK)*
S. Eardley, R.A. Smith *(Blackett Laboratory, Imperial College London, UK)*
J.-N. Gruse, S.P.D. Mangles, Z. Najmudin, S. Rozario *(The John Adams Institute for Accelerator Science, Imperial College London, UK)*
J. Hah, K. Krushelnick, J. A. Nees *(Center for Ultrafast Optical Science, University of Michigan, USA)*
D. Hazra *(Laser Plasma Section, Raja Ramanna Centre for Advanced technology, Indore, India)*
J. Osterhoff, P. Pourmoussavi *(Deutsches Elektronen-Synchrotron DESY, Hamburg, Germany)*
S.V. Rahul *(TIFR Centre for Interdisciplinary Sciences, Hyperabad, India)*
J.D.E. Scott *(Physics Department, Lancaster University, UK)*
S. Tata *(Tata Institute of Fundamental research, Colaba, India)*
A.G.R. Thomas *(Physics Department, Lancaster University, UK; Center for Ultrafast Optical Science, University of Michigan, USA)*
M.J.V. Streeter *(Physics Department, Lancaster University, UK; The John Adams Institute for Accelerator Science, Imperial College London, UK)*

We describe the use of a genetic algorithm to apply active feedback to a laser wakefield accelerator at a higher power (10 TW) and a lower repetition rate (5 Hz) than previous work. The temporal shape of the drive laser pulse was adjusted automatically to optimize the properties of the electron beam. By changing the software configuration, different properties could be improved. This included the total accelerated charge per bunch, which was doubled, and the average electron energy, which was increased from 22 to 27 MeV. Using experimental measurements directly to provide feedback allows the system to work even when the underlying acceleration mechanisms are not fully understood, and, in fact, studying the optimized pulse shape might reveal new insights into the physical processes responsible. Our work suggests that this technique, which has already been applied with low-power lasers, can be extended to work with petawatt-class laser systems.

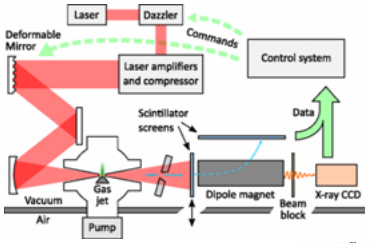

Schematic diagram of the experimental set-up.

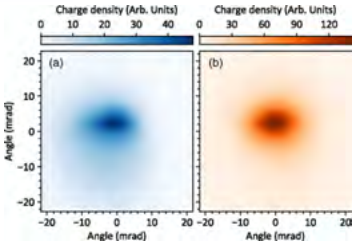

Images of the electron beam spatial profile (a) before and (b) after optimization.

Reprinted from S.J.D. Dann et al. Laser wakefield acceleration with active feedback at 5 Hz, Phys. Rev. Accel. Beams 22, 041303 (2019) published by the American Physical Society, under the terms of the Creative Commons Attribution 4.0 International License doi: 10.1103/PhysRevAccelBeams.22.041303

Contact: S.J.D. Dann (stephen.dann@stfc.ac.uk)

High order mode structure of intense light fields generated via a laser-driven relativistic plasma aperture

M.J. Duff, R. Wilson, M. King, B. Gonzalez-Izquierdo, A. Higginson, S.D.R. Williamson, Z.E. Davidson, R. Capdessus, D. Neely, R.J. Gray, P. McKenna *(SUPA Department of Physics, University of Strathclyde, Glasgow, UK)*
N. Booth, S. Hawkes *(Central Laser Facility, STFC Rutherford Appleton Laboratory, Harwell Campus, Didcot, UK)*
D. Neely *(SUPA Department of Physics, University of Strathclyde, Glasgow, UK; Central Laser Facility, STFC Rutherford Appleton Laboratory, Harwell Campus, Didcot, UK)*

The spatio-temporal and polarisation properties of intense light is important in wide-ranging topics at the forefront of extreme light-matter interactions, including ultrafast laser-driven particle acceleration, attosecond pulse generation, plasma photonics, high-field physics and laboratory astrophysics. Here, we experimentally demonstrate modifications to the polarisation and temporal properties of intense light measured at the rear of an ultrathin target foil irradiated by a relativistically intense laser pulse.

The changes are shown to result from a superposition of coherent radiation, generated by a directly accelerated bipolar electron distribution, and the light transmitted due to the onset of relativistic self-induced transparency. Simulations show that the generated light has a high-order transverse electromagnetic mode structure in both the first and second laser harmonics that can evolve on intra-pulse time-scales. The mode structure and polarisation state vary with the interaction parameters, opening up the possibility of developing this approach to achieve dynamic control of structured light fields at ultrahigh intensities.

Reprinted from Duff, M.J., Wilson, R., King, M. et al. High order mode structure of intense light fields generated via a laser-driven relativistic plasma aperture. Sci Rep 10, 105 (2020), published by Springer Nature, under the terms of the Creative Commons CC BY license. https://doi.org/10.1038/s41598-019-57119-x

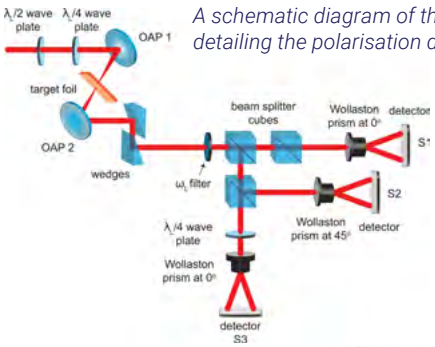

A schematic diagram of the experimental set-up detailing the polarisation diagnostic.

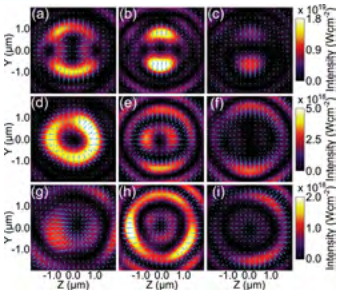

Right: Spatial intensity distributions and electric field vectors (blue arrows) for $2\omega_L$ light, from the full laser-foil simulations, measured 10 μm behind the target rear. Three values of target thickness are compared; (a–c), 5 nm; (d–f), 20 nm; and (g–i), 30 nm.

Contact: P. McKenna (paul.mckenna@strath.ac.uk)

Low-density hydrodynamic optical-field-ionized plasma channels generated with an axicon lens

R.J. Shalloo, C. Arran, A. Picksley, A. von Boetticher, J. Holloway, J. Jonnerby, R. Walczak, S.M. Hooker *(John Adams Institute for Accelerator Science and Department of Physics, University of Oxford, UK)*
L. Corner *(Cockcroft Institute for Accelerator Science and Technology, School of Engineering, University of Liverpool, UK)*
G. Hine, H.M. Milchberg *(Institute for Research in Electronics and Applied Physics, University of Maryland, USA)*
C. Thornton *(Central Laser Facility, STFC Rutherford Appleton Laboratory, Harwell Campus, Didcot, UK)*

We demonstrate optical guiding of high-intensity laser pulses in long, low-density hydrodynamic optical-field-ionized (HOFI) plasma channels. An axicon lens is used to generate HOFI plasma channels with on-axis electron densities as low as n_e (0) = 1.5 × 10^{17} cm^{-3} and matched spot sizes in the range 20 μm ≲ W_M ≲ 40 μm. Control of these channel parameters via adjustment of the initial cell pressure and the delay after the arrival of the channel-forming pulse is demonstrated. For laser pulses with a peak axial intensity of 4 × 10^{17} W cm^{-2}, highly reproducible, high-quality guiding over more than 14 Rayleigh ranges is achieved at a pulse repetition rate of 5 Hz, limited by the available channel-forming laser and vacuum pumping system. Plasma channels of this type would seem to be well suited to multi-GeV laser wakefield accelerators operating in the quasilinear regime.

Reprinted from R.J. Shalloo, C. Arran, A. Picksley et al. Low-density hydrodynamic optical-field-ionized plasma channels generated with an axicon lens, Phys. Rev. Accel. Beams 22, 041302 (2019) published by the American Physical Society, under the terms of the Creative Commons Attribution 4.0 International License doi: 10.1103/PhysRevAccelBeams.22.041302

Contact: S.M. Hooker (simon.hooker@physics.ox.ac.uk)

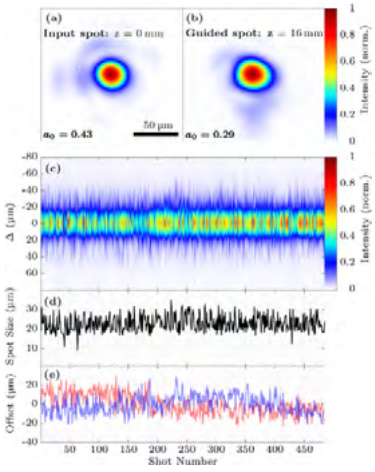

Transverse fluence profiles of the guided laser pulse at (a) the entrance and (b) the exit of a 16-mm-long HOFI channel, at τ = 1.5 ns. (c) shows, for each shot, the average of the horizontal and vertical fluence profiles through the center of mass; the coordinate Δ has its origin at the center of mass. In (d), the D4σ spot size of the transmitted beam (averaged along the principal axes of the spot) is shown for each of the 485 shots; (e) shows the vertical (blue) and horizontal (red) offsets of the spot center. In (a)–(c), the peak fluence has been normalized to the highest value in each plot.

Single-shot multi-keV X-ray absorption spectroscopy using an ultrashort laser-wakefield accelerator source

B. Kettle, E. Gerstmayr, R.A. Baggott, J.M. Cole, S.J. Rose, R. Watt, S.P.D. Mangles *(The John Adams Institute for Accelerator Science, Imperial College London, UK)*
M.J.V. Streeter, S. Dann, Y. Ma *(Physics Department, Lancaster University, UK)*
F. Albert, N. Lemos *(Lawrence Livermore National Laboratory (LLNL), California, USA)*
N. Bourgeois, C. Spindloe, D.R. Symes *(Central Laser Facility, STFC Rutherford Appleton Laboratory, Harwell Campus, Didcot, UK)*
K. Falk *(Helmholtz-Zentrum Dresden-Rossendorf, Germany; Institute of Physics of the ASCR, Prague, Czech Republic; Technische Universität Dresden, 01062, Dresden, Germany)*
I. Gallardo González, O. Lundh *(Department of Physics, Lund University, Sweden)*
A.E. Hussein *(Center for Ultrafast Optical Science, University of Michigan, USA)*
N.C. Lopes *(GoLP/Instituto de Plasmas e Fusão Nuclear, Instituto Superior Técnico, Lisboa, Portugal)*
M. Šmíd *(Helmholtz-Zentrum Dresden-Rossendorf, Germany)*
A.G.R. Thomas *(Center for Ultrafast Optical Science, University of Michigan, USA; Physics Department, Lancaster University, UK)*

Single-shot absorption measurements have been performed using the multi-keV X-rays generated by a laser-wakefield accelerator. A 200 TW laser was used to drive a laser-wakefield accelerator in a mode which produced broadband electron beams with a maximum energy above 1 GeV and a broad divergence of ≈15 mrad FWHM. Betatron oscillations of these electrons generated $1.2 \pm 0.2 \times 10^6$ photons/eV in the 5 keV region, with a signal-to-noise ratio of approximately 300:1. This was sufficient to allow high-resolution X-ray absorption near-edge structure measurements at the *K* edge of a titanium sample in a single shot. We demonstrate that this source is capable of single-shot, simultaneous measurements of both the electron and ion distributions in matter heated to eV temperatures by comparison with density functional theory simulations. The unique combination of a high-flux, large bandwidth, few femtosecond duration X-ray pulse synchronized to a high-power laser will enable key advances in the study of ultrafast energetic processes, such as electron-ion equilibration.

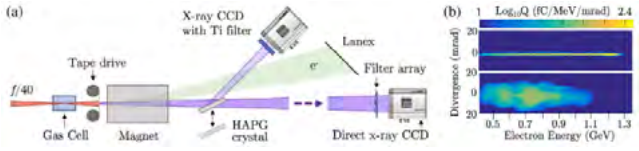

(a) Experiment setup. The LWFA x rays can be measured on axis or with a high-resolution crystal spectrometer. (b) Electron spectra where, for the first stage of the gas cell, $n_e = 1.2 \times 10^{18}$ cm^{-3} (top) and ne = 2.6×10^{18} cm^{-3} (bottom).

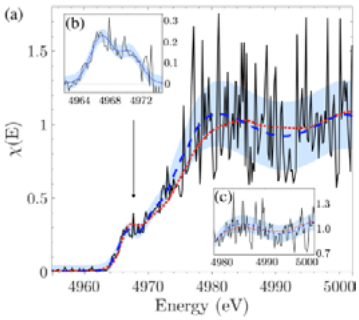

(a) Single-shot normalized absorption data (solid black curve) compared to a synchrotron reference measurement (dotted red curve). The fitted profile for our data is given (dashed blue curve) with the light blue area indicating the measurement error. (b) Double Gaussian fit to the preedge features. (c) The same result as in (a), but averaged over 11 shots.

Figures reprinted with permission from B. Kettle, E. Gerstmayr, M.J.V. Streeter et al. Single-shot multi-keV X-ray absorption spectroscopy using an ultrashort laser-wakefield accelerator source, Phys. Rev. Lett. 123, 254801 (2019) © American Physical Society DOI: 10.1103/PhysRevLett.123.254801

Contact: B. Kettle (b.kettle@imperial.ac.uk)

Dosimetry of laser-accelerated carbon ions for cell irradiation at ultra-high dose rate

G. Milluzzo *(School of Mathematics and Physics, Queen's University Belfast, UK; INFN-LNS, Via Santa Sofia 62, Catania, Italy)*
H. Ahmed *(Central Laser Facility, STFC Rutherford Appleton Laboratory, Harwell Campus, Didcot, UK; School of Mathematics and Physics, Queen's University Belfast, UK)*
L. Romagnani *(LULI - CNRS, Ecole Polytechnique, CEA, Universite Paris -Saclay, France)*
D. Doria *(Extreme Light Infrastructure (ELI-NP) and Horia Hulubei National Institute for R&D in Physics and Nuclear Engineering (IFIN-HH), Romania)*
P. Chaudhary, C. Maiorino, K. Prise *(The Patrick G. Johnston Centre for Cancer Research, Queen's University Belfast, UK)*
A. McIlvenny, A. McMurray, K. Polin, M. Borghesi *(School of Mathematics and Physics, Queen's University Belfast, UK)*
Y. Katzir, P. P. Rajeev *(Central Laser Facility, STFC Rutherford Appleton Laboratory, Harwell Campus, Didcot, UK)*
P. McKenna *(Department of Physics, SUPA, University of Strathclyde, Glasgow, UK)*

Carbon ions are particularly attractive for the treatment of radioresistant tumours, thanks to their higher Linear Energy Transfer (LET) and Relative Biological Effectiveness (RBE). Recent developments in ion acceleration have allowed to investigate for the first time the biological effects of carbon ions at ultra-high dose-rate (10^{10} Gy/s) using the Gemini laser system at the Rutherford Appleton Laboratory (RAL). Carbon ions were accelerated from ultrathin (10-20 nm) carbon foils and energy selected by a magnet allowing to irradiate the cells with an average carbon energy of 10 MeV/nucleon ± 8%. The details of the dosimetry arrangement as well as the measurement of the dose distribution at the cell plane are reported.

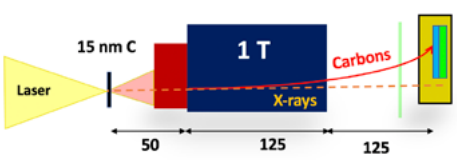

Schematic of the experimental setup.

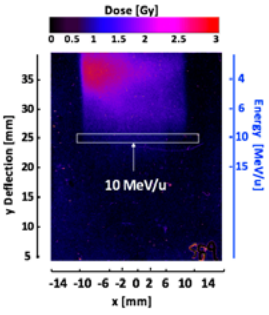

Image of the unlaminated EBT3 irradiated with carbon ions during one shot. The region corresponding to 10 MeV/nucleon carbon ions is also shown (white square).

Figures adapted from G. Milluzzo et al. Dosimetry of laser-accelerated carbon ions for cell irradiation at ultra-high dose rate, J. Phys.: Conf. Ser. 1596 012038 (2020), published by IOP Publishing Ltd, under the terms of the Creative Commons Attribution 3.0 Licence (CC BY 3.0). doi: 10.1088/1742-6596/1596/1/012038

Contact: G. Milluzzo (g.milluzzo@qub.ac.uk)

Characteristics of ion beams generated in the interaction of ultra-short laser pulses with ultra-thin foils

A. McIlvenny, H. Ahmed, C. Scullion, P. Martin, K. Naughton, S. Kar, M. Borghesi *(Centre for Plasma Physics, Queen's University Belfast, UK)*
D. Doria *(Centre for Plasma Physics, Queen's University Belfast, UK; Extreme Light Infrastructure—Nuclear Physics (ELI-NP), Horia Hulubei National Institute for R&D in Physics and Nuclear Engineering (IFIN-HH), Romania*
L. Romagnani *(Centre for Plasma Physics, Queen's University Belfast, UK; LULI, École Polytechnique, CNRS, Palaiseau Cedex, France)*
A. Sgattoni *(CNR/INO (National Institute of Optics), Pisa, Italy)*
D.R. Symes *(Central Laser Facility, STFC Rutherford Appleton Laboratory, Harwell Campus, Didcot, UK)*
A. Macchi *(CNR/INO (National Institute of Optics), Pisa, Italy; Enrico Fermi Department of Physics, University of Pisa, Italy)*
P. McKenna *(SUPA, Department of Physics, University of Strathclyde, Glasgow, UK)*
M. Zepf *(Centre for Plasma Physics, Queen's University Belfast, UK; Helmholtz Institute Jena, Germany)*

Experiments investigating ion acceleration from laser-irradiated ultra-thin foils on the Gemini laser facility at the Rutherford Appleton Laboratory indicate a transition to 'light sail' radiation pressure acceleration when using circularly polarised, high contrast laser pulses. This paper complements previously published results with additional data and modelling which provide information on the multispecies dynamics taking place during the acceleration, and provides an indication on expected scaling of these processes at higher laser intensities.

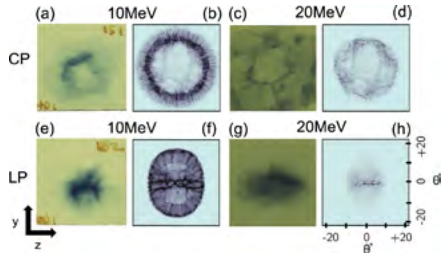

Average maximum ion energy measured from the Thomson Parabola Spectrometer. A target thickness scan showing maximum ion energies for (a) C^{6+} and (b) protons for linear (LP) and circular polarisation (CP) is displayed.

Reprinted from A. McIlvenny et al. Characteristics of ion beams generated in the interaction of ultra-short laser pulses with ultra-thin foils, Plasma Phys. Control. Fusion 62 054001 (2020), published by IOP Publishing Ltd, under the terms of the Creative Commons Attribution 4.0 International License
doi: 10.1088/1361-6587/ab7d26

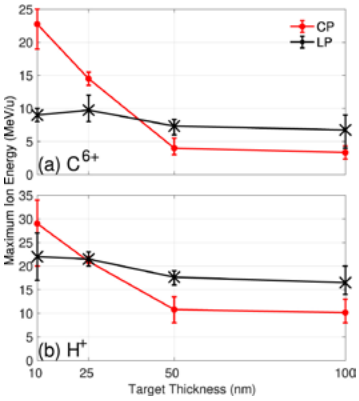

CP (a)–(d) and LP (e)–(h) proton beam profiles a 10 MeV (left) and 20 MeV (right) obtained experimentally from RCF (a), (c), (e), (g) and through 3D PIC simulations (b), (d), (f), (h).

Contact: M. Borghesi (m.borghesi@qub.ac.uk)

Selective ion acceleration by intense radiation pressure

A. McIlvenny, P. Martin, S. Kar, M. Borghesi *(Centre for Plasma Physics, Queen's University Belfast, UK)*
D. Doria *(Extreme Light Infrastructure (ELI-NP) and Horia Hulubei National Institute for R&D in Physics and Nuclear Engineering (IFIN-HH), Romania*
L. Romagnani *(LULI, Ecole Polytechnique, CNRS, Palaiseau Cedex, France)*
H. Ahmed, N. Booth, P.P. Rajeev, G.G. Scott, D. Neely *(Central Laser Facility, STFC Rutherford Appleton Laboratory, Harwell Campus, Didcot, UK)*
E.J. Ditter, O.C. Ettlinger, G.S. Hicks, Z. Najmudin *(The John Adams Institute for Accelerator Science, Blackett Laboratory, Imperial College London, UK)*
S.D.R. Williamson, P. McKenna *(SUPA, Department of Physics, University of Strathclyde, Glasgow, UK)*
A. Macchi *(Istituto Nazionale di Ottica, Consiglio Nazionale delle Ricerche (CNR/INO), Research Unit "Adriano Gozzini," Pisa, Italy)*

We report on preferential acceleration of heavy ions in an inherently multi-species target by the intense radiation pressure of the Gemini laser incident on ultra-thin foils with circular polarization. At the optimum thickness of 15 nm, heavy ion C^{6+} energies were detected up to 33 MeV/nucleon and protons with a maximum energy cut off of 18 MeV. This difference, the opposite to what is typically observed with laser-foil interactions, is attributed (via multi-dimensional Particle in Cell simulations) to the removal of contaminant protons (and their subsequent thermal acceleration) by the laser's coherent contrast, with the carbon ions being accelerated via Radiation Pressure Acceleration in the Light Sail regime. This is supported by the experimental measurement of different scaling of the maximum ion energy with laser intensity for the two species.

Contact: A. McIlvenny (a.mcilvenny@qub.ac.uk)

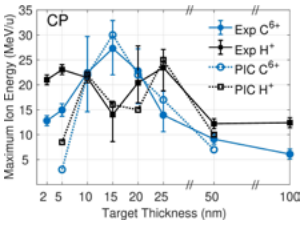

Maximum ion energy along the laser axis for C^{6+} (blue) and protons (black) for circular polarisation. The experimental data is shown with solid lines (and solid markers) and simulations with dotted lines (and empty markers). Preferential acceleration of carbon ions over protons is observed at 15 nm.

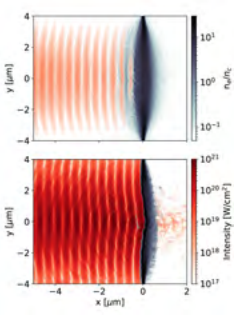

2D PIC maps of electron density (grey scale) and laser intensity (red scale) at -83 fs (top) and -23 fs (bottom) with respect to the peak of the pulse hitting the target at 0 fs (each colour-bar refers to both images). The laser enters from the left and is centred at y = 0 μm. Moderate target expansion prior to the peak of the pulse arriving is responsible for the removal of contaminant protons and allows for the acceleration of carbon ions only by radiation pressure.

Generation of electron high energy beams with a ring-like structure by a dual stage laser wakefield accelerator

R. Spesyvtsev, G. Vieux, M. Shahzad, A. Maitrallain, S. Yoffe, B. Ersfeld, A. Kornaszewski *(SUPA, Department of Physics, University of Strathclyde, UK)*
E. Brunetti, D.A. Jaroszynski *(SUPA, Department of Physics, University of Strathclyde, UK; The Cockcroft Institute, Daresbury, UK)*
M.J.V. Streeter *(Physics Department, Lancaster University, UK; The Cockcroft Institute, Daresbury, UK; The John Adams Institute for Accelerator Science, Imperial College London, UK)*
O. Finlay *(Physics Department, Lancaster University, UK)*
Y. Ma, A.G.R. Thomas *(Physics Department, Lancaster University, UK; The Cockcroft Institute, Daresbury, UK; Center for Ultrafast Optical Science, University of Michigan, USA)*
B. Kettle, J.M. Cole, E. Gerstmayr, S.P.D. Mangles, Z. Najmudin *(The John Adams Institute for Accelerator Science, Imperial College London, UK)*
S.J.D. Dann *(Physics Department, Lancaster University, UK; The Cockcroft Institute, Daresbury, UK)*
F. Albert, N. Lemos *(Lawrence Livermore National Laboratory, California, USA)*
N. Bourgeois, P.P. Rajeev, D.R. Symes *(Central Laser Facility, STFC Rutherford Appleton Laboratory, Harwell Campus, Didcot, UK)*
S. Cipiccia *(Diamond Light Source, Harwell Science and Innovation Campus, Didcot, UK)*
I.G. Gonzáles, O. Lundh *(Department of Physics, Lund University, Sweden)*
A. Higginbotham, C. Lumsdon *(York Plasma Institute, Department of Physics, University of York, UK)*
A.E. Hussein, K. Krushelnick *(Center for Ultrafast Optical Science, University of Michigan, USA)*
K. Falk, M. Smid *(ELI Beamlines, Institute of Physics of the ASCR, Prague, Czech Republic)*
N.C. Lopes *(The John Adams Institute for Accelerator Science, Imperial College London, UK; GoLP/Instituto de Plasmas e Fusão Nuclear, Instituto Superior Técnico, Lisboa, Portugal)*

The laser wakefield accelerator (LWFA) traditionally produces high brightness, quasi-monoenergetic electron beams with Gaussian-like spatial and angular distributions. In the present work we investigate the generation of ultra-relativistic beams with ring-like structures in the blowout regime of the LWFA using a dual stage accelerator. A density down-ramp triggers injection after the first stage and is used to produce ring-like electron spectra in the 300 – 600 MeV energy range. These well-defined, annular beams are observed simultaneously with the on-axis, high energy electron beams, with a divergence of a few milliradians. The rings have quasi-monoenergetic energy spectra with an RMS spread estimated to be less than 5%. Particle-in-cell simulations confirm that off-axis injection provides the electrons with the initial transverse momentum necessary to undertake distinct betatron oscillations within the plasma bubble during their acceleration process.

Reprinted with permission from Spesyvtsev, R., et al. Generation of electron high energy beams with a ring-like structure by a dual stage laser wakefield accelerator. Relativistic Plasma Waves and Particle Beams as Coherent and Incoherent Radiation Sources III. Vol. 11036. International Society for Optics and Photonics, 2019. https://doi.org/10.1117/12.2522781

Contact: D.A. Jaroszynski (d.a.jaroszynski@strath.ac.uk)

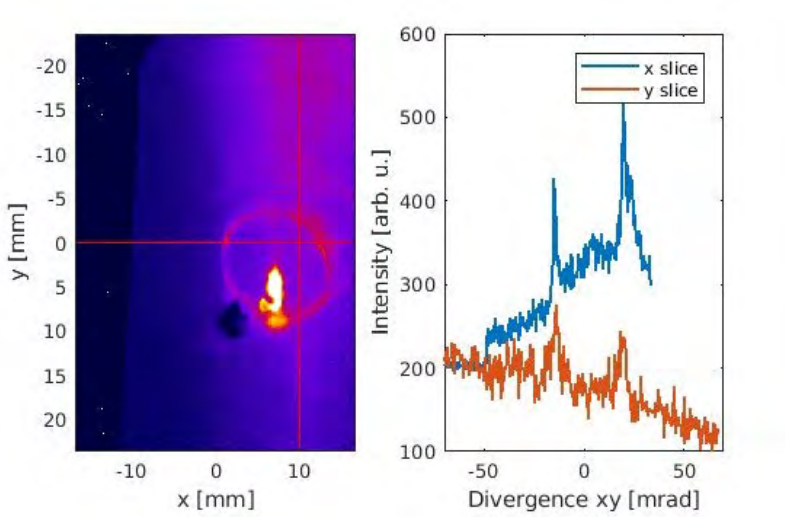

Electron beam profile measured on a LANEX electron profile monitor with cross-sections taken along the indicated lines.

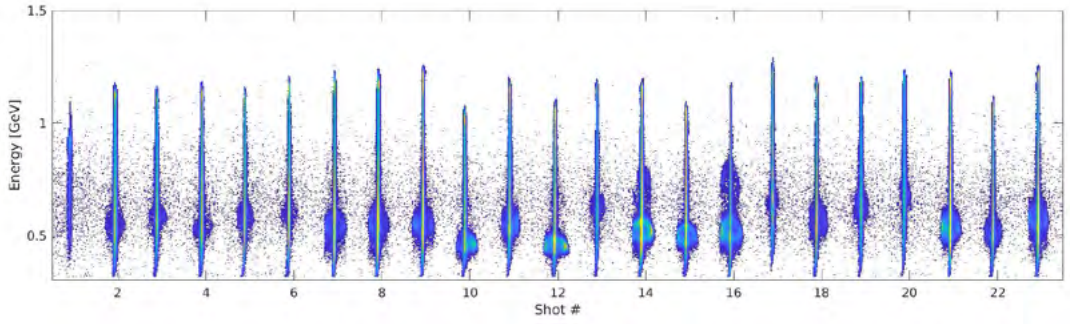

Electron energy spectrum measurements showing a broad energy distribution as well as a quasi-monoenergetic ring structure.

Absolute calibration of microchannel plate detector for carbon ions up to 250 MeV

A. McIlvenny, H. Ahmed, P. Martin, S. Kar, M. Borghesi *(Centre for Plasma Physics, Queen's University Belfast, UK)*
D. Doria *(Extreme Light Infrastructure—Nuclear Physics (ELI-NP), Horia Hulubei National Institute for R&D in Physics and Nuclear Engineering (IFIN-HH), Romania*
L. Romagnani *(LULI, École Polytechnique, CNRS, Palaiseau Cedex, France)*
S.D.R. Williamson, P. McKenna *(SUPA, Department of Physics, University of Strathclyde, Glasgow, UK)*
E.J. Ditter, O. Ettlinger, G.S. Hicks, Z. Najmudin *(The John Adams Institute, Imperial College London, UK)*
D. Neely *(Central Laser Facility, STFC Rutherford Appleton Laboratory, Harwell Campus, Didcot, UK)*

A 375 TW 40 fs pulse was used at the Gemini facility for investigating novel ion acceleration regimes employing ultrathin foil targets. An online detection system consisting of a Thomson Parabola Spectrometer (TPS) with a Microchannel Plate (MCP) was used to determine maximum energies and spectra per species. The response of the MCP was calibrated for absolute particle (carbon) number per steradian using CR-39 up to 21 MeV/nucleon. This calibration provides a useful reference for a widely used diagnostic arrangement.

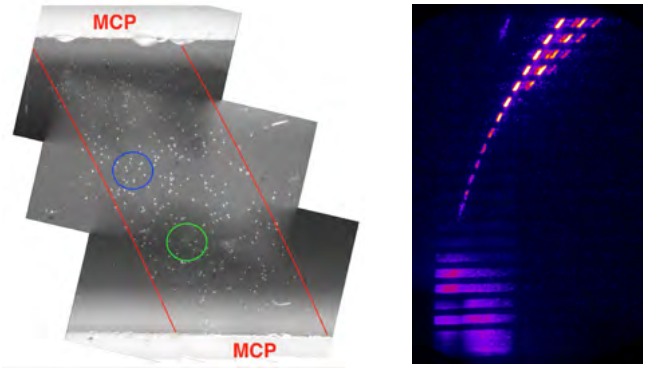

Left: Mosaic image of CR-39 at X10 magnification showing the width of the parabolic ion trace (red lines) and the CR-39–MCP interface at 4.1 MeV/nucleon (top) and 4.4MeV/u (bottom). The blue circle represents C^{6+} and green represents noise from damage particles. Right: Image of MCP with slotted CR-39 placed in front of it forming regular interfaces between the two.

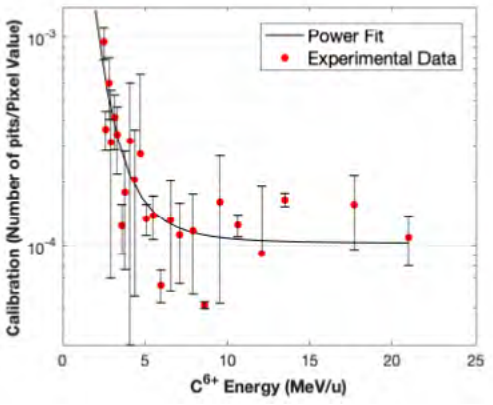

Calibration function for each energy bin for the Thomson Parabola Spectrometer at 0° (red dots):
Calibration = $1.257 \times 10^{-2} \times \text{energy}^{-3.331} + 1.028 \times 10^{-4}$ (black line).

Reprinted with permission from A. McIlvenny et al. Absolute calibration of microchannel plate detector for carbon ions up to 250 MeV, JINST 14 C04002 (2019), © IOP Publishing Ltd & Sissa Medialab doi: 10.1088/1748-0221/14/04/C04002

Contact: M. Borghesi (m.borghesi@qub.ac.uk)

Wakefields in a cluster plasma

M.W. Mayr, L. Ceurvorst, M.F. Kasim, J.D. Sadler, B. Spiers, A.F. Savin, A.J. Ross, R. Aboushelbaya, J. Holloway, N. Ratan, R.H.W. Wang, P.N. Burrows *(Department of Physics, University of Oxford, UK)*
K. Glize, N. Bourgeois, D.R. Symes, R.M.G.M. Trines, P.P. Rajeev *(Central Laser Facility, STFC Rutherford Appleton Laboratory, Harwell Campus, Didcot, UK)*
F. Keeble, M. Wing *(Department of Physics and Astronomy, University College London, UK)*
R.A. Fonseca *(ISCTE - Instituto Universitário de Lisboa, Portugal; GoLP/Instituto de Plasmas e Fusão Nuclear, Instituto Superior Tecnico, Lisbon, Portugal)*
R. Bingham *(Central Laser Facility, STFC Rutherford Appleton Laboratory, Harwell Campus, Didcot, UK; Department of Physics, University of Strathclyde, Glasgow, UK)*
L.O. Silva *(GoLP/Instituto de Plasmas e Fusão Nuclear, Instituto Superior Técnico, Lisboa, Portugal)*
P.A. Norreys *(Department of Physics, University of Oxford, UK; Central Laser Facility, STFC Rutherford Appleton Laboratory, Harwell Campus, Didcot, UK)*

We report the first comprehensive study of large amplitude Langmuir waves in a plasma of nanometre-scale clusters. Using an oblique angle single-shot frequency domain holography diagnostic, the shape of these wakefields is captured for the first time. The wavefronts are observed to curve backwards, in contrast to the forwards curvature of wakefields in uniform plasma. Due to the expansion of the clusters, the first wakefield period is longer than those trailing it. The features of the data are well described by fully relativistic two-dimensional particle-in-cell simulations and by a quasianalytic solution for a one-dimensional, nonlinear wakefield in a cluster plasma.

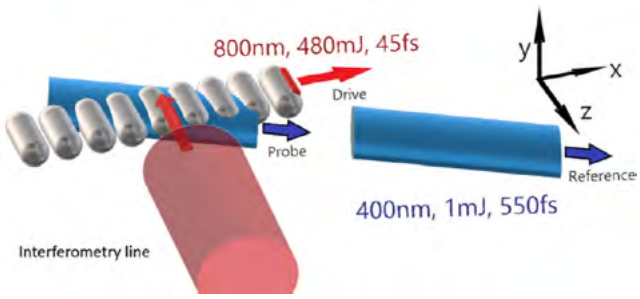

Schematic of the experimental set-up, including a single-shot oblique-angle frequency domain holography diagnostic and a transverse optical probe.

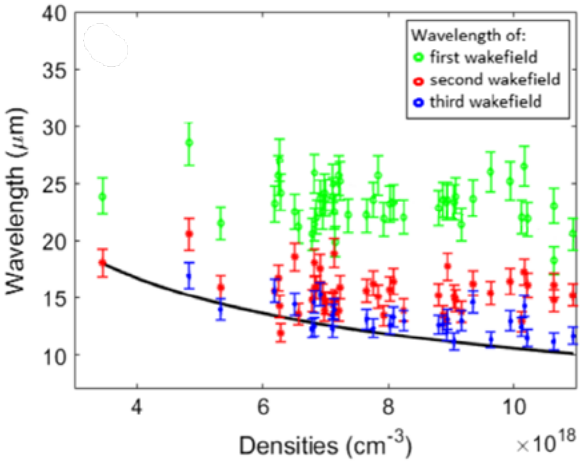

Measurement of the first (green), second (red), and third (blue) wakefield wavelengths as a function of the average plasma electron density measured by the transverse interferometry, with data from 30 separate laser shots.

Reprinted from M.W. Mayr, L. Ceurvorst, M.F. Kasim et al. Wakefields in a cluster plasma, Phys. Rev. Accel. Beams 22, 113501 (2019) published by the American Physical Society, under the terms of the Creative Commons Attribution 4.0 International License doi: 10.1103/PhysRevAccelBeams.22.113501

Contact: M.W. Mayr (marko.mayr@physics.ox.ac.uk)

Calorimetry techniques for absolute dosimetry of laser-driven ion beams

S. McCallum *(Centre for Plasma Physics, Queen's University Belfast, UK; National Physical Laboratory, Medical Radiation Science, Teddington, UK)*
G. Milluzzo, H. Ahmed, A. McIlvenny, M. Borghesi *(Centre for Plasma Physics, Queen's University Belfast, UK)*
N. Lee, A. Subiel *(National Physical Laboratory, Medical Radiation Science, Teddington, UK)*
F. Romano *(Istituto Nazionale di Fisica Nucleare, Sezione di Catania, Italy; National Physical Laboratory, Medical Radiation Science Teddington, UK)*

Laser-driven particle acceleration based on the use of intense, ultra-short laser pulses is emerging as a novel technique for the compact generation and delivery of energetic ion beams, particularly in view of the possible future use of these beams as a source for particle therapy of cancer. Precise measurement of the dose delivered to a given volume is essential to ensure safe delivery of treatment. Therefore, reliable methods allowing beam characterization and accurate dosimetry need to be established to first ensure reliable pre-clinical studies and, in a future perspective, optimal treatment. Absolute dosimetry of laser-driven ion beams, using a small portable graphite calorimeter developed at National Physical Laboratory is presented, with a first proof of principle experiment demonstrating the use of calorimetric techniques in a laser environment.

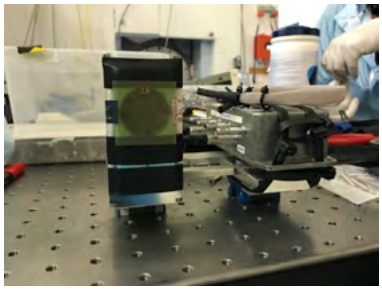

Left: The SPGC assembled in a makeshift holder dedicated for the measurement using Vulcan, and electronics close by. The calorimeter indicated is composed of a sensitive core containing 4 thermistors.

Right: Measured radiation induced temperature rise of the SPGC core for a shot performed with the Vulcan laser system. This represents the first laser-driven proton beam captured by through calorimetry.

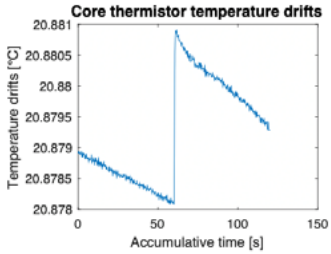

Contact: S. McCallum (smccallum05@qub.ac.uk)

Multi-species hybrid ion acceleration from ps, PW interactions with ultra-thin foils

O. McCusker, A. McIlvenny, P. Martin, S. Ferguson, S. Zhai, S. Kar, M. Borghesi *(Centre of Plasma Physics, Queen's University Belfast, UK)*
H. Ahmed, J. Green *(Central Laser Facility, STFC Rutherford Appleton Laboratory, Harwell Campus, Didcot, UK)*
J. Jarrett, M. King, P. McKenna *(SUPA Department of Physics University of Strathclyde, Glasgow, UK)*

The optimisation of heavy and light ion acceleration from intense laser interactions was investigated experimentally. Ultra-thin (10 - 340 nm) plastic (CH) foils were irradiated with intense, short (750 fs) laser pulses with maximum energies of 75 MeV and 25 MeV/μ obtained for H^+ and C^{6+} ions, respectively. Species resolved spectra suggest differences in the acceleration mechanism for each species. Further analysis through Particle in Cell simulations, identifies a hybrid acceleration scheme, which is enhanced by the onset of relativistically induced transparency. This report presents the analysis of the interplay of the different mechanisms and how it affects each species' acceleration dynamics.

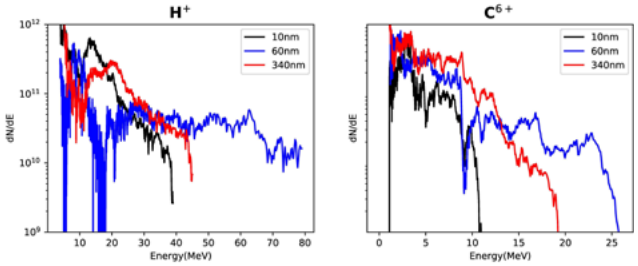

Spectra obtained for both H^+ (left) and C^{6+} (right) ions at TPS1 (+6.5°) for three target thicknesses, 10 nm, 60 nm and 340 nm.

2D colour-maps of average electric field at each time-step for three thicknesses, a) 40 nm, b) 140 nm, c) 300 nm. X positions of highest energy ions (H^+ (black) and C^{6+} ions (red)) for each thickness are tracked. The times at which transparency occurs are marked with a blue vertical line for each thickness.

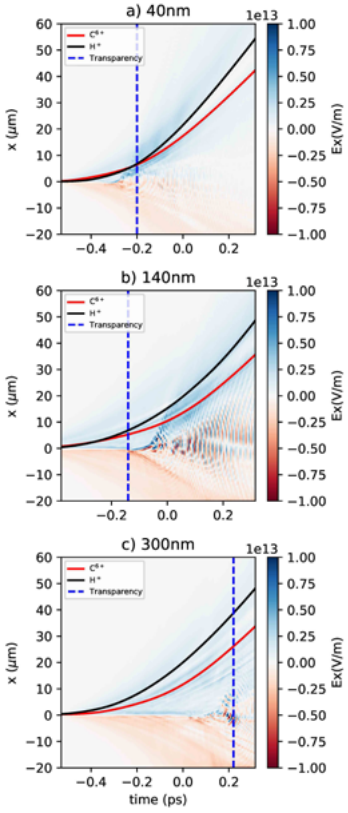

Contact: O. McCusker (omccusker03@qub.ac.uk)

Light-sail acceleration from two moderate intensity pulses

P. Martin, S. Ferguson, A. McIlvenny, S. Kar, M. Borghesi *(Centre for Plasma Physics, Queen's University Belfast, UK)*
H. Ahmed, J.S. Green *(Central Laser Facility, STFC Rutherford Appleton Laboratory, UK)*
D. Doria *(ELI NP, Magurele, Romania)*
J. Jarrett, P. McKenna *(Department of Physics, University of Strathclyde, UK)*
S. Zhai *(ELI Beamlines, Dolní Břežany, Czechia)*

The acceleration of ions from ultrathin deuterated plastic foils is demonstrated by implementing two pulses with intensities on the order of 10^{19} W/cm^2, which could be spatio-temporally separated by varying degrees. At the optimal arrangement of the two pulses, maximum proton and deuteron energies of 45 MeV and 33 MeV/u, respectively, were accelerated from 85 nm foils, exceeding what was achieved from a single pulse irradiating the same target at ~5 × 10^{20} W/cm^2, despite the double pulse setup sacrificing a ~60% average reduction in total laser fluence on target.

Contact: P. Martin (p.martin@qub.ac.uk)

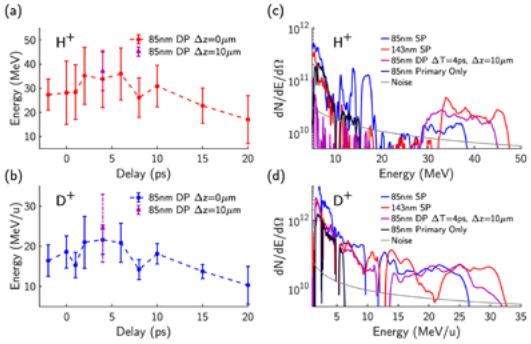

(a) Proton, and (b) deuteron central bunch energies along target normal direction vs time delay between the two beams in the double pulse setup. Also shown in purple is the highest energy reached when the secondary beam is focused 10 μm further along the laser axis. The bars on each data point represent bunch widths of individual shots. The maximum limit of the bars corresponds to the spectrum cut-off energies. (c) Proton and (d) deuteron TPS spectra, for selected single pulse (SP) and double pulse (DP) shots from the campaign, taken along the laser axis.

Extending proton energy gain in laser-driven helical coil targets

S. Ferguson, B. Greenwood, B. Odlozilik, M. Alanazi, M. Borghesi, S. Kar *(Centre for Plasma Physics, Queen's University Belfast, UK)*
E. Aktan, M. Cerchez *(Institute for Laser and Plasma Physics, Henrich Heine University of Dusseldorf, Germany)*
D. Doria *(Extreme Light Infrastructure – Nuclear Physics, Horia Hulubei National Institute, Romania)*
H. Ahmed, J. Green *(Central Laser Facility, STFC Rutherford Appleton Laboratory, Harwell Campus, Didcot, UK)*

Laser driven helical coil targets post-accelerate and focus TNSA beams to form a quasi-collimated, narrow energy band of protons. Increasing the length of helical coil extends the duration protons remain in phase with the strong electric fields formed by the helical coil target. Therefore, longer helical coils are expected to enhance the acceleration and focussing effects, which was observed in our recent experiment at Vulcan's target area west with helical coil length up to ~12 mm. Particle tracing simulations closely resemble the experimental data and reveal that the helical coil effectiveness is significantly reduced after ~12 mm. The reduced effectiveness is attributed to accelerated protons outrunning, thus de-phasing with the strong electric field region produced by helical coils of fixed pitch and radius.

Contact: S. Ferguson (sferguson25@qub.ac.uk)

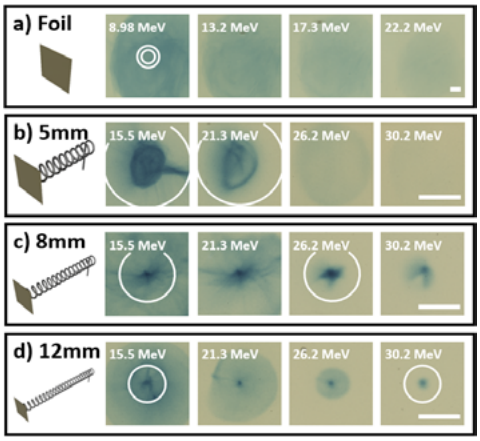

(a-d) Proton beam spatial profiles at different energies produced from helical coils of varying lengths, obtained from an experimental campaign at Vulcan's target area west. HCs had 0.5 mm pitch, 0.7 mm diameter. RCF was deployed 75 mm from the proton source and scale bars correspond 5 mm at the RCF plane. White circles represent the helical coil apertures with half-angle divergences (b) 4.0°, (c) 2.5° and (d) 1.7°. As a reference, 4.0° and 2.5° divergences are also shown in (a).

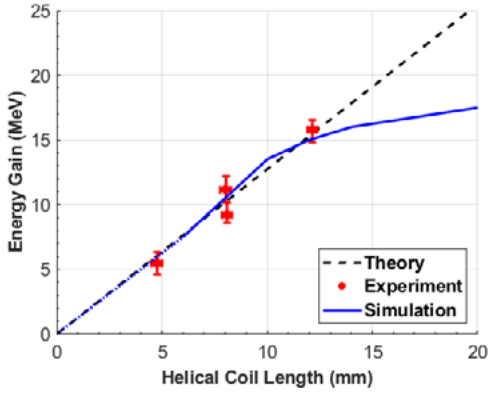

Energy gain as a function of helical coil length for experimental data (red dots) and PTRACE particle tracing simulations (blue line). Energy gain remains uniform at ~1.25 MeV/mm for the first 12 mm of the helical coil length, as expected from theory (black dashed line). However, the de-phasing between accelerated protons and EM field saturates energy gain beyond 12 mm, as studied through PTRACE simulations.

Field reconstruction from proton radiography of intense laser-driven magnetic reconnection

C.A.J. Palmer *(Clarendon Laboratory, University of Oxford, UK; Cockcroft Institute, Daresbury, UK; Physics Department, Lancaster University, UK)*
P.T. Campbell, Y. Ma, P. Kordell, K. Krushelnick, A.G.R. Thomas *(Center for Ultrafast Optical Science, University of Michigan, USA)*
L. Willingale *(Center for Ultrafast Optical Science, University of Michigan, USA; Cockcroft Institute, Daresbury, UK; Physics Department, Lancaster University, UK)*
L. Antonelli, C.P. Ridgers, N. Woolsey *(Department of Physics, University of York, UK)*
A.F.A. Bott, G. Gregori, A.A. Schekochihin *(Clarendon Laboratory, University of Oxford, UK)*
J. Halliday, S.V. Lebedev, E.R. Tubman, M.J.V. Streeter *(Blackett Laboratory, Imperial College London, UK)*
Y. Katzir, E. Montgomery, M. Notley, D.C. Carroll *(Central Laser Facility, STFC Rutherford Appleton Laboratory, Harwell Campus, Didcot, UK)*

Relativistic magnetic reconnection is a potential source of particle energisation in extreme astrophysical environments. Non-thermal particle populations have been produced in laboratory reconnection events driven by two high intensity laser pulses (A. E. Raymond *et al.*, PRE, 98, 043207 (2018)). Here proton radiography was used to map the field evolution around two such laser foci. The azimuthal magnetic fields around each focus is established rapidly (<6 ps) and are distorted as the fields of each focus meet in the midplane region. The measurements reveal that these continue to grow for 10s ps after the laser drive before decaying. An algorithm developed by A. F. A. Bott *et al.*, JPP, 83, 905830614 (2017), was used to retrieve the fields and multiple initial proton fluxes are tested to determine the sensitivity of the retrieval to initial beam profile.

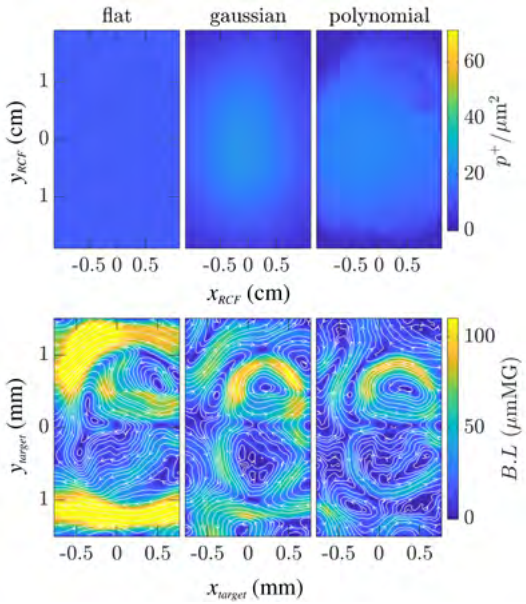

Field retrievals (bottom row) at the interaction plane of proton radiography at t = 33 ps using different assumed 'undisturbed' proton flux distributions shown at the detector plane (top row) including, from left to right, a flat mean-field, a σ=150-pixel Gaussian filter with 200-pixel kernal size, and a custom 2D 3rd-order polynomial, masked with the beam edge, in which the low flux regions are replaced with the original image. Taken from Palmer et al., PoP, 26, 083109 (2019)

Contact: C. Palmer (c.palmer@qub.ac.uk)

Collisionless shock acceleration from laser-irradiated foam targets

B.T. Spiers, A.F. Savin, R. Aboushelbaya, M. Mayr, R.W. Paddock, R.H.W. Wang, P.A. Norreys *(Department of Physics, University of Oxford, UK)*
L. Ceurvorst, A. Casner *(CELIA, Université de Bordeaux-CNRS-CEA, France)*
M. Fajardo *(Department of Physics, Instituto Superior Técnico, Lisbon, Portugal)*
C.D. Baird, M. Notley, C. Spindloe, S. Irving *(Central Laser Facility, STFC Rutherford Appleton Laboratory, Harwell Campus, Didcot, UK)*
R. Bingham *(Central Laser Facility, STFC Rutherford Appleton Laboratory, Harwell Campus, Didcot, UK; University of Strathclyde, Glasgow, UK)*
R.A. Cairns *(University of St. Andrews, UK)*
E. Boella *(Physics Department, Lancaster University, UK)*

An experiment was carried out at the Vulcan 100 TW laser facility to investigate the potential for collisionless shock acceleration in low-density plastic foam targets. To assist in interpretation of the spectra obtained, advances are made in the kinetic theory approach to collisionless shock theory first presented by Cairns *et al.* in 2014. Experimental signatures consistent with acceleration from a collisionless shock were detected and parameter values which fit the form of the ion spectra are found. The parameter values found correspond to somewhat sub optimal plasma conditions that arose due to experimental constraints.

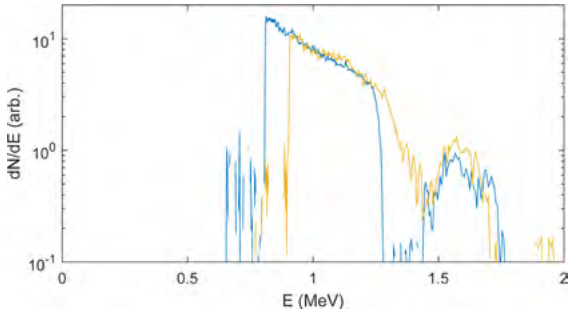

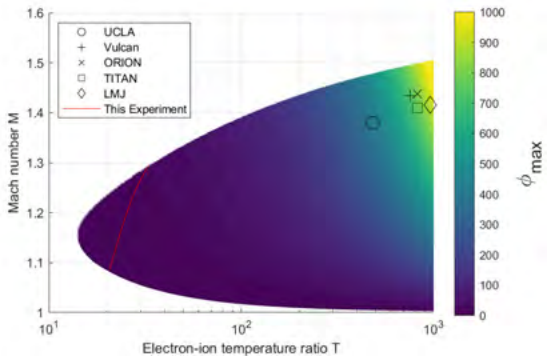

Above: The parameter space compatible with this experiment's results. The red line is produced by varying the ion temperature while keeping the maximum energy and energy FWHM of the reflected ions constant. Shown with markers are predictions for the parameter space attainable at Vulcan and other facilities under ideal conditions.

Left: Ion spectra collected on two representative shots, showing the quasi-monoenergetic ion feature indicative of acceleration by a collisionless shock.

Contact: B. Spiers (benjamin.spiers@physics.ox.ac.uk)

Supersonic plasma turbulence in the laboratory

T.G. White, M.T. Oliver *(Department of Physics, University of Nevada, Reno, USA; Department of Physics, University of Oxford, UK)*
P. Mabey *(Department of Physics, University of Oxford, UK; LULI—CNRS, Ecole Polytechnique, France)*
M. Kühn-Kauffeldt *(Universität der Bundeswehr München, Germany)*
A.F.A. Bott, A.R. Bell, J. Meinecke, F. Miniati, S. Sarkar, A.A. Schekochihin, G. Gregori *(Department of Physics, University of Oxford, UK)*
L.N.K. Döhl, N. Woolsey *(York Plasma Institute, University of York, UK)*
R. Bingham *(Central Laser Facility, STFC Rutherford Appleton Laboratory, Harwell Campus, Didcot, UK; Department of Physics, SUPA, University of Strathclyde, Glasgow, UK)*
R. Clarke, R. Heathcote, M. Notley, M.P. Selwood, R.H.H. Scott *(Central Laser Facility, STFC Rutherford Appleton Laboratory, Harwell Campus, Didcot, UK)*
J. Foster, P. Graham *(AWE, Aldermaston, UK)*
G. Giacinti *(Max-Planck-Institut für Kernphysik, Heidelberg, Germany)*
M. Koenig *(LULI—CNRS, Ecole Polytechnique, France; Graduate School of Engineering, Osaka University, Japan)*
Y. Kuramitsu *(Graduate School of Engineering, Osaka University, Japan)*
D.Q. Lamb, P. Tzeferacos *(Department of Astronomy and Astrophysics, University of Chicago, USA)*
Th. Michel *(LULI—CNRS, Ecole Polytechnique, France)*
B. Reville *(School of Mathematics and Physics, Queen's University Belfast, UK)*
D. Ryu *(Department of Physics, School of Natural Sciences, UNIST, Ulsan, Korea)*
Y. Sakawa *(Institute of Laser Engineering, Osaka, Japan)*
J. Squire *(Theoretical Astrophysics, 350-17, California Institute of Technology, USA; Physics Department, University of Otago, Dunedin, New Zealand)*

The Universe is full of turbulent plasmas. The characteristic large scales and small viscosities drive chaotic motion that governs the dynamics of the interstellar medium, molecular clouds, stars, supernovae, and accretion disks. However, unlike most terrestrial-based turbulence, in these astrophysical scenarios, the motions are often supersonic, i.e., faster than the speed of sound. The additional complexity has hampered our understanding compared to the subsonic case. In our latest paper, published in *Nature Communications*[1], we study the behaviour of turbulence generated from the collision of two supersonic plasma jets driven by high-energy lasers. We were able to use TAW laser to generate jets up to Mach 6, which is at velocities comparable to those found in star-forming molecular clouds. By passing these jets through a pair of grids and colliding them in the centre, we produced a region of supersonic turbulence. Utilizing a suite of diagnostics, we observed the formation of small shockwaves, a characteristic of supersonic turbulence. We ultimately watched the turbulence transition away from being Kolmogorov-like at low Mach number to matching what is seen in molecular clouds at higher Mach number.

1. White, T.G., Oliver, M.T., Mabey, P. et al. Supersonic plasma turbulence in the laboratory. Nat Commun 10, 1758 (2019). https://doi.org/10.1038/s41467-019-09498-y

Contact: T.G. White (tgwhite@unr.edu)

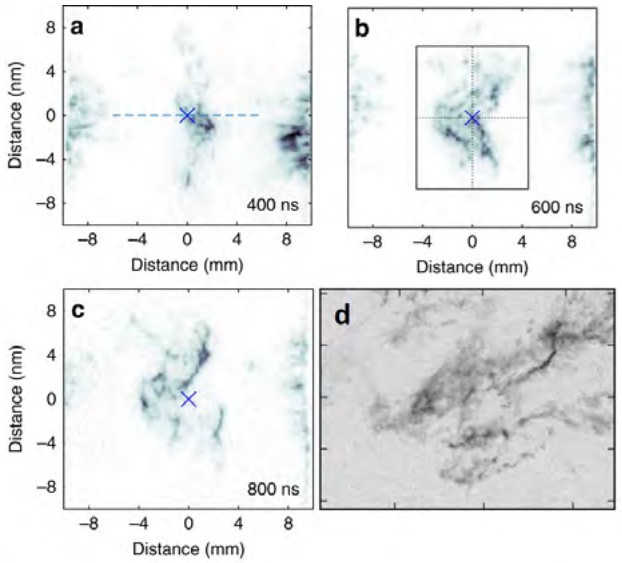

Schlieren images of the supersonic plasma generated in the experiment (a – 400 ns, b – 600 ns, c – 800ns) and CO integrated intensity map of the Taurus Molecular Cloud (d). Notice the formation of thin features in both, a characteristic of shock-wave formation and supersonic turbulence. The image in d is reproduced from Brunt, C. M. The density variance–Mach number relation in the Taurus molecular cloud. Astronomy & Astrophysics 513 (2010): A67. doi: 10.1051/0004-6361/200913506

Proton acceleration from a cryogenic hydrogen ribbon

P. Martin, S. Kar, D. Margarone, M. Borghesi *(Centre for Plasma Physics, Queen's University Belfast, UK)*
H. Ahmed, D. Carroll *(Central Laser Facility, STFC Rutherford Appleton Laboratory, UK)*
D. Doria *(ELI NP, Magurele, Romania)*
A. Alejo *(Department of Physics, University of Oxford, UK)*
P. Bonnay, D. Chatain, D. Garcia, S. Michaux, J.P. Perin *(CEA, Grenoble, France)*
F. Grepl, L. Giuffrida, P. Lutoslawski, F. Schillaci, V. Scuderi, A. Velyhan *(ELI Beamlines, Dolní Břežany, Czechia)*

We report on the interaction of an intense (~5 × 10^{20} W/cm^2) picosecond pulse with thin (75 – 100 µm) ribbons of cryogenically-cooled solid hydrogen. Beams of protons exhibiting the broadband TNSA-like spectrum seen in typical higher-density target types were observed, in addition to quasi-monoenergetic bunches, at energies exceeding the TNSA cutoff, directed predominantly along the laser axis. This suggests a significant hole boring radiation pressure contribution to the acceleration dynamics. 2D PIC simulations are also presented, which demonstrate a strong relativistic self-focusing and channelling of the pulse inside the target, enhancing proton energies via the hole boring mechanism.

Contact: P. Martin (p.martin@qub.ac.uk)

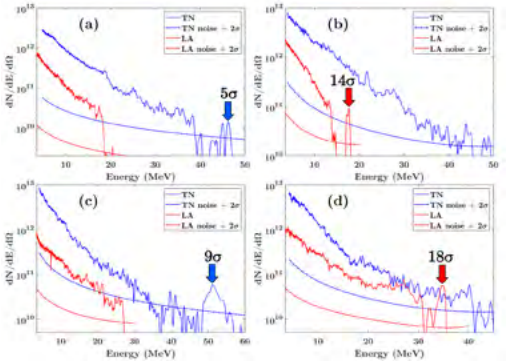

Proton spectra and the detection threshold taken along the target normal (TN) and laser axis (LA) TPS for solid hydrogen targets of (a) 75 µm and (b,c,d) 100 µm thickness. Quasi-monoenergetic bunches at high energy are indicated by the arrows, seen along target normal in (a) and (c), and laser axis in (b) and (d). The statistical heights of each peak above the noise level are displayed on the plots.

Laser science and development

Stable high-energy, high-repetition-rate, frequency doubling in a large aperture temperature-controlled LBO at 515 nm

J.P. Phillips, S. Banerjee, K. Ertel, P. Mason. J. Smith, T. Butcher, M. De Vido. C. Edwards, C. Hernadez-Gomez, J. Collier *(Central Laser Facility, STFC Rutherford Appleton Laboratory, Harwell Campus, Didcot, UK)*

We report on frequency doubling of high-energy, high-repetition-rate ns pulses from a cryogenically gas cooled, multi-slab Yb:YAG laser system, using a type-I phase-matched lithium triborate (LBO) crystal. Pulse energy of 4.3 J was extracted at 515 nm for a fundamental input of 5.4 J at 10 Hz (54 W), corresponding to a conversion efficiency of 77%. However, during long-term operation, a significant reduction of efficiency (more than 25%) was observed owing to the phase mismatch arising due to the temperature-dependent refractive index change in the crystal. This forced frequent angle tuning of the crystal to recover the second-harmonic generation (SHG) energy.

More than a five-fold improvement in energy stability of SHG was observed when the LBO crystal was mounted in an oven, and its temperature was controlled at 27°C. Stable frequency doubling with 0.8% rms energy variation was achieved at a higher input power of 74 W when the LBO temperature was controlled at 50°C.

Reproduced from Phillips, Jonathan P. et al., Stable high-energy, high-repetition-rate, frequency doubling in a large aperture temperature-controlled LBO at 515 nm, Opt. Lett. 45, 2946-2949 (2020) ©2020 Optical Society of America, under the terms of the OSA Open Publishing Agreement. doi:10.1364/OL.383129

Contact: J. Phillips (jonathan.phillips@stfc.ac.uk)

Photographs of LBO crystal oven components. The photo on the left shows the spring-loaded metallic crystal holder with the crystal in place. This is placed inside the oven unit (the photo on the right). The oven is then connected to a separate temperature control unit.

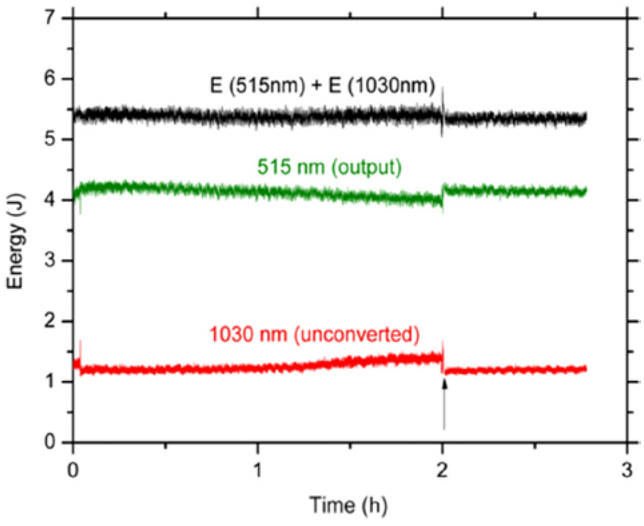

Long-term energy stability of type-I SHG in LBO in an oven set to 27°C using a 1 cm² beam. Total input energy of 5.4 J (black line) and average power of 54 W, 515 nm energy 4.1 J (green line) and unconverted fundamental energy 1.1 J (red line).

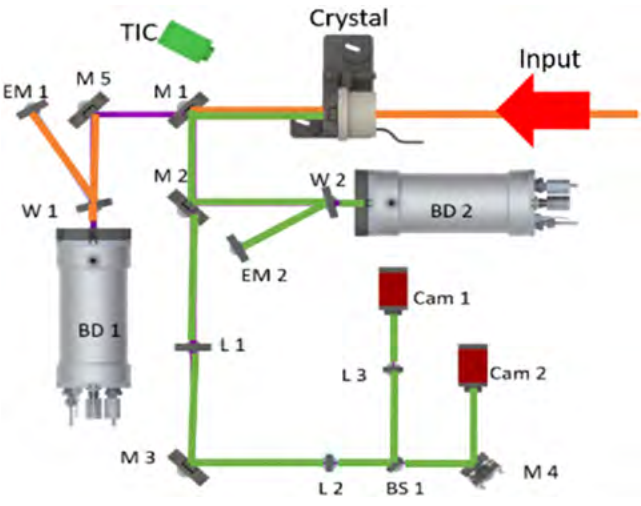

Schematic of the experimental setup used for frequency doubling energy stability experiments.

Pushing the boundaries of diode-pumped solid-state lasers for high-energy applications

S. Banerjee, P.D. Mason, P.J. Phillips, J.M. Smith, T.J. Butcher, J.L. Spear, M. De Vido, D. Clarke, K.G. Ertel, C. Hernandez-Gomez, C.B. Edwards, J.L. Collier *(Central Laser Facility, STFC Rutherford Appleton Laboratory, Harwell Campus, Didcot, UK)*

G. Quinn *(School of Engineering and Physical Sciences, Heriot-Watt University, Edinburgh, UK)*

We report on the successful demonstration of a 150 J nanosecond pulsed cryogenic gas cooled, diode pumped multi-slab Yb:YAG laser operating at 1 Hz. To the best of our knowledge, this is the highest energy ever recorded for a diode-pumped laser system.

Contact: S. Banerjee (saumyabrata.banerjee@stfc.ac.uk)

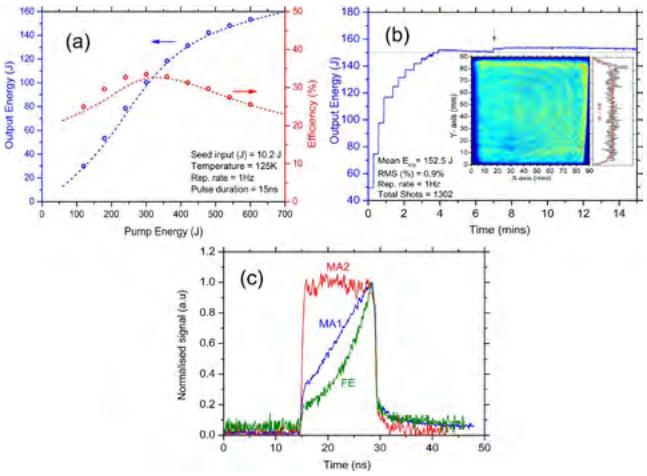

Right: a) Output energetics, experimentally measured (circle) and numerically calculated (dotted lines); (b) long-term operation at 150 J, 1 Hz, and the inset shows the near-field profile at 150 J, 1 Hz operation; (c) temporal profile of the front end (FE), main-amplifier 1 (MA1) and main-amplifier 2 (MA2) during 150 J, 1 Hz operation.

Figure reproduced from Banerjee, S. et al. Pushing the boundaries of diode-pumped solid-state lasers for high-energy applications. High Power Laser Science and Engineering, 8, E20, under the terms of the Creative Commons Attribution 4.0 International License. doi:10.1017/hpl.2020.20

High-resolution absorption measurement at the zero phonon line of Yb:YAG between 80K and 300K

M. De Vido *(Central Laser Facility, STFC Rutherford Appleton Laboratory, Harwell Campus, Didcot, UK; Institute of Photonics and Quantum sciences, Heriot-Watt University, Edinburgh, UK)*

A. Wojtusiak *(Loughborough University, UK; Central Laser Facility, STFC Rutherford Appleton Laboratory, Harwell Campus, Didcot, UK)*
K.G. Ertel *(Central Laser Facility, STFC Rutherford Appleton Laboratory, Harwell Campus, Didcot, UK)*

We present measurements of the temperature dependence of the absorption cross-section of Yb:YAG at the zero phonon line (ZPL) near 969 nm. Experiments were carried out on a 1.08 mm thick, ceramic, 1.1 at-% Yb-doped YAG sample over a temperature range between 80 K and 300 K. Results show that the ZPL characteristics strongly depend on temperature. The absorption cross-section increases from 0.8 x 10^{-20} cm^2 to above 49 x 10^{-20} cm^2 as temperature is decreased from 300 K to 80 K. The full-width at half maximum of the absorption line decreases with temperature, from 2.38 nm at 300 K to 0.05 nm at 80 K. The absorption peak shifts from 969.04 nm at 300 K to 968.39 nm at 80 K. To the best of our knowledge, this is the first time that the ZPL of Yb:YAG has been characterised with enough resolution at cryogenic temperatures and we expect that this data will assist in the design and optimisation of Yb:YAG lasers pumped on this absorption line.

Reproduced from M. De Vido, A. Wojtusiak, and K. Ertel, High-resolution absorption measurement at the zero phonon line of Yb:YAG between 80 K and 300 K, Opt. Mater. Express 10, 717-723 (2020), under the terms of the Creative Commons Attribution 4.0 International License. doi:10.1364/OME.386436

Contact: M. De Vido (mariastefania.de-vido@stfc.ac.uk)

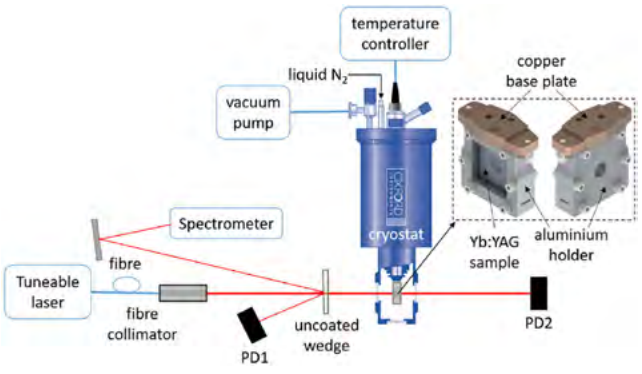

Experimental setup used to characterise absorption at the ZPL of Yb:YAG (PD1, PD2 = photo-detectors). The insert shows frontal and rear views of the holder in which the Yb:YAG sample is mounted.

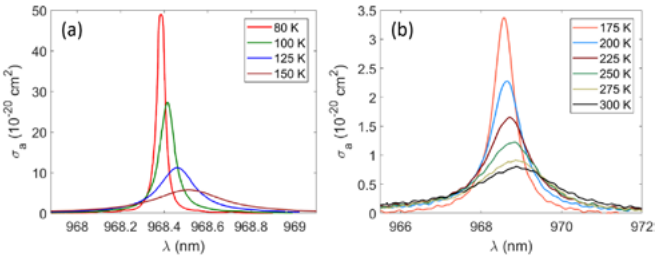

Absorption cross-section at the ZPL of Yb:YAG at temperatures between 80 K and 150 K (a) and between 175 K and 300 K (b).

Double rotating angled flanges for adjustable diagnostic pointing

B. Matthews *(Central Laser Facility, STFC Rutherford Appleton Laboratory, Harwell Campus, Didcot, UK)*

It is relatively common for diagnostics and optics on high-power laser experiments to need to be mounted onto the outside of the target chamber at an angle. This is generally achieved by manufacturing a custom angled flange to hold the device at the correct angle. This practice is extremely wasteful, however, as these flanges are usually large, difficult to store, and only usable by a particular diagnostic at a specific angle (preventing them from being reused). It also limits the ability for users to adjust and fine-tune their setup. A new design of flange is presented, comprising two counter-rotating 'wedges' that allow for the angle of orientation of an attached diagnostic or optic to be continuously varied within a range.

Contact: B. Matthews (barnaby.matthews@stfc.ac.uk)

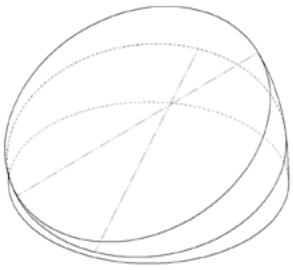

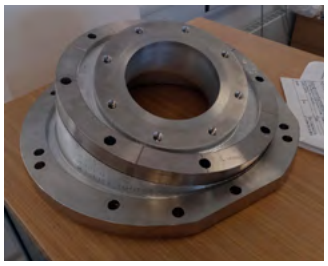

Left: Schematic diagram of the operating principle of a double-rotating flange.

Right: The manufactured low-profile double-rotating flange.

Software developments in Gemini

V.A. Marshall *(Central Laser Facility, STFC Rutherford Appleton Laboratory, Harwell Campus, Didcot, UK)*

Over the last year there have been significant updates to the Gemini facility metrology system. The system is now based on EPICS, following the trend of other control and diagnostic software in the CLF, and monitors nearly a hundred parameters of the Gemini beam and its environment. There have also been improvements connected to remote operation of the facility, namely an application to adjust timings on a critical Stanford delay box, improvements to the interface of the main Control System to allow the operator to move the Amp3 beam-dumps, plus the installation of a webcam to check that they are indeed in the expected position.

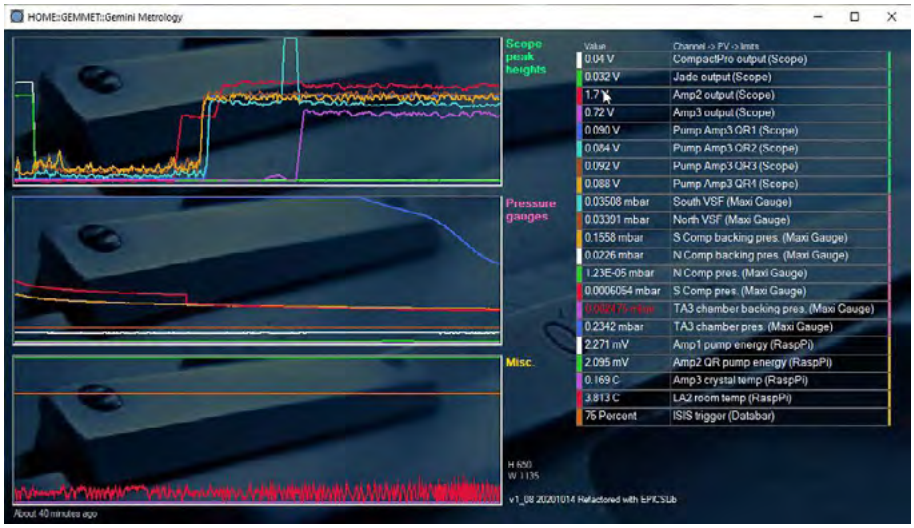

The Gemini Metrology application (formerly Mon&Cont). There was a spike on Amp3 output as the system was brought up, the TA3 Target Chamber is being pumped-down, and the ISIS trigger is holding steady.

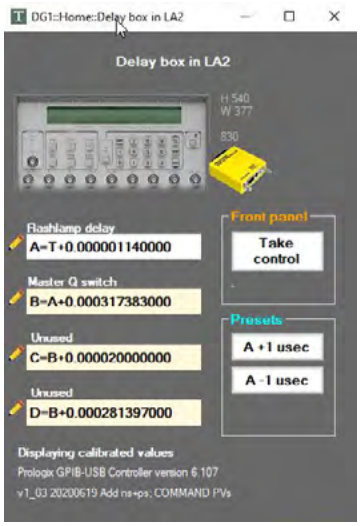

Screenshot of the DG535 control software showing the settings of the four channels (only two of which are in use), preset timing adjustment buttons, and physical control override button.

Contact: V.A. Marshall (victoria.marshall@stfc.ac.uk)

Installation of an independent probe beamline in Gemini TA3

M.M. Alderton *(Central Laser Facility, STFC Rutherford Appleton Laboratory, Harwell Campus, Didcot, UK; School of Physics, University of Bristol, UK)*
B.B. Boyde *(Department of Physics, Imperial College London, UK)*
N.C. Bourgeois, S.J.D. Dann, S.J. Hawkes, E. Raptodimos, D.R. Symes *(Central Laser Facility, STFC Rutherford Appleton Laboratory, Harwell Campus, Didcot, UK)*

A third beamline has been introduced to Gemini Target Area 3, to provide a short-pulse probe beam independently of the two main beams. The beam is derived from a leakage of the Gemini North beam after the fourth amplifier in LA3, and is compressed in the target area using a commercial compressor. This probe is designed to deliver up to 15 mJ in a pulse length < 50 fs with 25 mm beam diameter. Preliminary alignment of the probe compressor achieved a sub-100 fs duration that has been used for several user experiments.

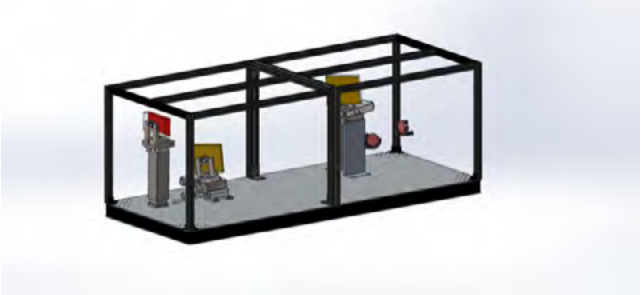

Design drawing of Crunch Technologies quadruple pass compressor installed in TA3 to provide a short-pulse independent probe beam.

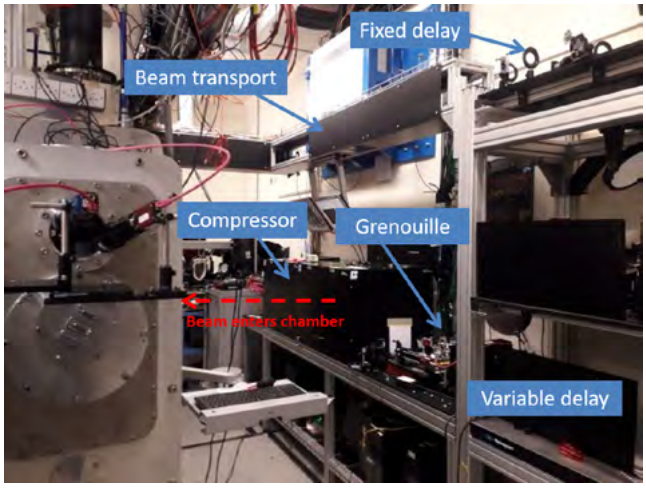

Photograph showing the location of the probe beam within Target Area 3. The beam is transported in an overhead gantry to fixed and variable delay lines. It passes through the compressor and is directed into the vacuum chamber from the East side.

Contact: D.R. Symes (dan.symes@stfc.ac.uk)

Replacement of the transmission grating in the Gemini pulse stretcher

C.J. Hooker, Y. Tang *(Central Laser Facility, STFC Rutherford Appleton Laboratory, Harwell Campus, Didcot, UK)*

Precision measurements of the surface profiles of diffraction gratings used in the pulse stretcher of the Gemini laser facility have been analysed. Detailed modelling showed that the surface roughness of a reflection grating, and refractive index non-uniformities in the substrate of a transmission grating, both introduced spectral phase noise into the pulse. This leads to a reduction of contrast ahead of the compressed pulse, known as the pedestal, which can potentially cause problems with experiments. The existing transmission grating was replaced in 2020 with a new grating, fabricated on a higher grade of fused silica with 5x lower inhomogeneity. Contrast scans of the compressed pulse following the change show a tenfold reduction in intensity of the pedestal near the main pulse. The pulse duration is also slightly shorter than before, which is believed to be due to greater uniformity in the grating groove structure resulting from improved fabrication techniques.

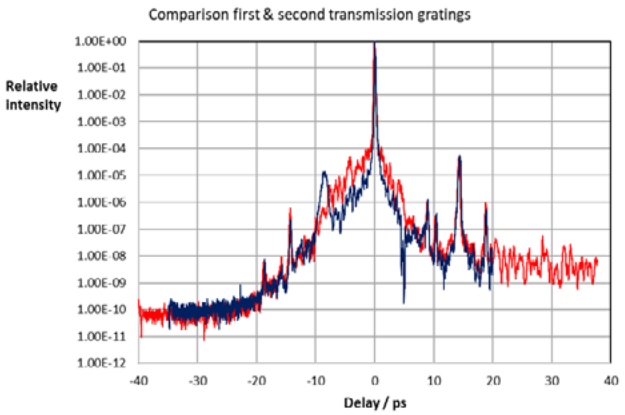

Comparison of Sequoia scans taken with the original transmission grating (red) and the new grating (blue). The level of the pedestal just before the main pulse is almost a factor of 10 lower with the new grating. The origin of the broad pre-pulse at -8.8 ps has not yet been identified.

Contact: C.J. Hooker (chris.hooker@stfc.ac.uk)

Redesign of Gemini double plasma mirror system

T.W.J. Dzelzainis, D. Treverrow, K. Fowell, B. Matthews, Y. Katzir, M. Alderton *(Central Laser Facility, STFC Rutherford Appleton Laboratory, Harwell Campus, Didcot, UK)*

Since the original plasma mirror system was installed in the Gemini target chamber in 2008, there have been many changes to the layout and modes of operation. The use of support frameworks and extension chambers now allows more efficient use of the space, which prompted a redesign of the plasma mirror system. The new layout is horizontal rather than vertical, and fits on a breadboard in a standard TA3 extension chamber. This allows more flexible use of alignment devices, and provides options for future upgrades. The parabolas are mounted on translation stages for focusing, with manual adjustment in the other axes. The plasma mirrors are mounted on a common vertical stage with separate horizontal stages to allow for rastering and independent selection of the spot sizes on each substrate. New debris shields have been designed with rotation and translation adjustments for accurate positioning, and kinematic mounts to allow easy replacement.

Contact: T.W.J. Dzelzainis (thomas.dzelzainis@stfc.ac.uk)

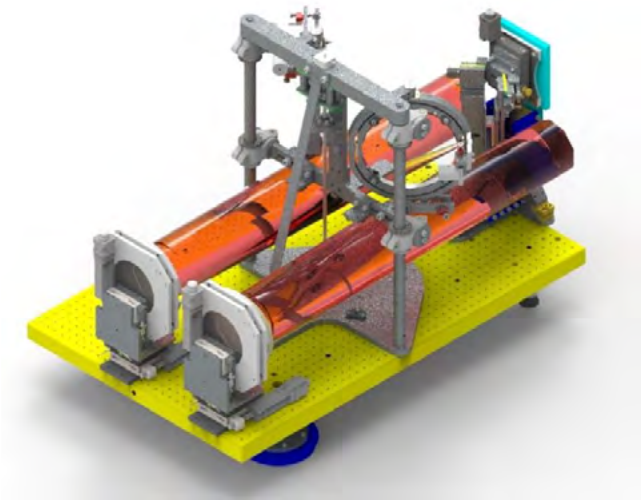

CAD render of the new Gemini plasma mirror system, shown mounted on a standard extension chamber breadboard.

Characterisation of duration-tuneable heavily-chirped pulses from the Gemini beamline using a streak camera

T. de Faria Pinto, M. Notley, S. Hawkes, R. Clarke *(Central Laser Facility, STFC Rutherford Appleton Laboratory, Harwell Campus, Didcot, UK)*

In this paper, we report on a recent experiment where a streak camera was used to characterise long pulses from the Gemini beamline, creating a calibration curve between pulse duration and grating position. Using this calibration, the experimental scientists could easily change the pulse duration in a reproducible way between 20 ps and 39 ps, using only automated translation stages, with minimal impact on compressor alignment.

We evaluated the lower limit of operation of the streak camera by measuring a compressed 45 fs pulse, which was measured as having a duration of 7.2 ps. While a more thorough characterisation is needed for the streak camera to be used accurately for pulses of similar duration, this value can be used as an indicator for the suitability of this diagnostic for future experiments.

The timing jitter of the trigger signal was measured to be 165 ps over a period of 12 minutes.

Contact: T. de Faria Pinto (tiago.pinto@stfc.ac.uk)

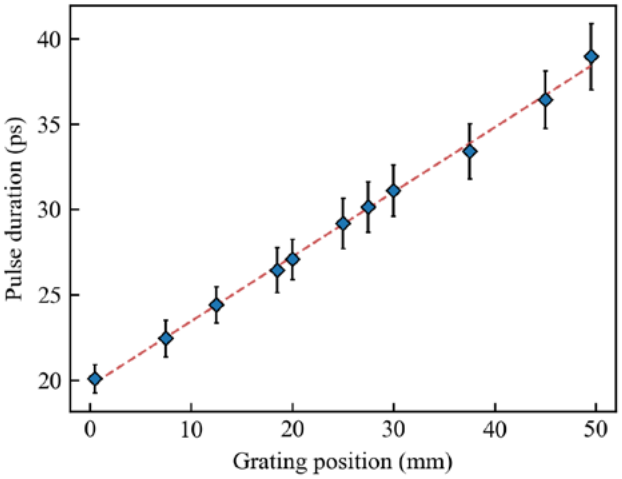

Pulse duration calibration curve, ranging from 20 ps to 38.9 ps, used by the experimental scientists to set a desired pulse duration using the G2 automated stage position.

Upgrading the kHz pump laser for the Gemini front-end

Y. Tang, T. de Faria Pinto, S. Hawkes *(Central Laser Facility, STFC Rutherford Appleton Laboratory, Harwell Campus, Didcot, UK)*

After many years of operation, the kHz Jade 2 pump laser in the front end of the Gemini facility has been replaced with a modern Ascend 40 laser. The Ascend is an industrial diode-pumped solid-state Q-switched laser manufactured by Spectra-Physics, which can deliver more than 25 W of average output power at a wavelength of 527 nm and a repetition rate of 1 kHz. The kHz pre-amplifier was also given a full service and re-optimised. The average output of the amplifier increased by a factor of 2.2x, the shot-to-shot stability was greatly improved and a high-amplitude slow drift with a period of ~200 s is no longer present. Overall, the RMS stability of the system improved from 19 % to 0.9%. This has led to a reduction in pump power required for the early amplifiers, and better stability throughout the amplifier chain.

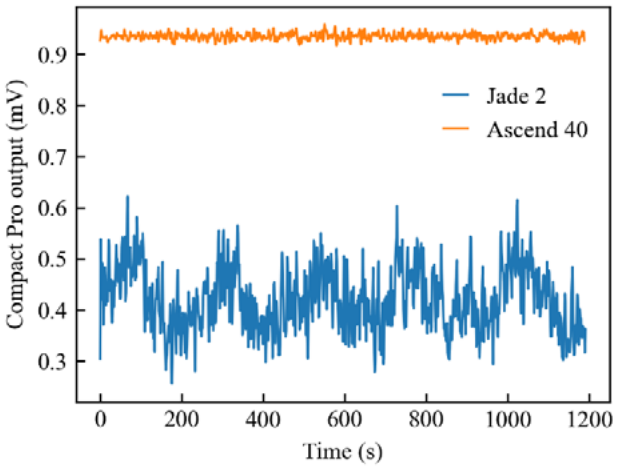

Stability measurement of the FemtoPower Compact Pro output before (blue) and after (orange) the pump laser upgrade and system maintenance.

Contact: Y. Tang (yunxin.tang@stfc.ac.uk)

Development of low-density sine wave targets for high-power laser experiments

P. Ariyathilaka *(Scitech Precision Ltd, STFC Rutherford Appleton Laboratory, Harwell Campus, Didcot, UK)*

C. Spindloe, A. Hughes *(Central Laser Facility, STFC Rutherford Appleton Laboratory, Harwell Campus, Didcot, UK)*

Methods are described for the production of a low-density foam target incorporating a sine-wave textured, brominated plastic disk. The targets were used in high power laser experiments to study Rayleigh-Taylor instabilities. Modifications to production processes giving target quality improvements are discussed.

Contact: P. Ariyathilaka (pawala.ariyathilaka@scitechprecision.com)

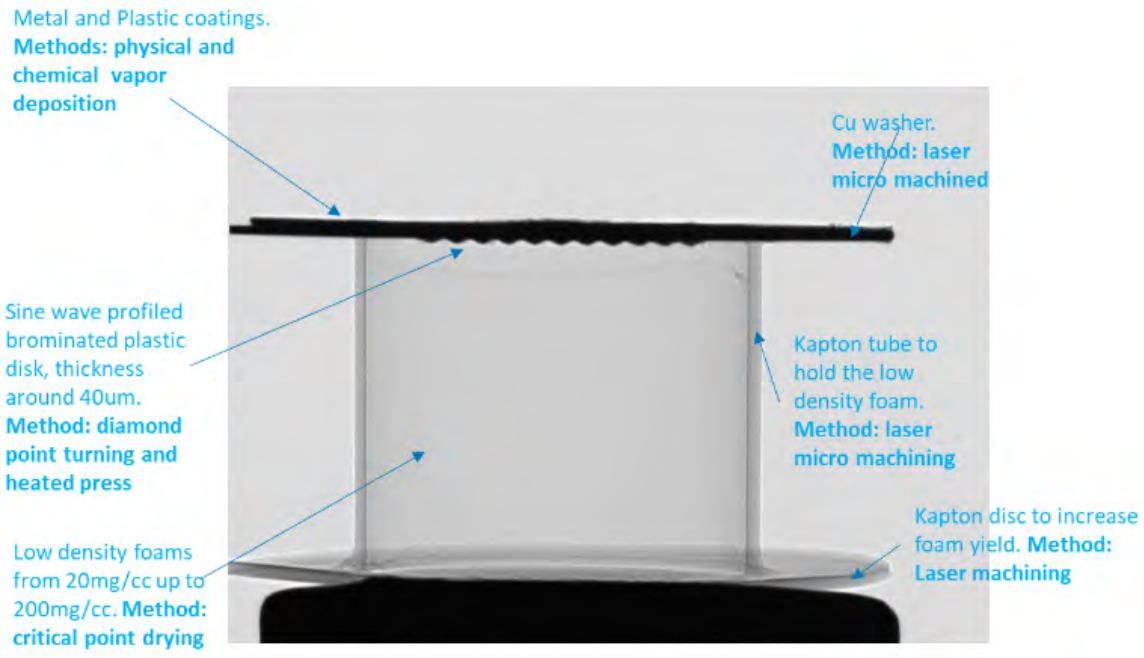

Computer tomography (CT) image of sine-wave target showing major components.

Super-resolution cryogenic correlative light and electron microscopy reveals protein organisation in the context of intact cellular ultrastructure

L. Wang, B. Bateman, L.C. Zanettti-Domingues, M.L. Martin-Fernandez *(Central Laser Facility, STFC Rutherford Appleton Laboratory, Harwell Campus, Didcot, UK)*

To understand how cells work, we need elucidate how proteins interact inside cellular ultrastructure. Super-resolution microscopy, e.g. stochastic optical reconstruction microscopy (STORM), underpins our understanding of interacting molecular networks in cells at the resolution of dozens of nanometres. However, to ascertain protein structure and function relationship, cryogenic correlative light and electron microscopy (cryo-CLEM) is highly sought after because it combines the functional information from molecular tagging in light microscopy with the intact ultrastructure information in electron microscopy. The challenge is the discrepancy in resolving power and imaging volume between cryo-EM and conventional cryo-FM. To address this challenge, we developed cryogenic STORM (cryo-STORM) to achieve sub-10 nm localization precision, and 3D Double Helix STORM with extended imaging volume to a few microns in a single shot. We are developing super-resolution cryo-CLEM workflow, aiming at unravelling the structure-function relationship of proteins and their partners throughout the cells with unprecedented precision.

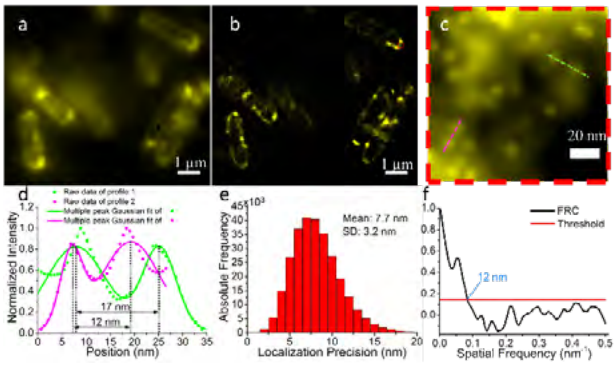

Cryo-STORM of Escherichia coli cells. (a) Wide-field and (b) STORM image of a field of cells. (c) The enlarged image of the region of the cell indicated by the red dashed border box in (b). (d) Line profiles of the cross-section of two adjacent single molecules. (e) Localization precision histogram. (f) FRC curve.

Contact: L. Wang (lin.wang@stfc.ac.uk)

Improving signal to noise ratios for transient absorption spectroscopy using an alternative referencing method

A. Edmeades, G.M. Greetham, M. Towrie, P.M. Donaldson *(Central Laser Facility,STFC Rutherford Appleton Laboratory, Harwell Campus, Didcot, UK)*

Improvements to signal-to-noise ratios in transient spectroscopies have been enabled by recently published schemes for better calculation of laser noise from reference measurements. In this article we describe the principles of these schemes and show them implemented on the CLF-Ultra transient spectrometers.

Contact: P.M. Donaldson (paul.donaldson@stfc.ac.uk)

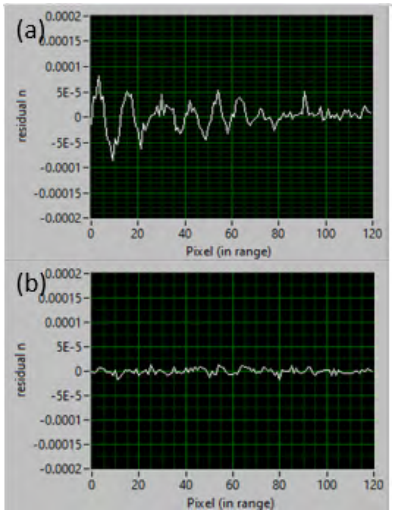

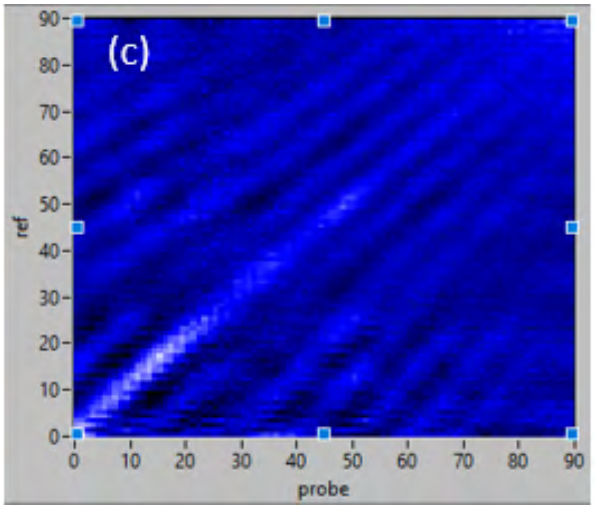

Pump on–off difference spectrum dispersed across 120 pixels of a Si photodiode array from a spectrally unstable WLC probe, referenced. (a) conventional referencing; (b) spectrum from same data as (a), but with B correlation referencing applied; (c) the correlation matrix.

Synchronised sample movement and pump laser timing in Time Resolved Multiple Probe Spectroscopy (TRMPS)

P.M. Donaldson, G.M. Greetham, M. Towrie *(Central Laser Facility, STFC Rutherford Appleton Laboratory, Harwell Campus, Didcot, UK)*

R.L. Owen *(Diamond Light Source Ltd, Harwell Science and Innovation Campus, Didcot, UK)*

Transient absorption spectroscopy often requires the sample studied to be moved in the laser beams to ensure measurement of a pristine sample. This is typically done unsynchronised to the measurement lasers, which convolutes the motion of the sample into the measured data and adds noise. Here we explore a rapid sample translation scheme which can be triggered from the lasers and demonstrate its operation in a transient infrared setup.

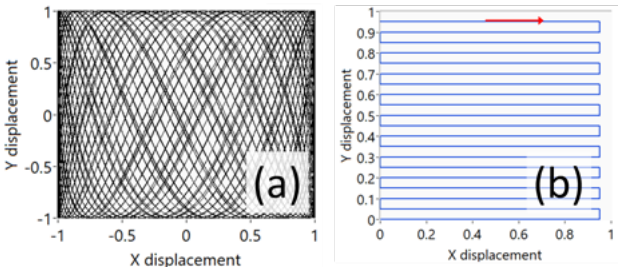

Position of a focussed laser spot in a moving sample for (a) 'Lissajous'-type sample motion and (b) 'Serpentine' motion.

Contact: P.M. Donaldson (paul.donaldson@stfc.ac.uk)

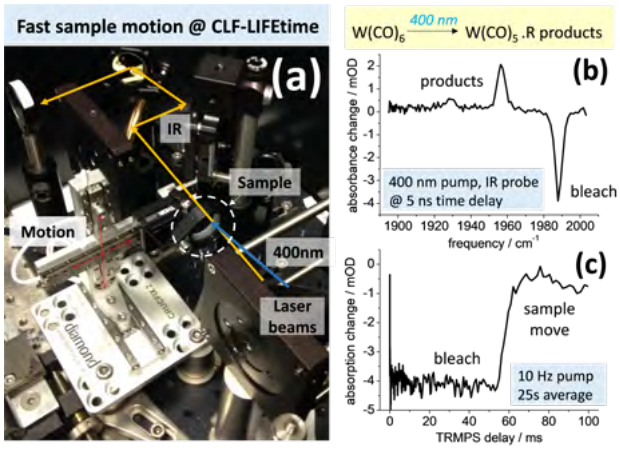

TRMPS-IR spectroscopy on a sample moving in synchronisation with the pump laser (a). The sample is $W(CO)_6$ in heptane. The effect of its permanent bleaching by a 400 nm laser pulse is clear in the transient infrared spectrum (b). Tracking the absorption change of the bleach (c), 50 ms after the photoproducts are created, the sample is moved 100 µm, exposing fresh sample for the next laser shot. (c) is an average of 250 pump laser / move events.

Development of a single-shot third-order cross-correlator for Vulcan

A.C. Aitken, P. Oliveira, L.E. Bradley, E. Dilworth, M. Galetti, B. Parry, M. Galimberti, I.O. Musgrave *(Central Laser Facility, STFC Rutherford Appleton Laboratory, Harwell Campus, Didcot, UK)*

In this paper we present the development of a near-field single-shot third-order cross-correlator (TOCC). We present measurements of sub-ps pulses at λ = 1055:5 nm demonstrating the device has a temporal window of ΔT = 36:4 ps and a resolution of δt = 91 fs. We also discuss the spectral acceptance and the minimum required operational conditions.

Contact: P. Oliveira (pedro.oliveira@stfc.ac.uk)

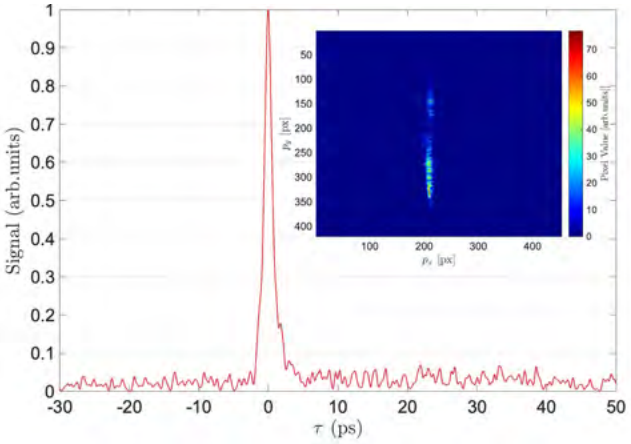

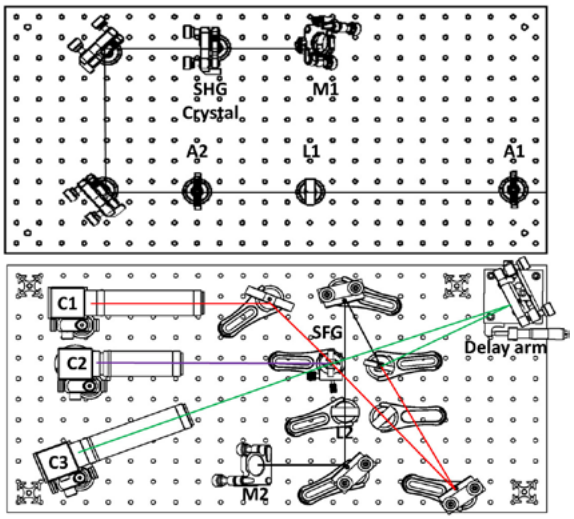

Above Schematic showing a top-down view of the upper (top) and lower (bottom) decks of the single-shot TOCC

Left: TOCC profile of the pulse retrieved through the lineout of the trace image. The signal in arbitrary units, normalised to the maximum value, is plotted against time in picoseconds from the point of maximum signal. (Inset) Single-shot measurement of the 2 Hz ns OPCPA

Comparing temporal contrast measurements taken in the Vulcan front-end and target area petawatt

L.E. Bradley, A.C. Aiken, P. Oliveira, M. Galimberti, I.O. Musgrave *(Central Laser Facility, STFC Rutherford Appleton Laboratory, Harwell Campus, Didcot, UK)*

Producing high-intensity laser pulses with a high temporal contrast is essential to establishing the mechanisms that drive particle acceleration at petawatt class laser facilities. Here we present measurements taken in both the Vulcan front-end and target area petawatt (TAP) using a third-order cross-correlator giving a contrast of 10^{10}. Comparing these measurements with an historical scan demonstrates that changes to the front-end can have a significant effect for the pre-pulses arriving in TAP.

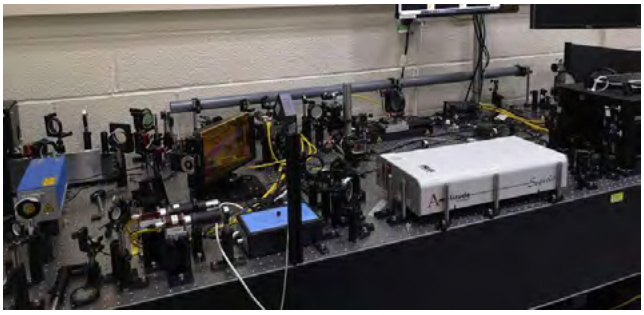

Setup showing the third-order cross-correlator in TAP.

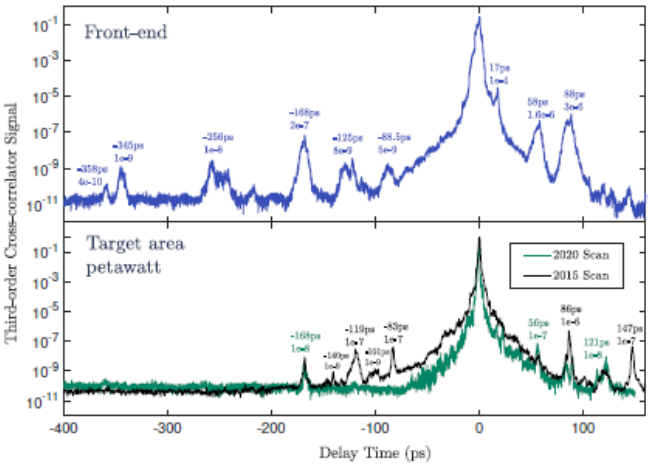

Third-order cross-correlator measurements from the Vulcan front-end and TAP compared with an historical 2015 scan. A single pre-pulse is left at time -168 ps at 10^{-8} in the target area after changing various optics in the front-end.

Contact: L.E. Bradley (laurence.bradley@stfc.ac.uk)

Progress on improving stability of the short picosecond pulse by fast stabilisation in Vulcan

L.E. Bradley, M. Galimberti, A. Kidd, P. Oliveira, A. Aiken, C. Suciu, J. Patel, I.O. Musgrave *(Central Laser Facility, STFC Rutherford Appleton Laboratory, Harwell Campus, Didcot, UK)*

Energy stability of the short picosecond CPA pulse in Vulcan can vary over time. This creates operationally dynamic conditions, as the energies between shots can deviate from user requested energies. We present progress in stabilising the beams near-field, while identifying future interventions to improve stability.

Contact: L.E. Bradley (laurence.bradley@stfc.ac.uk)

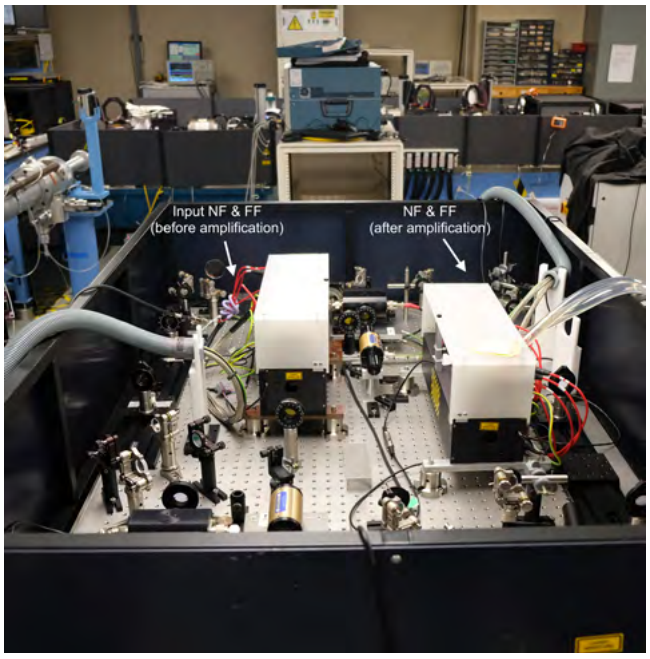

Right: Near-field and far-field diagnostics installed before and after the short pulse is amplified through the two double pass 9 mm amplifiers

Facility upgrades for Artemis in new laboratory

C. E. Sanders, A. S. Wyatt, R. T. Chapman, G. Karras, Y. Zhang, G. G. Greetham, A. Cox, P. Rice, D. Rose, S. Spurdle, P. Brummitt, L. Benson, J. Suarez, R. Sarasola, I. Shaw, M. Dominey, R. Bickerton, N. Crook, P. Amos, M. Towrie, and E. Springate
(*Central Laser Facility, Research Complex at Harwell, STFC Rutherford Appleton Laboratory, Harwell Campus, Didcot, UK)*

Contact: emma.springate@stfc.ac.uk

Introduction

The Artemis lab has been relocated to the Research Complex at Harwell since 2018, when it was moved across campus (from its old location in building R7) and reassembled with new beamlines and a new vacuum system[1]. In 2019-20, the lab made numerous planned upgrades to its experimental capabilities, including the installation of a new 100 kHz laser system.

New 100-kHz laser

In autumn 2019, Artemis received its new 100 kHz laser system – a customised system from the FastLite company in France. This new laser, based on optical parametric chirped pulse amplification of output from a Yb:YAG thin-disc pump, represents a major improvement in repetition rate over Artemis's older, 1 kHz laser system. The laser was installed (Figure 1) on a new beamline that is being built for the material science programme. This will ultimately support beamtimes for pump-probe photoemission spectroscopy with improved signal-to-noise characteristics, and will also be the basis for new capabilities in pump-probe transient absorption spectroscopy. The beamline will generate short pulses in the tens-of-fs regime, with photon energies of tens of eV via high harmonic generation (HHG). It remains under construction, with plans for commissioning in the upcoming year.

Figure 1: Artemis's new 100 kHz laser system on the table in the new lab.

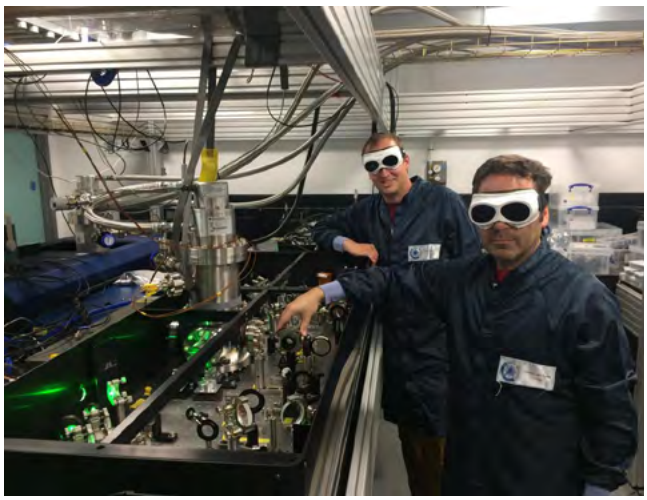

Figure 2: Laser engineer Ben Langdon of Crunch Technologies and Artemis staff member Richard Chapman, aligning the upgraded 1 kHz Ti:sapp laser system in the new laboratory

Upgrades to 1-kHz laser

The 1 kHz KLM Labs 'Red Dragon' titanium-sapphire (Ti:sapp) laser system that has served Artemis since 2008 has received upgrades from Crunch Technologies, USA. These include new Pockels cells, stretcher and compressor upgrades, and a third amplifier. The laser and beamline are now installed in the new lab (Figure 2). With these upgrades, along with upgrades to the beamline, users will be able to see intensity improvements in HHG. The Artemis access panel met to evaluate the first round of proposals on this system in November 2019.

New lab layout improves user experience

The layout of the new lab will allow improvements to the user experience. Four independent beamlines will now support user experiments in imaging, infrared spectroscopy, and photoemission from the gas and solid states on the basis of short pulses by HHG (Figures 3 and 4). The two laser systems are sequestered in a temperature- and humidity-controlled laser room, while the experimental stations are housed in the neighbouring room. Furthermore, a plant room (Figure 5) now segregates compressors and mechanical pumps from the lab, so as to reduce noise and vibrations in the measurement area.

Engineering upgrades

A new laser interlock system has been designed and installed, offering better trouble-shooting capability and upgraded logic. This will minimise disruption to the lasers when the interlock system is tripped. The engineering and mechanical sections, working in close collaboration with each other, also designed and installed a new vacuum control system for the HHG beamlines. With this, Artemis

Figure 3: User area in the new laboratory. The beamline closest to the camera is the flat-field imaging beamline; the beamline behind it is for photoemission spectroscopy from the gas phase (see the chamber on a blue table-frame, docked at the beamline's end). At the back of the lab, behind the partition, are beamlines for solid-state photoemission (the material science chamber is just visible at left) and – not visible here – a beamline for infrared spectroscopy.

Figure 4: Another view of the lab. A partition, at centre, allows the lab to be divided into two separate rooms. The beamline at left is the solid-state photoemission beamline, under construction. Just to the right of the partition is the beamline for photoemission from the gas phase. At far right is the flat-field imaging beamline.

can reduce the number of vacuum pumps it needs to use, along with energy usage and noise levels.

Current status

User operations have now been restarted on the 1 kHz beamline, which has been recommissioned with ten times higher HHG flux than in the old lab. The 100 kHz beamline is undergoing further assembly, and laser commissioning is in progress. More details of the current status are posted on the Artemis section of the CLF website[2].

Conclusions

The Artemis programme is installed in its new lab in the Research Complex at Harwell, and has executed major upgrades to its laser capabilities. With a new laser, upgrades to the existing laser, new beamlines, and a new lab layout, users can expect major improvements in measurement capabilities and in the user experience.

References

1. www.clf.stfc.ac.uk/Pages/Annual-Report-2018-19.aspx
2. www.clf.stfc.ac.uk/Pages/Artemis.aspx

Figure 5: Pumps and compressors are now housed in a separate plant room that opens out onto the back of the building. By segregating these from the experimental stations, we achieve major improvements in noise, and we free up space in the lab.

Plasma diagnostics

A characterisation of the Figaro electromagnet electron spectrometer

I. Gerenstein *(Department of Physics, Loughborough University, UK)*

D.C. Carroll *(Central Laser Facility, STFC Rutherford Appleton Laboratory, Harwell Campus, Didcot, UK)*

The aim of this project is to characterize the magnetic field of the CLF Figaro electromagnet electron spectrometer. A Hall probe is used to map the magnetic field and how it varies spatially and temporally. The relationship between the power supply current and magnetic field was deduced, and resistive heating effects were investigated including an on-off cycle typical for a sequence of Vulcan laser shots. The magnetic field produced varies with current by the following equation: B = 281.3I +3.5, where B is the magnetic field strength in mT and I is the current in A. The optimum current range to minimise decline in current due to resistive heating is between 0A and up to 2A.

Contact: I. Gerenstein (i.gerenstein-17@student.lboro.ac.uk)

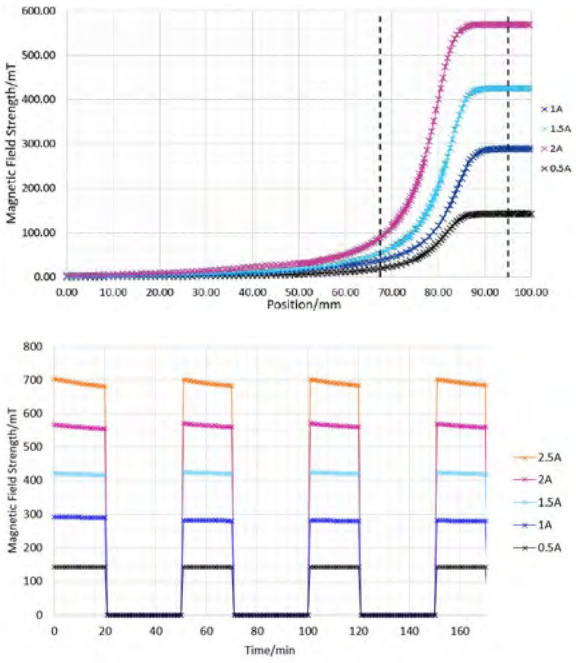

Top right: Spatial measurements of the magnetic field of the spectrometer. The dashed lines represent the edge (left) and the centre (right) of the electromagnet.

Bottom right: Repeat on-off measurements of magnetic field strength with time for different electromagnet currents.

Compact scintillator – silicon photomultiplier hard X-ray detectors for laser-plasma diagnosis

J. K. Patel *(Loughborough University, UK)*

D. Neely, C.D. Armstrong, R.J. Clarke, K. Fowell, I. Symonds *(Central Laser Facility, STFC Rutherford Appleton Laboratory, Harwell Campus, Didcot, UK)*

Decaying emission of 511 keV annihilation X-rays from materials activated by >3 MeV photons can be used to diagnose laser-plasma interactions. Low-voltage operable silicon-photomultipliers (SiPM) coupled to scintillators are a favourable alternative to large, high voltage photomultiplier tube (PMT) detectors for measuring low photon numbers.

To optimise the design, the performance of scintillators of varying size is explored, and a simple model is presented which achieves good agreement with the spectra obtained from bismuth germanate (BGO) - SiPM detector combinations tested.

Contact: C.D. Armstrong (chris.armstrong@stfc.ac.uk)

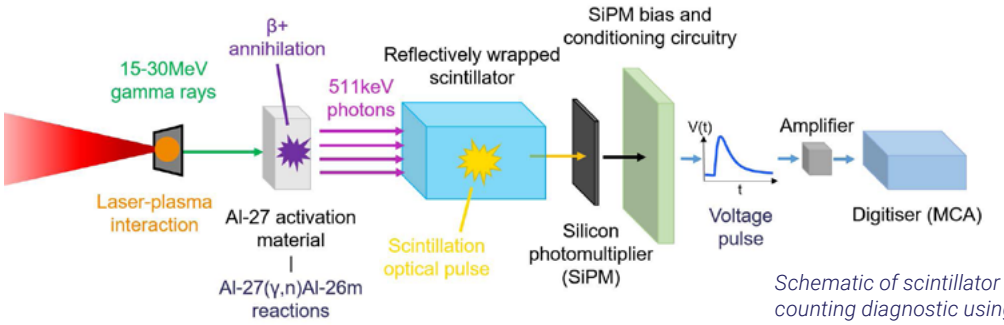

Schematic of scintillator - SiPM detector for gamma counting diagnostic using activation of ^{27}Al.

Assessing collection efficiency for a scintillator-based high repetition radiography detector

J.K. Patel *(Loughborough University, Loughborough, UK)*

C.D. Armstrong, D. Neely *(Central Laser Facility, STFC Rutherford Appleton Laboratory, Harwell Campus, Didcot, UK)*

Next generation high repetition laser driven sources offer advancements for industrial and medical radiography applications, including techniques like Computed Tomography (CT) which requires 100s to 1000s of images. Optical imaging of slab or pixelated scintillators offers a solution for a high repetition detector to pair with these sources. To this end, analytical models for the collection efficiency of camera and lens systems at high and low magnification, have been developed.

Application of the models predicts the sensitivity and dynamic range of several proposed configurations with respect to X-ray deposition. As a result, the suitability of a detector specification with a source of given flux and spectral shape can be assessed. In addition, it is shown that pixelated scintillator arrays are better suited to a set up with high geometrical magnification, where the detector plane is at a significant distance from a sample object and a point-like source. A figure of merit has also been established to compare potential X-ray scintillator candidates based on the relevant properties; light yield, density, and refractive index.

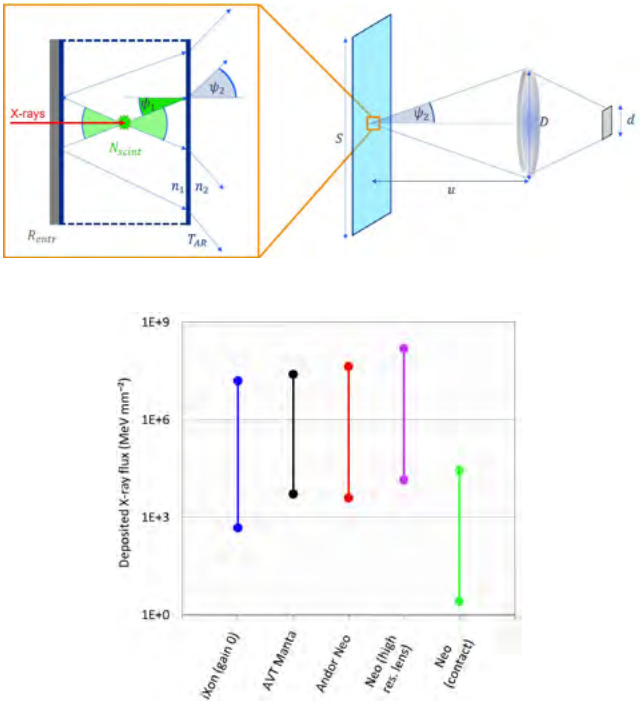

Contact: C.D. Armstrong (chris.armstrong@stfc.ac.uk)

Top: Scintillator imaging diagram on the right-hand side illustrating geometry of lens collection, and blown up cross section of modelled isotropic scintillation event, with relevant angles for calculating lens collection efficiency based on Snell's law and solid angles. Reflected rear cone and refractive indices of the scintillator and air (or alternate immersion medium) are also shown.

Bottom: The model predicted dynamic ranges of various camera and lens or contact optical couplings of a slab LYSO scintillator detector. Given in deposited energy per scintillator area, the model can be used to predict the suitability of a given imaging system with a source of given flux and spectral shape.

Improving collimation of optical flux emission from scintillator crystals

J.K. Patel *(Loughborough University, UK)*

D. Neely, C.D. Armstrong, R.J. Clarke *(Central Laser Facility, STFC Rutherford Appleton Laboratory, Harwell Campus, Didcot, UK)*

A linear array of scintillator crystals can be used to characterise a hard X-ray spectrum. Reflective PTFE wrapping of individual crystals improves the incident signal onto a lens coupled detector. Increasing the collimation of scintillator emission will enable further improved yield in the angular range close to the normal to the front crystal face, for better quality electron temperature measurements on laser-plasma experiments.

Using the inherent phosphorescence of LYSO and scintillation from an X-ray source, an investigation of the impact that the surface finish and width of scintillator crystals has on the angular flux distribution, with and without PTFE wrapping, is reported here.

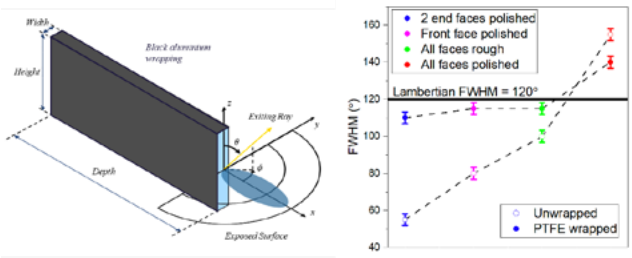

Contact: C.D. Armstrong (chris.armstrong@stfc.ac.uk)

Left: Crystal schematic showing the angle, between the normal to the exposed front face and the line to the centre of the camera sensor, which is varied. Anodised aluminium wrapping was used to prevent light transmitted from the other faces from falling on the sensor. Crystal depth and height dimensions used were 30 x 12 mm, and the widths were varied between 1, 2 and 5 mm.

Right: FWHM for each surface finish, with and without PTFE wrapping.

Accounting for spectral bandwidth broadening due to self-phase modulation in measurements of laser pulse transmission through a dense plasma

E.J. Dolier, R. Wilson, T. P. Frazer, J. Goodman, A. Lofrese, A. Horne, M. King, R.J. Gray, P. McKenna *(SUPA Department of Physics, University of Strathclyde, UK)*

T. Dzelzainis, D. Neely *(Central Laser Facility, STFC Rutherford Appleton Laboratory, Harwell Campus, Didcot UK)*

A method has been developed to characterise the fraction of laser energy transmitted through an initially over-dense plasma whilst accounting for broadening in the transmitted pulse spectrum. As such, this method accounts for the effect of self-phase modulation which may occur as an intense pulse propagates through beamline optics before being detected.

Contact: E.J. Dolier (ewan.dolier.2015@uni.strath.ac.uk)

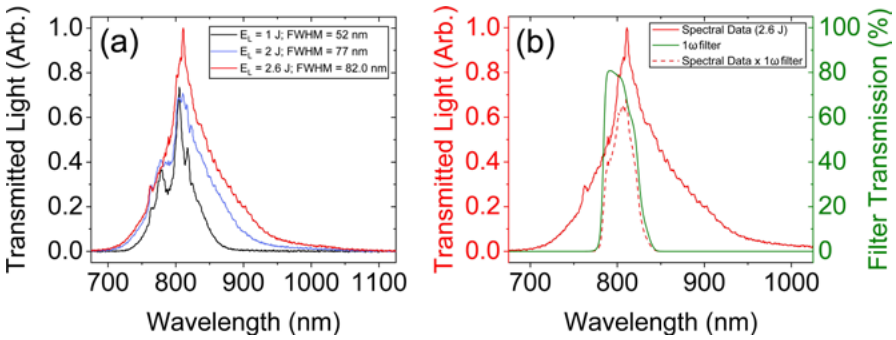

(a) Transmitted light spectra for several no target shots display increased bandwidth (FWHM) with increasing incident laser energy, suggesting SPM-induced broadening. (b) An example transmitted light spectrum (solid red) is shown for a no target shot, alongside the transmission curve of the $\Delta\lambda$ = 40 nm interference filter placed in front of the CCD camera (green). Spectral measurements were multiplied by this transmission curve (dashed red), indicating the proportion of transmitted light which has gone undetected by the filtered camera.

Absolute Cherenkov photon measurements via angular calibration of a fused silica scatter screen

J.K. Patel *(Loughborough University, UK)*
D. Neely, C.D. Armstrong, Y. Katzir, A. Dasgupta, D. Treverrow, S. Hawkes *(Central Laser Facility, STFC Rutherford Appleton Laboratory, Harwell Campus, Didcot, UK)*
E. Zemaityte, R. Gray, A. Horne, T. Frazier, P. McKenna *(University of Strathclyde, Glasgow, UK)*

S. Rozario, J. Wood, M. Backhouse *(Imperial College London, UK)*
R. Deas, H. Thomas, J. Wilkinson, S. Dorkings, R. Giordmaina, P. Dodd, J. May *(Defence Science and Technology Laboratory (Dstl), Fort Halstead, Kent, UK)*

Cherenkov radiation is the electromagnetic emission (typically of visible to ultraviolet wavelength) produced when a charged particle travels faster than the speed of light in a medium with refractive index >1. Cherenkov radiation can be used to diagnose the charge of high energy electron bunches, such as those produced in laser-plasma interactions, by placing a medium in the path of electrons. The expected light yield in photons can be derived from Cherenkov theory, which can be used to verify experimental results. Herein an absolute calibration of the scatter screen is carried out using cooled Andor NEO scientific linear CMOS cameras. The results and methods of such a calibration are reported here, for direct calibration of experimental Cherenkov measurements.

Contact: C.D. Armstrong (chris.armstrong@stfc.ac.uk)

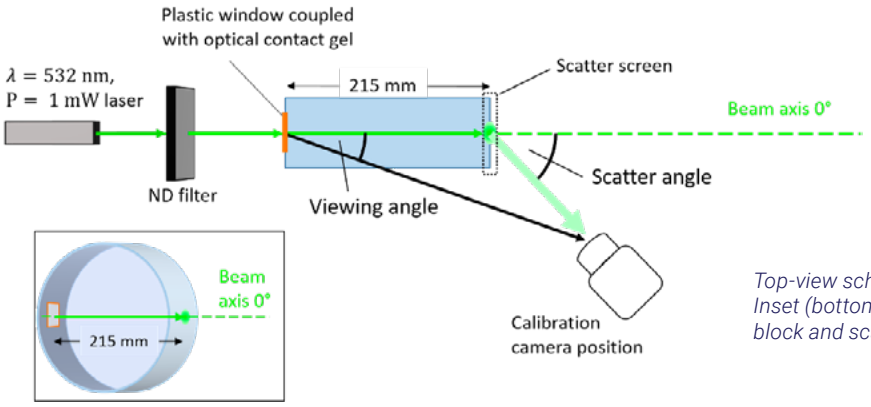

Top-view schematic of scatter screen calibration set up. Inset (bottom-left) is side-view illustration of fused silica block and scatter surface.

Imaging and dynamics for physical and life sciences

Multimodal imaging of autofluorescent sites reveals varied chemical speciation in zeolites for catalysis

N.E. Omori, I. Lezcano-Gonzalez, A.G. Greenaway, A.M. Beale *(Department of Chemistry, University College London, UK; Research Complex at Harwell, STFC Rutherford Appleton Laboratory, Harwell Campus, Didcot, UK)*
A. Candeo, S. Mosca *(Central Laser Facility, Research Complex at Harwell, STFC Rutherford Appleton Laboratory, Harwell Campus, Didcot, UK),*
I.K. Robinson *(London Centre for Nanotechnology, University College London, UK; Brookhaven National Laboratory, Upton, New York, USA)*
L. Li *(Advanced Photon Source, Argonne National Laboratory, Lemont, Illinois, USA)*
P. Collier (Johnson Matthey Technology Centre, Reading UK)

A multimodal imaging study of chabazite is used to show the distribution of and discriminate between different emissive deposits arising as a result of the detemplation process. 3D confocal imaging, fluorescence lifetime imaging, spectral imaging, and Raman mapping are used to show three different types of emissive behaviours each characterised by different spatial distributions, trends in lifetime, spectral signals, and Raman signatures. A notable difference is seen in the morphology of agglomerated surface deposits and larger subsurface deposits, which experience lifetime augmentation due to spatial confinement. The distribution of organic residue throughout the crystal volume is comparable to XRF mapping that shows Si enrichment on the outer edges and higher Al content through the centre, demonstrating that the technique can also be used to indirectly comment on the compositional chemistry of the inorganic framework.

Reproduced from Omori, N. et al. Multimodal Imaging of Autofluorescent Sites Reveals Varied Chemical Speciation in SSZ-13 Crystals. Angew. Chem. Int. Ed. 2021, 60, 5125 – 5131, © 2020 Wiley-VCH GmbH. doi:10.1002/anie.202015016

Contact: A.M. Beale (andrew.beale@ucl.ac.uk)

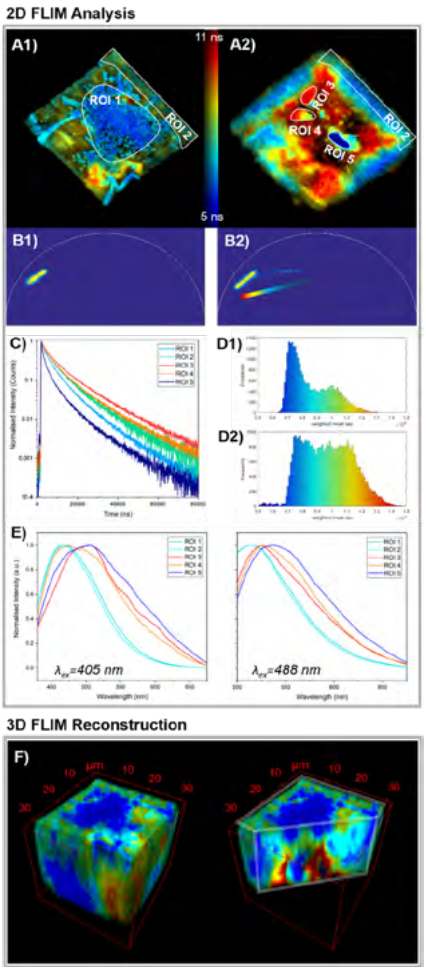

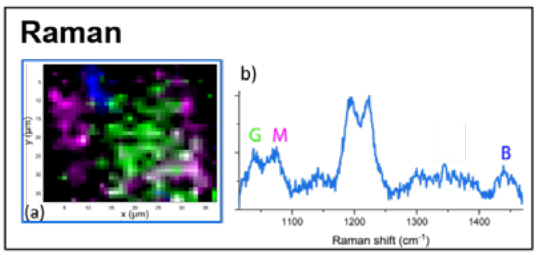

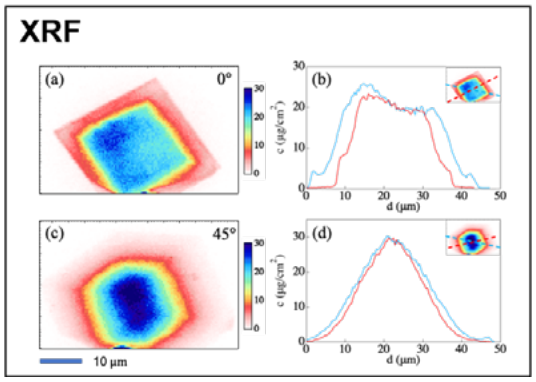

Left: FLIM ensemble of chabazite calcined at 550°C acquired at λ_{ex} = 488 nm including the A) map of weighted average lifetimes (1) for the uppermost plane and (2) for the central plane, B) phasor plots, C) fluorescence decays for selected ROIs, D) frequency histograms of lifetimes, and E) spectra for ROIs acquired at λ_{ex}= 405 nm and 488 nm.

Right: Raman maps showing the distribution of selected vibrations for chabazite calcined at 550°C (top) and XRF tomography of wet-ion exchanged Cu-SSZ-13 crystals obtained at the Argonne National Laboratory with 10 keV photons (bottom) where (a) & (c) are the projected Cu maps at 0º and 45º to the crystal and (b) & (d) are the respective line profiles.

Detection of drug-protein complexes in aqueous serum using two-dimensional infrared spectroscopy

S.H. Rutherford *(Department of Physics, University of Strathclyde, Glasgow, UK)*
G.M. Greetham, M. Towrie, A.W. Parker *(Central Laser Facility, STFC Rutherford Appleton Laboratory, Harwell Campus, Didcot, UK)*
M.J. Baker *(Department of Chemistry, University of Strathclyde, Glasgow, UK)*
N.T. Hunt *(Department of Chemistry, University of York, UK)*

This report demonstrates proof of concept for the use of 2D-IR spectroscopy to detect drug binding to the serum albumin protein in blood serum. 2D-IR spectroscopy of blood serum to which the common drug molecules paracetamol, ibuprofen and warfarin have been added showed characteristic changes in the amide I region due to binding of the drugs to serum albumin. These results will motivate further work to clarify limits of detection and to assign the structural origins of the changes observed definitively. The demonstrated ability to measure different protein structural responses due to binding of drugs at physiological concentrations, however, suggests that the 2D-IR method has the potential to be used for rapid screening of protein-drug combinations or for monitoring of serum concentrations of specific drugs.

Contact: N.T. Hunt (neil.hunt@york.ac.uk)

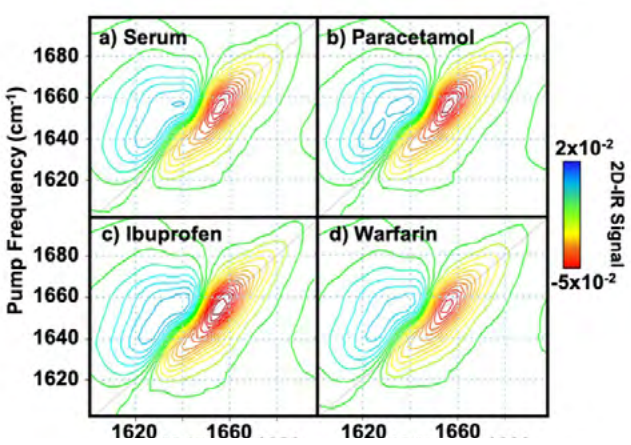

2D-IR spectra of a) serum, and serum spiked with b) paracetamol 2:1, c) ibuprofen 2:1 and d) warfarin 0.07:1. All spectra are plotted using the same scale, see colour bar.

Identification of a rare manganese dinitrogen complex

J.B. Eastwood, L.A. Hammarback, M.T. McRobie, I.J.S. Fairlamb, J.M. Lynam *(Department of Chemistry, University of York, UK)*
I.P. Clark, M. Towrie *(Central Laser Facility, STFC Rutherford Appleton Laboratory, Harwell Campus, Didcot, UK)*

A novel manganese dinitrogen complex has been identified by time-resolved infra-red spectroscopy. Light-induced loss of a carbonyl ligand from a stable precursor results in a highly reactive solvent complex. Displacement of the weakly held solvent then permits binding of N_2 to the manganese. The presence of the dinitrogen ligand was identified with the aid of isotopically enriched $^{15}N_2$ inducing the predicted shift in the MnN≡N vibrational mode. Kinetic simulations revealed the nature of competitive N_2 and H_2O binding to the metal and allowed for the rate constants for solvent substitution to be determined.

Contact: J.M. Lynam (jason.lynam@york.ac.uk)

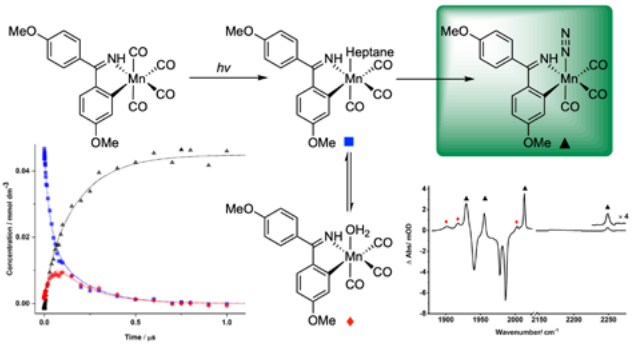

A new manganese-containing dinitrogen complex has been identified

Mapping photochemical cycles over femtosecond to millisecond timescales using transient absorption spectroscopy

L. Lewis-Borrell, M. Sneha, A. Bhattacherjee, A.J. Orr-Ewing *(School of Chemistry, University of Bristol, UK)*

Activation of chemical reactions using visible or ultraviolet light is a promising route to the sustainable synthesis of important compounds and materials such as pharmaceuticals or polymers. However, the mechanisms of such reactions follow complicated, multi-step pathways and the chemistry can be difficult to control. Systematic study of the short-lived reactive intermediates, their lifetimes, and their preferred reactions at each step along the reaction path using time-resolved infra-red spectroscopy offers new opportunities to understand and harness this light-activated chemistry.

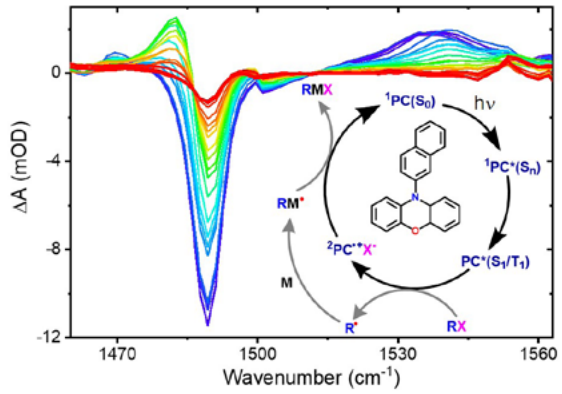

Time-resolved infra-red spectra of a UV-excited organic photocatalyst used to drive photoredox reaction cycles of the type shown.

Contact: A.J. Orr-Ewing (a.orr-ewing@bristol.ac.uk)

Understanding hydrogenases by ultrafast and 2D-IR spectroscopy: proof-of-concept, recent advances and future avenues

M. Horch *(Department of Physics, Freie Universität Berlin, Germany; Department of Chemistry & York Biomedical Research Institute, University of York, UK; Department of Chemistry, Technische Universität Berlin, Germany)*
N.T. Hunt, A. Parkin, B. Procacci, J. Walton, S.L.D. Wrathall *(Department of Chemistry & York Biomedical Research Institute, University of York, UK)*
G.M. Greetham *(Central Laser Facility, STFC Rutherford Appleton Laboratory, Harwell Campus, Didcot, UK)*
A. Al-Shameri, C.J. Kulka, L. Lauterbach, O. Lenz, C. Lorent, J. Schoknecht, C. Schulz, I. Zebger *(Department of Chemistry, Technische Universität Berlin, Germany)*
J.A. Birrell, W. Lubitz, E.J. Reijerse *(Max Planck Institute for Chemical Energy Conversion, Mülheim an der Ruhr, Germany)*
P. Rodríguez Maciá *(Department of Chemistry University of Oxford, UK; Max Planck Institute for Chemical Energy Conversion, Mülheim an der Ruhr, Germany)*

Utilizing active-site CO and CN^- ligands as vibrational reporter groups, the structure, function, and dynamics of hydrogen-transforming biocatalysts, so-called hydrogenases, have been investigated by ultrafast infrared (IR) pump-probe and two-dimensional (2D) IR spectroscopies. Using these techniques, detailed insights into bond properties of the catalytically relevant CO ligand were obtained. In addition, fast relaxation rates of the CO and two CN stretching modes revealed highly efficient energy transfer – both from the catalytic metal site towards the protein matrix and between the two sets of ligands. Coupling between all three CX ligand vibrations could also be inferred from 2D-IR cross peaks and quantum beats observed in time series of IR pump-probe spectra. Both features allow assigning catalytic intermediates in complex reaction mixtures. Furthermore, analysis of the quantum beat decay revealed the time and length scales of active-site equilibrium dynamics, highlighting the relevance of entatic states in biological hydrogen transformation.

Reproduced from https://doi.org/10.1039/C9SC02851J with permission from the Royal Society of Chemistry

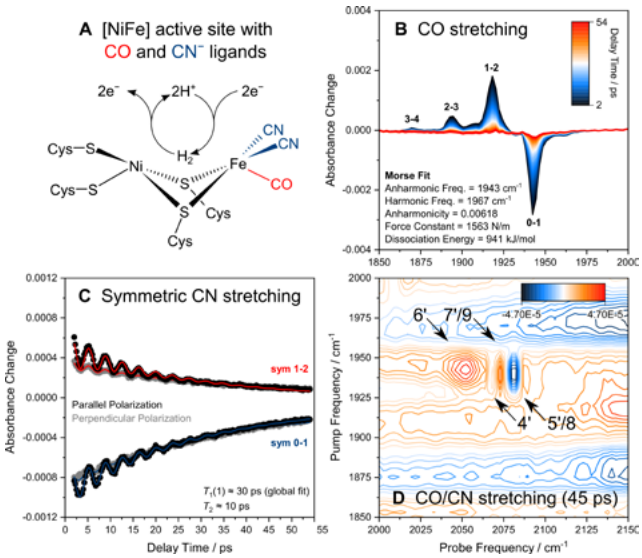

(A) Active site structure of [NiFe] hydrogenases. Diatomic ligands used as IR reporter groups are highlighted. (B) CO stretch transitions observed by ultrafast IR pump-probe spectroscopy and extracted bond properties. (C) Population and coherence decay observed for coupled CN stretch modes by ultrafast IR pump-probe spectroscopy. Time traces reflect the symmetric CN stretch mode. Extracted quantities are indicated. (D) Cross peaks observed by 2D-IR-spectroscopy, reflecting energy transfer between CO and CN stretch modes.

Contact: M. Horch (marius.horch@fu-berlin.de)

Understanding cation dynamics in caesium substituted organohalide perovskites

N.P. Gallop, A.A. Bakulin *(Department of Chemistry, Imperial College London, Molecular Sciences Research Hub, London, UK)*
J. Ye, R. Hoye *(Department of Materials, Imperial College London, Royal School of Mines, London, UK)*
G. Greetham *(Central Laser Facility, STFC Rutherford Appleton Laboratory, Harwell Campus, Didcot, UK)*

In this work, we aim to understand the effect of caesium substitution on the cation dynamics of organohalide perovskites (OHPs). This family of materials show immense promise as next-generation solar cells; however, there are still many aspects to them that we do not entirely understand. Amongst these is a complete understanding of the dynamics of the organic cations within the cell. To this end, we use 2DIR transient anisotropy measurements to probe the dynamics of methylammonium (MA) within the archetypal perovskite $MA_xCs_{1-x}PbI_3$. We find that the addition of as little as 10% caesium results in a 2.5-fold slowdown in the reorientation of the organic cation. Comparison with previous DFT and Raman studies suggests that distortion of the octahedral cavity, coupled with rigidisation of the PbI_3 cage, prevents facile rotation of the MA ion. Our work also highlights the interplay between static and dynamic disorder within OHPs, which is highly relevant for future improvements to their stability and optoelectronic properties.

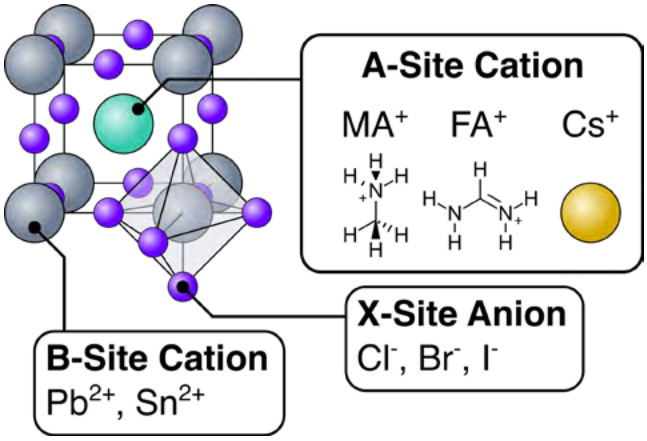

Generalised crystal structure of a metal-halide perovskite.

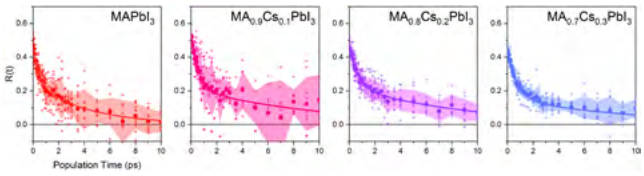

Rotational anisotropy decays of $MA_xCs_{1-x}PbI_3$ (x = 0.0—0.3). The solid points represent averages across all runs (semitranspatent points), whilst the solid lines represent a fit of this data using Eqn. 2. The shaded region denotes the standard error of the measurements.

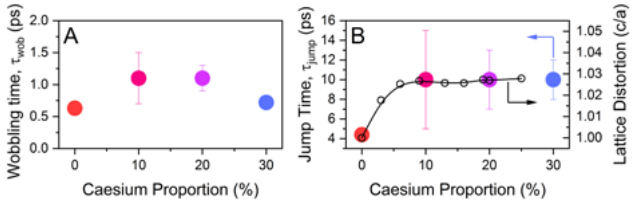

Extracted wobbling and jump time parameters, obtained by fitting the four anisotropy decays in Fig. 2 to Eqn. 2. The black line in (B) is digitally extracted from Ghosh, D. et al. Good Vibrations: Locking of Octahedral Tilting in Mixed-Cation Iodide Perovskites for Solar Cells. ACS Energy Lett. 2017, 2 (10), 2424–2429

Equation 2:

$$R(t) = \frac{2}{5}\left[S^2 e^{-t/\tau_{jump}} + (1 - S^2) e^{t/\tau_{wob} - t/\tau_{jump}}\right]$$

Contact: A. Bakulin (a.bakulin@imperial.ac.uk)

Functional dynamics of a single tryptophan residue in a BLUF protein revealed by fluorescence spectroscopy

K. Karadi, S.M. Kapetanaki, M. Nyitrai, A. Lukacs *(Department of Biophysics, Medical School, University of Pécs, Hungary; Szentagothai Research Center, University of Pécs, Hungary)*
K. Raics, I. Pecsi, R. Kapronczai, Z. Fekete, J. Orban *(Department of Biophysics, Medical School, University of Pécs, Hungary)*
J.N. Iuliano, J. Tolentino Collado, A.A. Gil, P.J. Tonge *(Department of Chemistry, Stony Brook University, Stony Brook, New York, USA)*
G.M. Greetham *(Central Laser Facility, STFC Rutherford Appleton Laboratory, Harwell Campus, Didcot, UK)*
M.H. Vos *(LOB, CNRS, INSERM, Ecole Polytechnique, Institut Polytechnique de Paris, France)*
S.R. Meech *(School of Chemistry, University of East Anglia, Norwich, UK)*

Blue Light Using Flavin (BLUF) domains are increasingly being adopted for use in optogenetic constructs. Despite this, much remains to be resolved on the mechanism of their activation. The advent of unnatural amino acid mutagenesis opens up a new toolbox for the study of protein structural dynamics. The tryptophan analogue, 7-aza-Trp (7AW) was incorporated in the BLUF domain of the Activation of Photopigment and PUC A (AppA) photoreceptor in order to investigate the functional dynamics of the crucial W104 residue during photoactivation of the protein. The 7-aza modification to Trp makes selective excitation possible using 310 nm excitation and 380 nm emission, separating the signals of interest from other Trp and Tyr residues. We used Förster energy transfer (FRET) between 7AW and the flavin to estimate the distance between Trp and flavin in both the light- and dark-adapted states in solution. Nanosecond fluorescence anisotropy decay and picosecond fluorescence lifetime measurements for the flavin revealed a rather dynamic picture for the tryptophan residue. In the dark adapted state, the major population of the tryptophan 104 is pointing away from the flavin and can move freely, in contrast to previous results reported in the literature. Upon blue-light excitation, the tryptophan population is reorganized, the dominant population moves closer to the flavin occupying a rigidly bound state participating in the hydrogen-bond network around the flavin molecule.

Reproduced from Karadi, K., Kapetanaki, S.M., Raics, K. et al. Functional dynamics of a single tryptophan residue in a BLUF protein revealed by fluorescence spectroscopy. Sci Rep 10, 2061 (2020), under the terms of the Creative Commons Attribution 4.0 International License. https://doi.org/10.1038/s41598-020-59073-5

Contact: A. Lukacs (andras.lukacs@aok.pte.hu)

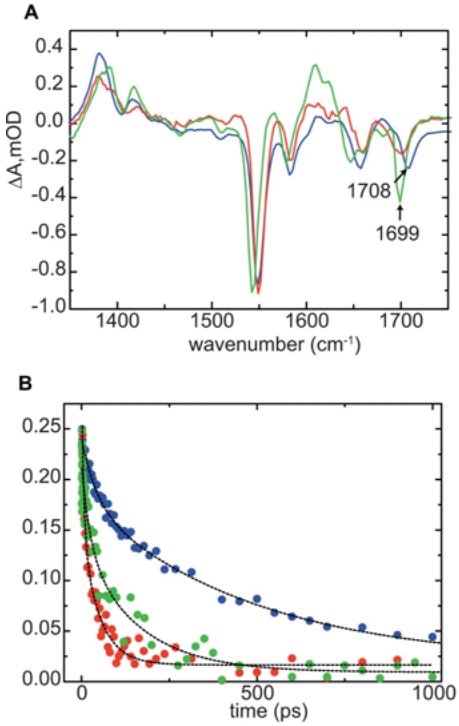

(A) TRIR spectra of dark- and light-adapted (blue and red respectively) W64F and the Y21F/Y56F/W64F AppA mutants (green) recorded at 10 ps; (B) Kinetics of the excited state of the flavin in the dark- and light-adapted (blue and red respectively) states of W64F $AppA_{BLUF}$ and in the Y21F/Y56F/W64F $AppA_{BLUF}$ (green) observed at 1380 cm^{-1}.

Overcoming the challenges of measuring the irreversible photochemical dynamics of a 'tricky' protein using time-resolved infrared spectroscopy: the B_{12}-dependent transcriptional regulator, CarH

I.S. Camacho, A.R. Jones *(Biometrology, Chemical and Biological Sciences, National Physical Laboratory, Teddington, Middlesex, UK)*
I.V. Sazanovich, E. Gozzard, M. Towrie *(Central Laser Facility, STFC Rutherford Appleton Laboratory, Harwell Campus, Didcot, UK)*
N.T. Hunt *(Department of Chemistry and York Biomedical Research Institute, University of York, UK)*

Photoreceptor proteins enable organisms to respond to their environment and can be engineered into light-activated tools and novel phototherapies. Time-resolved infrared (TRIR) spectroscopy has significant potential to elucidate the photophysical, photochemical and structural dynamics of photoreceptors. Not all such proteins are straightforwardly amenable to investigation by TRIR, however. Here we describe the development of a sample preparation and data acquisition protocol for TRIR with a 'tricky' protein: the B_{12}-dependent bacterial photoreceptor, CarH. At the concentrations required for TRIR, CarH precipitates during its irreversible photoconversion, resulting in light scattering. We therefore developed a one-way flow and sample recycling system (figure below left) that yields high quality, reproducible TRIR data (figure below right) from limited sample. This approach should be adaptable for the investigation by TRIR of similarly challenging samples, providing data that details photoreceptor dynamics and that informs the developments of light-activated, molecular biotechnologies.

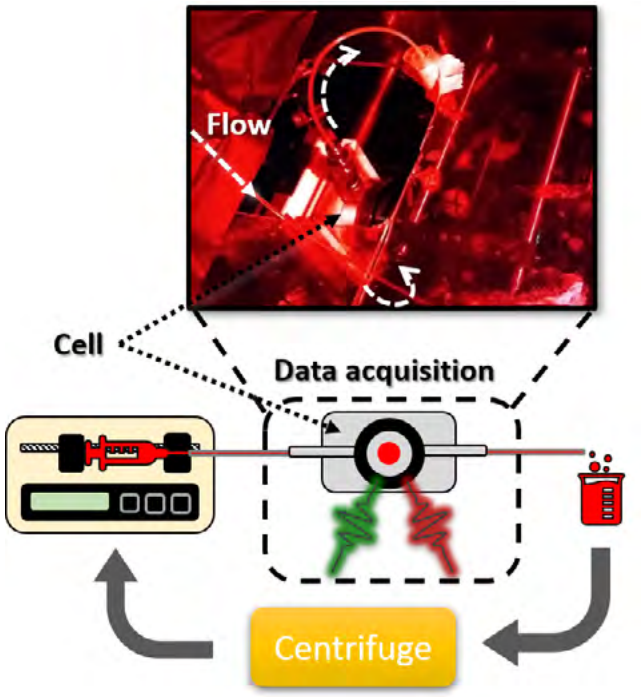

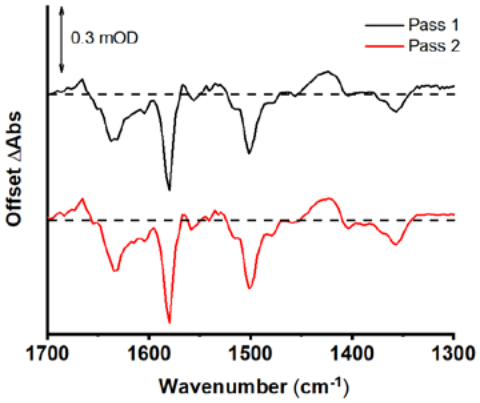

Above: TRIR difference spectra at 2 ps following photoexcitation of CarH at 525 nm in aqueous buffer. The data illustrate the reproducibility of sequential acquisition 'passes' following centrifugation as shown in the figure left. Plots are offset for clarity; dashed lines indicate zero spectral amplitude; and a scale bar is indicated.

Left: Schematic of the final experimental setup (bottom) where the sample (red) flows (left to right) from a syringe pump, via tubing, through the modified cell to waste. The 'waste' is then centrifuged to remove photoconverted precipitate and the supernatant recycled for further data acquisition. Visible pump (green) and midIR probe (red) laser light are shown incident to the cell window. A photograph (top) shows the flow set up in situ under red ambient light. The direction of sample flow from the pump (out of shot) is indicated using white dashed arrows.

Contact: A.R. Jones (alex.jones@npl.co.uk)

Unraveling the mechanism of a LOV domain optogenetic sensor: a glutamine lever induces unfolding of the Jα Helix

J.N. Iuliano, J.T. Collado, S-Y. Shin, H.A. Woroniecka, T. Daryaee, C.L.Simmerling, P.J. Tonge *(Department of Chemistry, Stony Brook University, New York, USA)*
A.A. Gil, P.T. Ravindran, J.E. Toettcher *(Department of Molecular Biology, Princeton University, Princeton, New Jersey 08544, United States)*
A. Lukacs *(School of Chemistry, University of East Anglia, Norwich, UK; Department of Biophysics, Medical School, University of Pecs, Hungary)*
K. Adamczyk, C.R. Hall, S.R. Meech *(School of Chemistry, University of East Anglia, Norwich, UK)*
J.M. Aramini *(Structural Biology Initiative, CUNY Advanced Science Research Center, New York, USA)*
U.R. Edupuganti *(Structural Biology Initiative, CUNY Advanced Science Research Center, New York, USA; PhD Program in Biochemistry, CUNY Graduate Center, New York, USA)*
G.M. Greetham, I.V. Sazanovich, I.P. Clark *(Central Laser Facility, Research Complex at Harwell, STFC Rutherford Appleton Laboratory, Harwell Campus, Didcot, UK)*
J.B. French *(Department of Chemistry, Stony Brook University, New York, USA; Hormel Institute, University of Minnesota, USA)*
K.H. Gardner *(Structural Biology Initiative, CUNY Advanced Science Research Center, New York, USA; PhD Programs in Biochemistry, Biology, and Chemistry, CUNY Graduate Center, New York, USA; Department of Chemistry and Biochemistry, City College of New York, USA)*

Light-activated protein domains provide a convenient, modular, and genetically encodable sensor for optogenetics and optobiology. Although these domains have now been deployed in numerous systems, the precise mechanism of photoactivation and the accompanying structural dynamics that modulate output domain activity remain to be fully elucidated. In the C-terminal light–oxygen–voltage (LOV) domain of plant phototropins (LOV2), blue light activation leads to formation of an adduct between a conserved Cys residue and the embedded FMN chromophore, rotation of a conserved Gln (Q513), and unfolding of a helix (Jα-helix) which is coupled to the output domain. In the present work, we focus on the allosteric pathways leading to Jα helix unfolding in Avena sativa LOV2 (AsLOV2) using an interdisciplinary approach involving molecular dynamics simulations extending to 7 μs, time-resolved infrared spectroscopy, solution NMR spectroscopy, and in-cell optogenetic experiments. In the dark state, the side chain of N414 is hydrogen bonded to the backbone N–H of Q513. The simulations predict a lever-like motion of Q513 after Cys adduct formation resulting in a loss of the interaction between the side chain of N414 and the backbone C=O of Q513, and formation of a transient hydrogen bond between the Q513 and N414 side chains. The central role of N414 in signal transduction was evaluated by site-directed mutagenesis supporting a direct link between Jα helix unfolding dynamics and the cellular function of the Zdk2-AsLOV2 optogenetic construct. Through this multifaceted approach, we show that Q513 and N414 are critical mediators of protein structural dynamics, linking the ultrafast (sub-ps) excitation of the FMN chromophore to the microsecond conformational changes that result in photoreceptor activation and biological function.

Contact: P.J. Tonge (peter.tonge@stonybrook.edu)

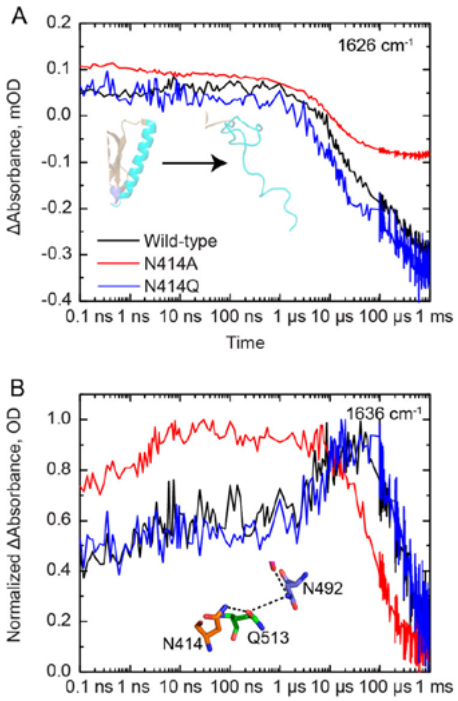

Selected kinetic traces from TRIR spectra of wild-type and mutant AsLOV2. (A) The unfolding of the Jα helix is tracked by the increase in bleach intensity at 1626 cm^{-1} for the wild-type (black), N414A (red), and N414Q (blue) AsLOV2 proteins. (B) A rise and decay of the signal at 1636 cm^{-1} is assigned to structural dynamics associated with a transient hydrogen bond between N414 and Q513 due to the rotation of Q513. This signal decays to zero with the time constant of the fourth EAS.

Reproduced with permission from Iuliano, James N et al. Unraveling the Mechanism of a LOV Domain Optogenetic Sensor: A Glutamine Lever Induces Unfolding of the Jα Helix. ACS chemical biology vol. 15,10 (2020): 2752-2765. Copyright © 2020 American Chemical Society. doi:10.1021/acschembio.0c00543

A time-resolved spectroscopic study of BODIPY copolymers and their application as photosensitisers for hydrogen evolution

A.A. Cullen, K. Heintz, L. O'Reilly, C. Long, M.T. Pryce *(School of Chemical Sciences, Dublin City University, Ireland)*
A. Heise, R. Murphy *(Department of Chemistry, Royal College of Surgeons in Ireland, Dublin, Ireland)*
J. Karlsson, E. Gibson *(Energy Materials Laboratory, Chemistry, School of Natural and Environmental Science, Newcastle University, UK)*
G.M. Greetham, M. Towrie *(Central Laser Facility, Research Complex at Harwell, STFC Rutherford Appleton Laboratory, Harwell Campus, Didcot, UK)*

A novel BODIPY copolymer with diethynylbenzene linkers has been studied as a photosensitising unit for photocatalytic hydrogen generation. Time-resolved infrared and transient absorption studies spanning the ps- to ns-timescales were used to probe the excited state dynamics of this photosensitising centre. Visible light irradiation of solutions containing the BODIPY copolymer together with a cobaloxime catalyst under various conditions generates hydrogen.

Reproduced from Cullen, Aoibhín A et al. A Time-Resolved Spectroscopic Investigation of a Novel BODIPY Copolymer and Its Potential Use as a Photosensitiser for Hydrogen Evolution. Frontiers in chemistry vol. 8 584060. 19 Oct. 2020, under the terms of the Creative Commons Attribution License (CC BY). doi:10.3389/fchem.2020.584060

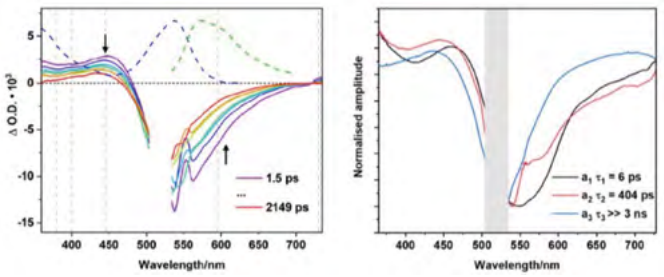

Transient absorption spectra of the BODIPY copolymer in CD_3CN following excitation at 525 nm at various time points together with the Decay Associated Spectra.

Contact: M.T. Pryce (mary.pryce@dcu.ie)

From sunscreens to medicines: Can a dissipation hypothesis explain the beneficial aspects of many plant compounds?

A.V.W. Nunn, J.D. Bell *(Research Centre for Optimal Health, Department of Life Sciences, University of Westminster, London, UK)*
G.W. Guy *(GW pharmaceuticals, Salisbury, Wiltshire, UK)*
S.W. Botchway *(Central Laser Facility, Research Complex at Harwell, STFC Rutherford Appleton Laboratory, Harwell Campus, Didcot, UK; Department of Biological and Medical Sciences, Oxford Brookes University, UK)*

Medicine has utilised plant-based treatments for millennia, but precisely how they work is unclear. One approach is to use a thermodynamic viewpoint that life arose by dissipating geothermal and/or solar potential. Hence, the ability to dissipate energy to maintain homeostasis is a fundamental principle in all life, which can be viewed as an accretion system where layers of complexity have built upon core abiotic molecules. Many of these compounds are chromophoric and are now involved in multiple pathways. Plants have further evolved a plethora of chromophoric compounds that can not only act as sunscreens and redox modifiers, but also have now become integrated into a generalised stress adaptive system. This could be an extension of the dissipative process. In animals, many of these compounds are hormetic, modulating mitochondria and calcium signalling. They can also display anti-pathogen effects. They could therefore modulate bioenergetics across all life due to the conserved electron transport chain and proton gradient. In this review paper, we focus on well-described medicinal compounds, such as salicylic acid and cannabidiol and suggest, at least in animals, their activity reflects their evolved function in plants in relation to stress adaptation, which itself evolved to maintain dissipative homeostasis.

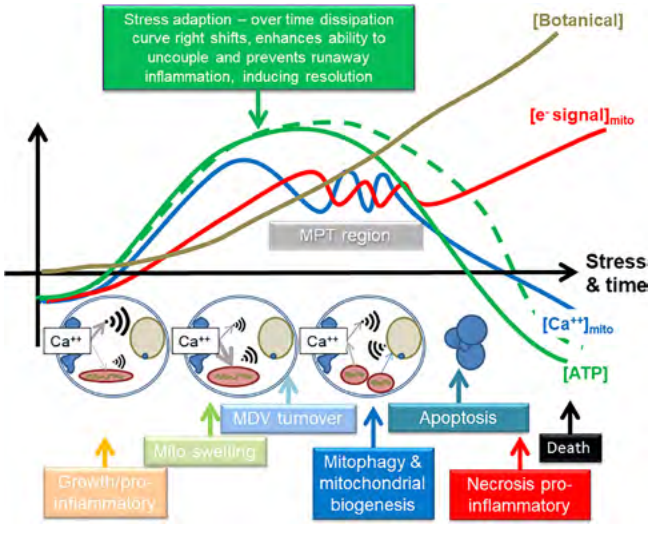

Reproduced from A.V.W. Nunn, G.W. Guy, S.W. Botchway, J.D. Bell. From sunscreens to medicines: Can a dissipation hypothesis explain the beneficial aspects of many plant compounds? Phytotherapy Research 2020, 34(8), 1868-1888, published by John Wiley & Sons Ltd, under the terms of the Creative Commons Attribution License. doi: 10.1002/ptr.6654

Contact: A.V.W. Nunn (a.nunn@westminster.ac.uk)

Biphasic effects of plant compounds on mitochondrial function, from a calcium-centric viewpoint
Key:
MPT = mitochondrial permeability transition
MDV = mitochondrially derived vesicles
Blue line = mitochondrial calcium concentration
Red line = electron leak leading to ROS
Green line = dissipation & ATP
Brown line = possible plant compound concentration

Controlling the fluorescence and room-temperature phosphorescence behaviour of carbon nanodots with inorganic crystalline nanocomposites

D.C. Green, S. Zhang, F.C. Meldrum *(School of Chemistry, University of Leeds, UK)*
M.A. Holden *(School of Chemistry, University of Leeds, UK; School of Physics and Astronomy, University of Leeds, UK)*
B.R.G. Johnson, J.Gala de Pablo *(School of Physics and Astronomy, University of Leeds, UK)*
M.A. Levenstein *(School of Chemistry, University of Leeds, UK; School of Mechanical Engineering, University of Leeds, UK)*
A. Ward, S.W. Botchway *(Central Laser Facility, Research Complex at Harwell, STFC Rutherford Appleton Laboratory, Harwell Campus, Didcot, UK)*

There is a significant drive to identify alternative materials that exhibit room temperature phosphorescence for technologies including bio-imaging, photodynamic therapy and organic light-emitting diodes. Ideally, these materials should be non-toxic and cheap, and it will be possible to control their photoluminescent properties. This was achieved here by embedding carbon nanodots within crystalline particles of alkaline earth carbonates, sulphates and oxalates. The resultant nanocomposites are luminescent and exhibit a bright, sub-second lifetime afterglow. Importantly, the excited state lifetimes, and steady-state and afterglow colours can all be systematically controlled by varying the cations and anions in the host inorganic phase, due to the influence of the cation size and material density on emissive and non-emissive electronic transitions. This simple strategy provides a flexible route for generating materials with specific, phosphorescent properties and is an exciting alternative to approaches relying on the synthesis of custom-made luminescent organic molecules.

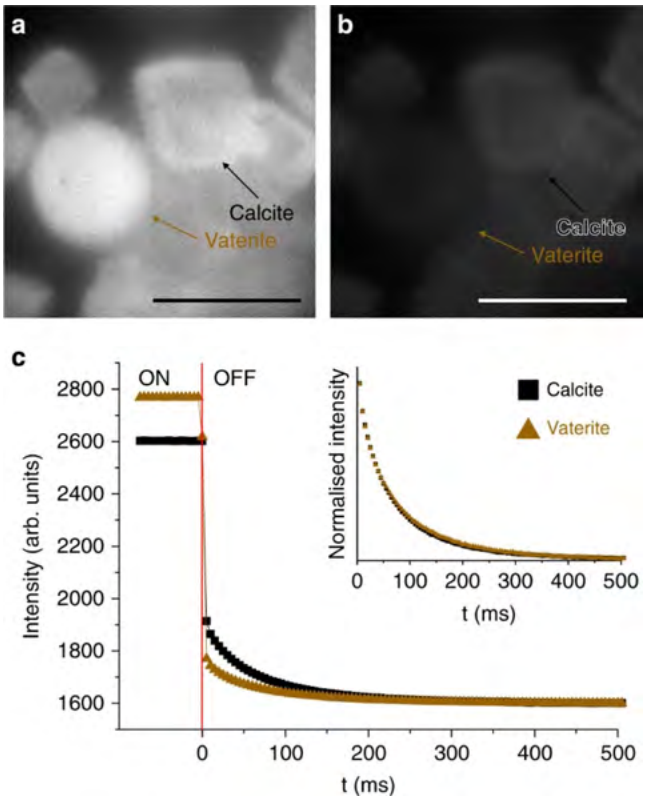

Dependence of room temperature phosphorescence activation on the crystal phase. Time-resolved phosphorescence microscopy images with UV excitation (a) on and (b) 5 ms after the removal of UV excitation, and (c) intensity vs time plots for calcite (black square) and vaterite (brown triangle)-based RTP nanocomposites. The plot in (c) shows the intensity with UV light on and off, and the point at which the light is removed is shown with a vertical red line at t = 0. The normalised decay curves for calcite and vaterite overlap, indicating identical phosphorescent lifetimes (inset; scale bar 50 μm)

Reproduced from Green, D.C., Holden, M.A., Levenstein, M.A. et al. Controlling the fluorescence and room-temperature phosphorescence behaviour of carbon nanodots with inorganic crystalline nanocomposites. Nat Commun 10, 206 (2019), under the terms of the Creative Commons Attribution 4.0 International (CC BY 4.0) License. doi: 10.1038/s41467-018-08214-6

Contact: D.C. Green (D.C.Green@leeds.ac.uk),
F.C. Meldrum (F.Meldrum@leeds.ac.uk)

Multiphoton fluorescence lifetime imaging microscopy (FLIM) and super-resolution fluorescence imaging with a supramolecular biopolymer for the controlled tagging of polysaccharides

H. Ge, F. Cortezon-Tamarit, H-C. Wang, R.L. Arrowsmith, V. Mirabello, T.D. James, S.I. Pascu *(Department of Chemistry, University of Bath, UK)*
A.C. Sedgwick *(Department of Chemistry, University of Texas at Austin, USA)*
S.W. Botchway *(Central Laser Facility, Research Complex at Harwell, STFC Rutherford Appleton Laboratory, Harwell Campus, Didcot, UK*

A fluorophore based on a new boronic acid derivative of coumarin and its corresponding β-D-glucan supramolecular conjugate were prepared and investigated by optical fluorescence techniques (one-photon and two-photon fluorescence spectroscopy together with time correlated singlephoton counting), AFM and Raman. The binding of this functional boronic acid to β-D-glucan from barley produced a kinetically stable nano-dimensional, soft material composite, denoted 5@β-D-glucan, with a binding affinity allowing for the retention of the complexed state even upon cellular uptake over a range of concentrations. Solution phase investigations by fluorescence spectroscopies both in single photon and two-photon excitation modes combined with *in vitro* studies (in HeLa and PC-3 cells, macrophage). The supramolecular conjugate was also evaluated as cellular imaging probes in different cancer cell lines (HeLa and PC-3) as well as J774.2 macrophages using single- and two-photon fluorescence lifetime imaging microscopy (FLIM) showing that the conjugates enter cells successfully; studies by multiphoton fluorescence confocal imaging and super-resolution imaging indicate that both 5-P and 5@β-D-glucan can enter cells and distribute in the cytoplasm at both 37°C and 4°C. Fluorescence lifetime studies confirmed for the first time the successful binding of a coumarin boronic acid with β-D-glucan which remains intact as a kinetically stable complex in aqueous environments. We describe a new coumarin-appended boronate ester as a fluorogenic reagent, which binds to both mono and polysaccharides. This new glucan hybrid could serve as cellular imaging probe: a simple coumarin boronic acid can thus act to bridge the gap between the development and application of small molecules and bio-nanomaterials for the labelling of living cancer cells. We believe that biopolymers such as β-D-glucan from barley used as a scaffold for boronate-tagging methodologies could lead to new synthetic approaches to deliver non-invasive and affordable early diagnostics for cancers which are difficult to access non-invasively such as prostate cancers.

Reproduced from Ge H, Cortezon-Tamarit F, Wang H-C, et al. Multiphoton fluorescence lifetime imaging microscopy (FLIM) and super-resolution fluorescence imaging with a supramolecular biopolymer for the controlled tagging of polysaccharides. Nanoscale, 2019,11, 9498, © 2019 The Royal Society of Chemistry, under the terms of a Creative Commons Attribution NonCommerical 3.0 Unported License. DOI: 10.1039/c8nr10344e

Contact: S.I. Pascu (s.pascu@bath.ac.uk)

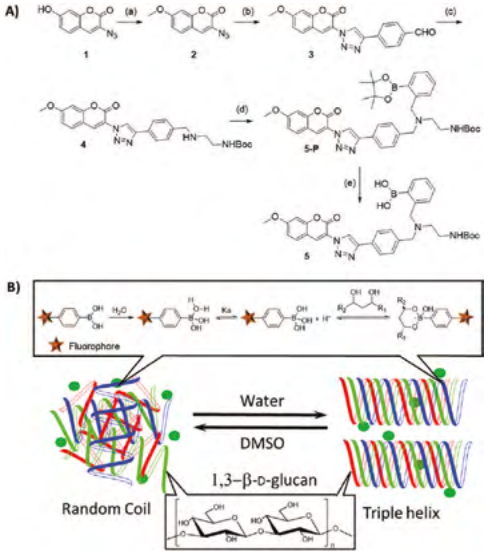

Scheme 1: A) Synthesis of the pinacol-protected coumarin monoboronate ester of 5-P: (a) MeI, K_2CO_3, acetone, reflux. (100%) (b) 4-ethynylbenzaldehyde 2, $CuSO_4{\cdot}5H_2O$ (5 mol%), NaAsc (10 mol%), H_2O/EtOH = 1 : 1, rt. (80%) (c) (i) mono Boc-diamine (1 eq.), DCM/MeOH, rt. (ii) $NaBH_3CN$, MeOH, rt. (74%) (d) 2-(bromomethyl) phenylboronic acid pinacol ester, K_2CO_3, ACN, reflux. (B) Schematic representation of the β-D-glucan triple helix in water and the diagram of boronic acid fluorophore reversible binding with the diols of the 1,3-β-D-glucan. Pinacol deprotection of 5-P proceeded to 5 in situ in presence of glucan diols, at pH 8–9.5 to form the desired diol-boronate and covalently-bonded supramolecular biopolymer complex, denoted 5@β-D-glucan.

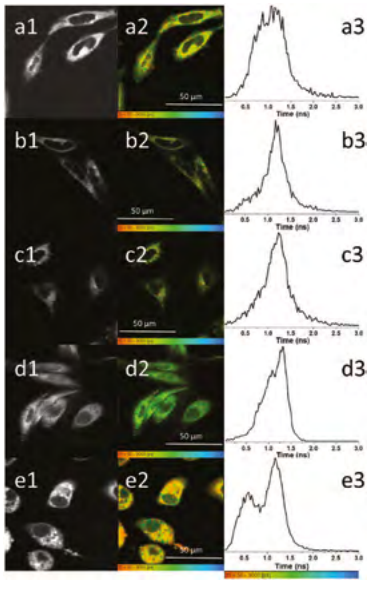

Two-photon fluorescence imaging including lifetime microscopy mapping of 5-P (100 μM in 0.5 : 99.5% DMSO : RPMI) (a_{1-2}; b_{1-2}; d_{1-2}) and 5@β-D-glucan (0.5 : 99.5% DMSO : RPMI) (c_{1-2}; e_{1-2}) in HeLa (a_{1-2}; b_{1-2}; c_{1-2}) and PC-3 cells (d_{1-2}; e_{1-2}) after 15 min incubation. Corresponding fluorescence lifetime distribution curves: a_3, b_3, c_3, d_3, e_3; λ_{ex} = 810 nm. Scale bar: 50μm. The micrographs show that 5-P and 5@β-D-glucan are capable of penetrating the cell membrane at either 4°C (b_{1-2}; c_{1-2}) or at 37°C (a_{1-2}; d_{1-2}; e_{1-2}), although the lower temperature reduces the extent of cellular uptake. Legend colours provide a direct correlation between the lifetime maps a2–e2 and the histograms showing the corresponding lifetimes distribution (a3–e3).

A dinuclear Ruthenium(II) complex excited by Near-infrared light through two-photon absorption induces phototoxicity deep within hypoxic regions of melanoma cancer spheroids

A. Raza, S. MacNeil, J.W. Haycock *(Materials Science & Engineering, University of Sheffield, UK)*
S.A. Archer, S.D. Fairbanks, K.L. Smitten, J.A. Thomas *(Department of Chemistry, University of Sheffield, UK)*
S.W. Botchway *(Central Laser Facility, Research Complex at Harwell, STFC Rutherford Appleton Laboratory, Harwell Campus, Didcot, UK)*

The dinuclear photo-oxidizing Ru^{II} complex $[\{Ru(TAP_2)\}_2(tpphz)]^{4+}$ (TAP = 1,4,5,8- tetraazaphenanthrene, tpphz = tetrapyrido- [3,2-*a*:2′,3′-*c*:3″,2″-*h*:2‴,3‴-*j*]phenazine), 1^{4+}, is readily taken up by live cells localizing in mitochondria and nuclei. In this study, the two-photon absorption cross section of 1^{4+} is quantified and its use as a two-photon absorbing phototherapeutic is reported. It was confirmed that the complex is readily photoexcited using near-infrared, NIR, and light through two-photon absorption, TPA. In 2-D cell cultures, irradiation with NIR light at low power results in precisely focused phototoxicity effects in which human melanoma cells were killed after 5 min of light exposure. Similar experiments were then carried out in human cancer spheroids that provide a realistic tumor model for the development of therapeutics and phototherapeutics. Using the characteristic emission of the complex as a probe, its uptake into 280 µm spheroids was investigated and confirmed that the spheroid takes up the complex. Notably TPA excitation results in more intense luminescence being observed throughout the depth of the spheroids, although emission intensity still drops off toward the necrotic core. As 1^{4+} can directly photo-oxidize DNA without the mediation of singlet oxygen or other reactive oxygen species, phototoxicity within the deeper, hypoxic layers of the spheroids was also investigated. To quantify the penetration of these phototoxic effects, 1^{4+} was photoexcited through TPA at a power of 60 mW, which was progressively focused in 10 µm steps throughout the entire z-axis of individual spheroids. These experiments revealed that, in irradiated spheroids treated with 1^{4+}, acute and rapid photoinduced cell death was observed throughout their depth, including the hypoxic region.

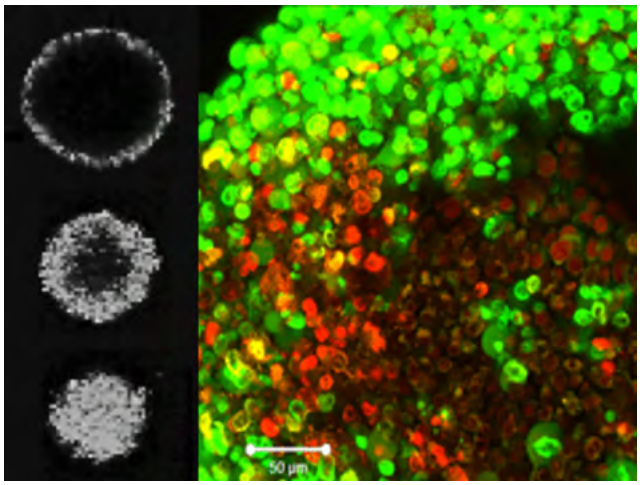

Reprinted from Raza A, Archer SA, Fairbanks SD, et al. A Dinuclear Ruthenium(II) Complex Excited by Near-Infrared Light through Two-Photon Absorption Induces Phototoxicity Deep within Hypoxic Regions of Melanoma Cancer Spheroids. J Am Chem Soc. 2020;142:4639-4647, © 2020 American Chemical Society, under the terms of the Creative Commons Attribution (CC-BY) License. DOI: 10.1021/jacs.9b11313

Contact: J.A. Thomas (james.thomas@sheffield.ac.uk)
S. MacNeil (s.macneil@sheffield.ac.uk)
J.W. Haycock (j.w.haycock@sheffield.ac.uk)

The photophysical properties of triisopropylsilyl-ethynylpentacene – a molecule with an unusually large singlet-triplet energy gap – in solution and solid phases

F.A. Schaberle, C. Serpa. L.G. Arnaut *(CQC, Department of Chemistry, University of Coimbra, Portugal)*
A.D. Ward *(Central Laser Facility, Research Complex at Harwell, STFC Rutherford Appleton Laboratory, Harwell Campus, Didcot, UK)*
J.K. Karlsson, A. Harriman *(Molecular Photonics Laboratory, SNES, Newcastle University, UK)*
A. Atahan *(Molecular Photonics Laboratory, SNES, Newcastle University, UK; Department of Polymer Engineering, Faculty of Technology, Duzce University, Turkey)*

The process of singlet-exciton fission (SEF) has attracted much attention of late. One of the most popular SEF compounds is TIPS-pentacene (TIPS P, where TIPS = triisopropylsilylethynyl) but, despite its extensive use as both a reference and building block, its photophysical properties are not so well established. In particular, the triplet state excitation energy remains uncertain. Here, we report quantitative data and spectral characterization for excited-singlet and -triplet states in dilute solution. The triplet energy is determined to be 7940 ± 1200 cm^{-1} on the basis of sensitization studies using time-resolved photoacoustic calorimetry. The triplet quantum yield at the limit of low concentration and low laser intensity is only ca. 1%. Self-quenching occurs at high solute concentration where the fluorescence yield and lifetime decrease markedly relative to dilute solution but we were unable to detect excimer emission by steady-state spectroscopy. Short-lived fluorescence, free from excimer emission or phosphorescence, occurs for crystals of TIPS P, most likely from amorphous domains.

Reprinted from F.A. Schaberle. C. Serpa, L.G. Arnaut et al. Chemistry, 2(2), 545-564 (2020), © 2020 by MDPI (http://www.mdpi.org), under the terms of the Creative Commons CC BY License. DOI: 10.3390/chemistry2020033

Contact: A. Harriman (anthony.harriman@ncl.ac.uk)

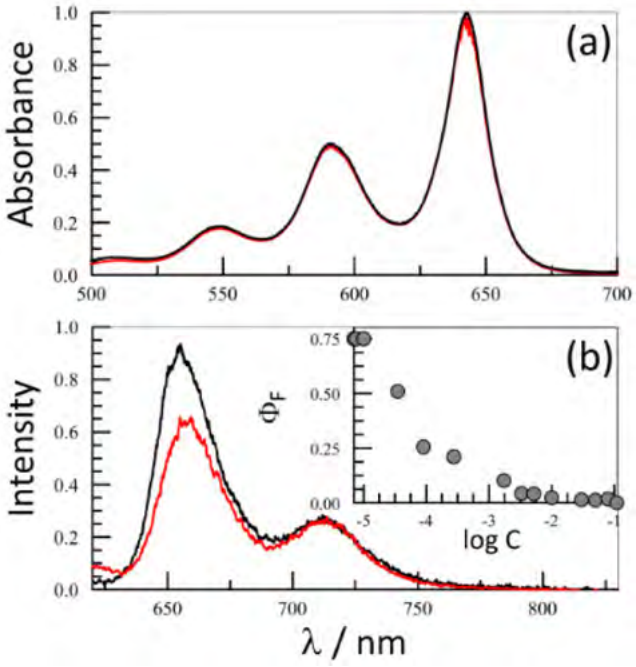

(a) Comparison of absorption spectra recorded for TIPS-P in toluene at concentrations of 1 μM (black curve) and 0.05 M (red curve). The spectra, which have been normalized at the respective maxima, were recorded with a variable path length optical cell to maintain a constant absorbance at any given wavelength. (b). Examples of fluorescence spectra recorded for the above solutions, with excitation at 595 nm and the same colour scheme. Note the minor distortion of the spectrum at high concentration caused by uncompensated self-absorption. The inset shows the effect of TIPS-P concentration on the fluorescence quantum yield.

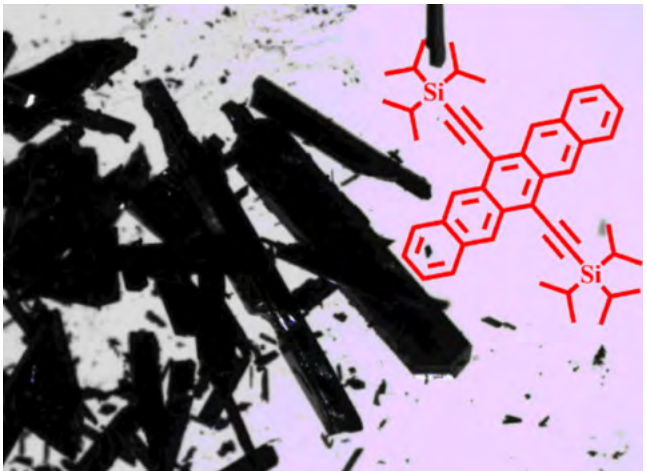

Chemical formula for TIPS-P superimposed over a photograph of crystals of the same material.

Measurement of the fluorescence lifetime of GFP in high refractive index levitated droplets using FLIM

N.M. Davidson, F.D. Pope *(School of Geography, Earth and Environmental Sciences, University of Birmingham, UK)*
P.J. Gallimore, M. Kalberer *(Department of Chemistry, University of Cambridge, UK)*
B.C. Bateman, S.W. Botchway, A.D. Ward *(Central Laser Facility, Research Complex at Harwell, STFC Rutherford Appleton Laboratory, Harwell Campus, Didcot, UK)*
M.K. Kuimova *(Department of Chemistry, Imperial College London, UK)*

Green fluorescent protein (GFP) is a widely used fluorescent probe in the life sciences and biosciences due to its high quantum yield and extinction coefficient, and its ability to bind to biological systems of interest. This study measures the fluorescence lifetime of GFP in sucrose/water solutions of known molarity in order to determine the refractive index dependent lifetime of GFP. A range of refractive indices from 1.43–1.53 were probed by levitating micron sized droplets composed of water/sucrose/ GFP in an optical trap under well-constrained conditions of relative humidity. This setup allows for the first reported measurements of the fluorescence lifetime of GFP at refractive indices greater than 1.46. The results obtained at refractive indices less than 1.46 show good agreement with previous studies. Further experiments that trapped droplets of deionised water containing GFP allowed the hygroscopic properties of GFP to be measured. GFP is found to be mildly hygroscopic by mass, but the high ratio of molecular masses of GFP to water (ca. 1500 : 1) signifies that water uptake is large on a per-mole basis. Hygroscopic properties are verified using brightfield microscope imaging, of GFP droplets at low and high relative humidity, by measuring the humidity dependent droplet size. In addition, this experiment allowed the refractive index of pure GFP to be estimated for the first time (1.72 ± 0.07). This work provides reference data for future experiments involving GFP, especially for those conducted in high refractive index media. The work also demonstrates that GFP can be used as a probe for aerosol studies, which require determination of the refractive index of the aerosol of any shape.

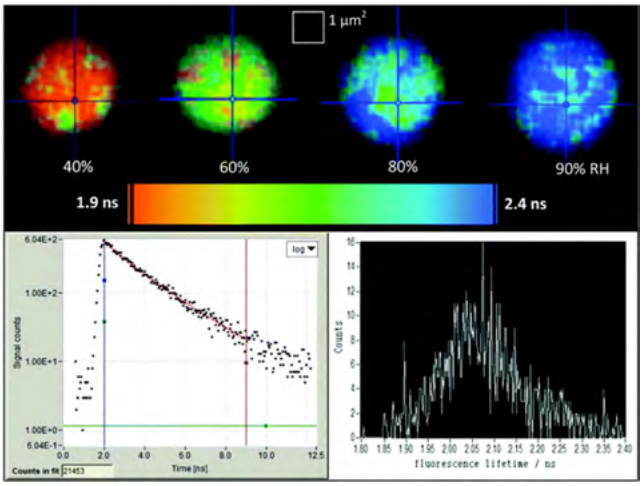

Top: Example fluorescence lifetime images of the same droplet of GFP in sucrose/water at 40, 60, 80 & 90% RH collected by SPCimage. Bottom left: Log time-resolved fluorescence decay of the 40% RH droplet in Tri2. Bottom right: Lifetime histogram of the same droplet, with lifetime on the x-axis and number of counts on the y-axis.

Reprinted from N.M. Davidson, P.J. Gallimore, B. Bateman, et al. Phys. Chem. Chem. Phys. 22, 14704 (2020), published by the PCCP Owner Societies, under the terms of the Creative Commons Attribution 3.0 Unported Licence. DOI: 10.1039/C9CP06395A

Contact: F.D. Pope (f.pope@bham.ac.uk)

Supramolecular clustering of the cardiac sodium channel Nav1.5 in HEK293F cells, with and without the auxiliary β3-subunit

S.C. Salvage, J.S. Rees, J.R. Irons, A.P. Jackson *(Department of Biochemistry, University of Cambridge, UK)*
A. McStea, M. Hirsch, L. Wang, C.J. Tynan, M.L. Martin-Fernandez *(Central Laser Facility, Research Complex at Harwell, STFC Rutherford Appleton Laboratory, Harwell Campus, Didcot, UK)*
M.W. Reed *(Department of Nuclear Physics, Research School of Physics and Engineering, Australian National University, Canberra, Australia)*
R. Butler *(Wellcome Trust/Cancer Research UK Gurdon Institute, University of Cambridge, UK)*
A.J. Thompson *(Department of Pharmacology, University of Cambridge, UK)*
C.L-H. Huang *(Department of Biochemistry, University of Cambridge, UK; Department of Physiology, Development and Neuroscience, University of Cambridge, UK)*

Voltage-gated sodium channels comprise an ion-selective ∝-subunit and one or more associated β-subunits. The β3-subunit (encoded by the SCN3B gene) is an important physiological regulator of the heart-specific sodium channel, Nav1.5. We have previously shown that when expressed alone in HEK293F cells, the full-length β3-subunit forms trimers in the plasma membrane. We extend this result with biochemical assays and use the proximity ligation assay (PLA) to identify oligomeric β3-subunits, not just at the plasma membrane, but throughout the secretory pathway. We then investigate the corresponding clustering properties of the ∝-subunit and the effects upon these of the β3-subunits. The oligomeric status of the Nav1.5 ∝-subunit in vivo, with or without the β3-subunit, has not been previously investigated. Using super-resolution fluorescence imaging, we show that under conditions typically used in electrophysiological studies, the Nav1.5 ∝-subunit assembles on the plasma membrane of HEK293F cells into spatially localized clusters rather than individual and randomly dispersed molecules.

Quantitative analysis indicates that the β3-subunit is not required for this clustering but β3 does significantly change the distribution of cluster sizes and nearest-neighbour distances between Nav1.5 ∝-subunits. However, when assayed by PLA, the β3-subunit increases the number of PLA-positive signals generated by anti-(Nav1.5 ∝-subunit) antibodies, mainly at the plasma membrane. Since PLA can be sensitive to the orientation of proteins within a cluster, we suggest that the β3-subunit introduces a significant change in the relative alignment of individual Nav1.5 ∝-subunits, but the clustering itself depends on other factors. We also show that these structural and higher-order changes induced by the β3-subunit do not alter the degree of electrophysiological gating cooperativity between Nav1.5 ∝-subunits. Our data provide new insights into the role of the β3-subunit and the supramolecular organization of sodium channels, in an important model cell system that is widely used to study Nav channel behaviour.

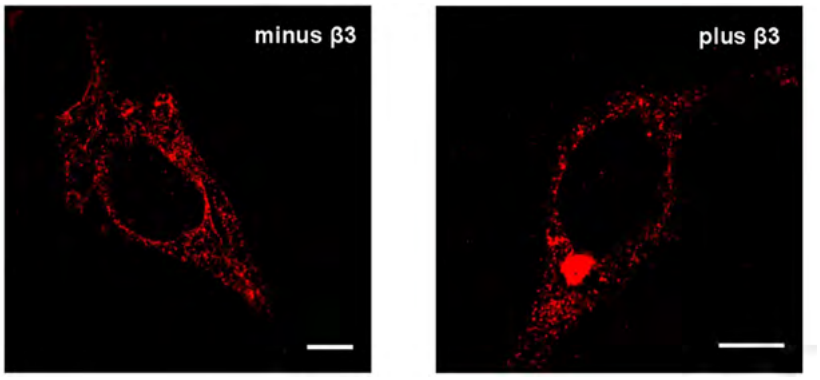

Super-resolution STORM imaging and of Nav1.5 ∝-subunits with and without β3-subunit at the CLF Octopus facility. Representative images are reconstructed from fluorophore AF-647 blinking in HEK293F cells co-transfected with Nav1.5-HA/EGFP and Nav1.5-HA/β3-EGFP. Bars = 5 μm.

Reproduced from Salvage, Samantha C et al. Supramolecular clustering of the cardiac sodium channel Nav1.5 in HEK293F cells, with and without the auxiliary β3-subunit. FASEB journal : official publication of the Federation of American Societies for Experimental Biology vol. 34,3 (2020): 3537-3553, under the terms of the Creative Commons Attribution 4.0 International (CC BY 4.0) License. doi:10.1096/fj.201701473RR.

Contact: S.C. Salvage (ss2148@cam.ac.uk)
A.P. Jackson (apj10@cam.ac.uk)

Direct imaging of the recruitment and phosphorylation of S6K1 in the mTORC1 pathway in living cells

A.R. Ahmed, C.D. Stubbs, A.W. Parker, S.W. Botchway *(Central Laser Facility, Research Complex at Harwell, STFC Rutherford Appleton Laboratory, Harwell Campus, Didcot, UK)*
R.J. Owens, R.B. Yadav *(Protein Production UK, Research Complex at Harwell, STFC Rutherford Appleton Laboratory, Harwell Campus, Didcot, UK; The Wellcome Centre for Human Genetics, Roosevelt Drive, Oxford, UK)*
R. Hitchman *(Evotec (UK) Ltd, Milton Park, Abingdon, UK)*
M. Dumoux *(Diamond Light Source, Harwell Campus, Didcot, UK; Protein Production UK, Research Complex at Harwell, STFC Rutherford Appleton Laboratory, Harwell Campus, Didcot, UK)*
C. Hawes *(Oxford Brookes University, Headington Campus, Oxford, UK)*

Knowledge of protein signalling pathways in the working cell is seen as a primary route to identifying and developing targeted medicines. In recent years there has been a growing awareness of the importance of the mTOR pathway, making it an attractive target for therapeutic intervention in several diseases. Within this pathway we have focused on S6 kinase 1 (S6K1), the downstream phosphorylation substrate of mTORC1, and specifically identify its juxtaposition with mTORC1. When S6K1 is co-expressed with raptor we show that S6K1 is translocated from the nucleus to the cytoplasm. By developing a novel biosensor we demonstrate in real-time, that phosphorylation and de-phosphorylation of S6K1 occurs mainly in the cytoplasm of living cells. Furthermore, we show that the scaffold protein raptor, that typically recruits mTOR substrates, is not always involved in S6K1 phosphorylation. Overall, we demonstrate how FRET-FLIM imaging technology can be used to show localisation of S6K1 phosphorylation in living cells and hence a key site of action of inhibitors targeting mTOR phosphorylation.

Reproduced from Ahmed, A.R., Owens, R.J., Stubbs, C.D. et al. Direct imaging of the recruitment and phosphorylation of S6K1 in the mTORC1 pathway in living cells. Sci Rep 9, 3408 (2019), under the terms of the Creative Commons Attribution 4.0 International (CC BY 4.0) License. doi: 10.1038/s41598-019-39410-z

Contact: S.W. Botchway (stan.botchway@stfc.ac.uk)

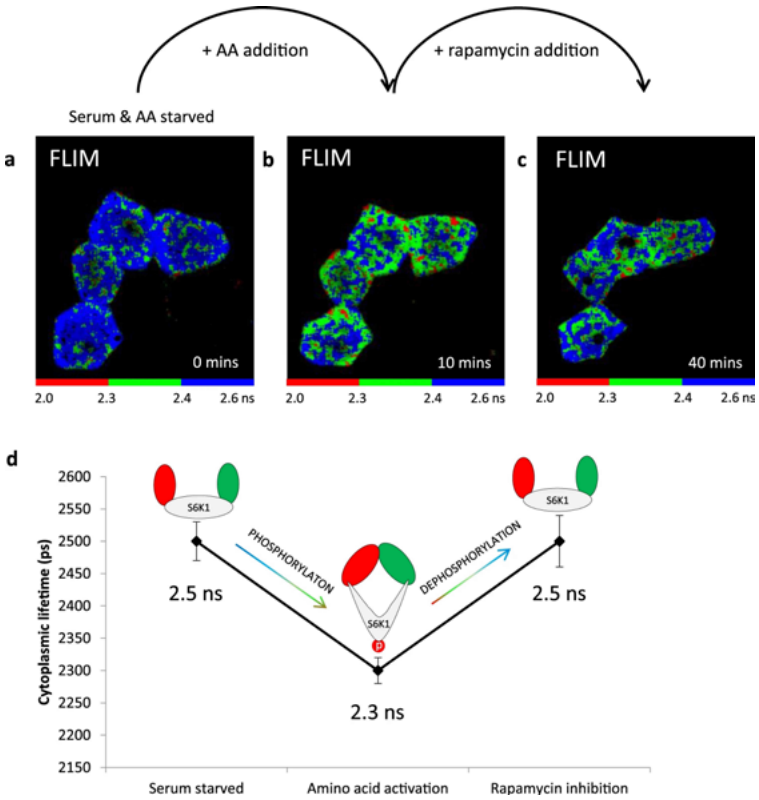

mTORC1 activation and inhibition using SensOR. (a) FLIM of serum and amino acid starved HEK293 cells expressing SensOR. (b) FLIM at 10 minutes following serine + leucine activation. (c) FLIM collected at 40 minutes after subsequent rapamycin treatment of serine + leucine activated cells for 30 minutes. (d) Summary of lifetime changes of SensOR with serum starvation, amino acid addition and rapamycin treatment from mean lifetimes and also pixel by pixel analysis of image with increased binning. Opening and closing of sensor also shown via schematics. Data representative of three independent experiments with errors representative of standard deviation, where two experiments were treated with leucine and the third treated with the combination of leucine and serine.

A highly dynamic F-actin network regulates transport and recycling of micronemes in *Toxoplasma Gondii* vacuoles

J. Periz, M. Del Rosario *(Wellcome Centre for Integrative Parasitology, Institute of Infection, Immunity & Inflammation, University of Glasgow, UK)*
A. McStea, L. Wang, M.L. Martin-Fernandez *(Central Laser Facility, Research Complex at Harwell, STFC Rutherford Appleton Laboratory, Harwell Campus, Didcot, UK)*
S. Gras *(Experimental Parasitology, Department for Veterinary Sciences, Ludwig-Maximilians-University Munich, Germany)*
M. Meissner *(Wellcome Centre for Integrative Parasitology, Institute of Infection, Immunity & Inflammation, University of Glasgow, UK; Experimental Parasitology, Department for Veterinary Sciences, Ludwig-Maximilians-University Munich, Germany)*
C. Loney *(MRC-University of Glasgow Centre for Virus Research, Sir Michael Stoker Building, Glasgow, UK)*

The obligate intracellular parasite *Toxoplasma Gondii* replicates in an unusual process, described as internal budding. Multiple daughter parasites are formed sequentially within a single mother cell, requiring replication and distribution of essential organelles such as micronemes. These organelles are thought to be formed de novo in the developing daughter cells. Using dual labelling of a microneme protein MIC2 and super-resolution microscopy, we show that micronemes are recycled from the mother to the forming daughter parasites using a highly dynamic F-actin network. While this recycling pathway is F-actin dependent, de novo synthesis of micronemes appears to be F-actin independent. The F-actin network connects individual parasites, supports long, multidirectional vesicular transport, and regulates transport, density and localisation of micronemal vesicles. The residual body acts as a storage and sorting station for these organelles. Our data describe an F-actin dependent mechanism in apicomplexans for transport and recycling of maternal organelles during intracellular development.

Reproduced from, Periz, J., Del Rosario, M., McStea, A. et al. A highly dynamic F-actin network regulates transport and recycling of micronemes in Toxoplasma Gondii vacuoles. Nat Commun 10, 4183 (2019), under the terms of the Creative Commons Attribution 4.0 International (CC BY 4.0) License. doi: 10.1038/s41467-019-12136-2

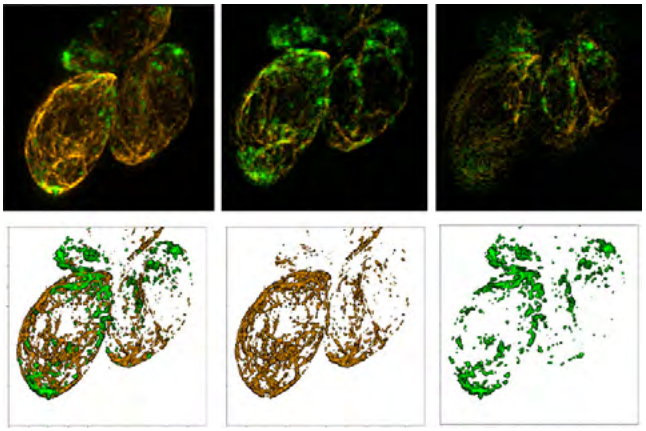

A mobile, interconnected F-actin network supports vesicular transport: 3D representative SIM image shows a continuous F-actin network connecting mother and daughter cells. Top row. 3D and z slices show continuous F-actin between mother and daughter. Bottom row. 3D surface rendered model and independent channel views comprising z stacks (z6–z15).

Contact: J. Periz (Javier.Periz@glasgow.ac.uk)
M. Meissner (Markus.Meissner@lmu.de)

Manipulation and deposition of complex, functional block copolymer nanostructures using optical tweezers

O.E.C. Gould, C.E. Boott (School of Chemistry, University of Bristol, UK)
S.J. Box, M.J. Miles *(School of Physics, University of Bristol, UK)*
A.D. Ward *(Central Laser Facility, Research Complex at Harwell, STFC Rutherford Appleton Laboratory, Harwell Campus, Didcot, UK)*
M.A. Winnik *(Department of Chemistry, University of Toronto, Canada)*
I. Manners *(School of Chemistry, University of Bristol, UK; Department of Chemistry, University of Victoria, Canada)*

Block copolymer self-assembly has enabled the creation of a range of solution-phase nanostructures with applications from optoelectronics and biomedicine to catalysis. However, to incorporate such materials into devices a method that facilitates their precise manipulation and deposition is desirable. Herein we describe how optical tweezers can be used to trap, manipulate, and pattern individual cylindrical micelles and larger hybrid micellar materials. Through the combination of TIRF imaging and optical trapping we can precisely control the three-dimensional motion of individual cylindrical block copolymer micelles in solution, enabling the creation of customizable arrays. We also demonstrate that dynamic holographic assembly enables the creation of ordered customizable arrays of complex hybrid block copolymer structures. By creating a program which automatically identifies, traps, and then deposits multiple assemblies simultaneously we have been able to dramatically speed up this normally slow process, enabling the fabrication of arrays of hybrid structures containing hundreds of assemblies in minutes rather than hours.

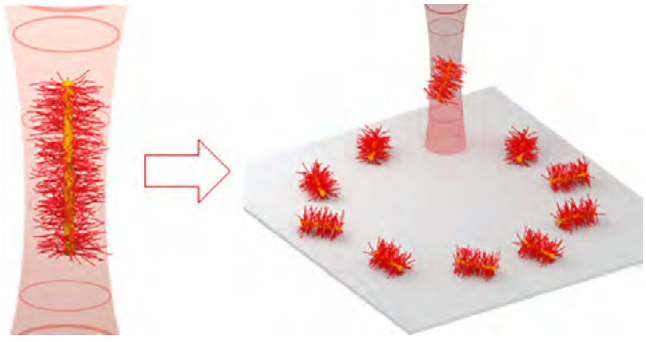

Reproduced from Gould OEC, Box SJ, Boott CE, et al. Manipulation and Deposition of Complex, Functional Block Copolymer Nanostructures Using Optical Tweezers. ACS Nano. 2019;13(4):3858-3866, © 2019 American Chemical Society, under the terms of an ACS AuthorChoice License. DOI: 10.1021/acsnano.9b00342

Contact M.J. Miles (mervyn.miles@bristol.ac.uk),
I. Manners (imanners@uvic.ca)

A global sampler of single particle tracking solutions for single molecule microscopy

M. Hirsch, D.J. Rolfe, L.C. Zanetti-Domingues, M.L. Martin-Fernandez *(Central Laser Facility, Research Complex at Harwell, STFC Rutherford Appleton Laboratory, Harwell Campus, Didcot, UK)*
R. Wareham, S.S. Singh *(Department of Engineering, University of Cambridge, UK)*
J.W. Yoon *(Center for Information Security Technology, Korea University, Seoul, South Korea)*
M.P. Hobson *(Department of Physics, University of Cambridge, UK)*
P.J. Parker *(School of Cancer and Pharmaceutical Sciences, King's College London, UK; Phosphorylation Laboratory, The Francis Crick Institute, London, UK)*

The dependence on model-fitting to evaluate particle trajectories makes it difficult for single particle tracking (SPT) to resolve the heterogeneous molecular motions typical of cells. We present here a global spatiotemporal sampler for SPT solutions using a Metropolis-Hastings algorithm. The sampler does not find just the most likely solution but also assesses its likelihood and presents alternative solutions. This enables the estimation of the tracking error. Furthermore the algorithm samples the parameters that govern the tracking process and therefore does not require any tweaking by the user. We demonstrate the algorithm on synthetic and single molecule data sets. Metrics for the comparison of SPT are generalised to be applied to a SPT sampler. We illustrate using the example of the diffusion coefficient how the distribution of the tracking solutions can be propagated into a distribution of derived quantities. We also discuss the major challenges that are posed by the realisation of a SPT sampler.

Reproduced from Hirsch, Michael et al. A global sampler of single particle tracking solutions for single molecule microscopy. PloS one vol. 14,10 e0221865. 28 Oct. 2019, under the terms of the Creative Commons Attribution 4.0 International (CC BY 4.0) License. doi:10.1371/journal.pone.0221865

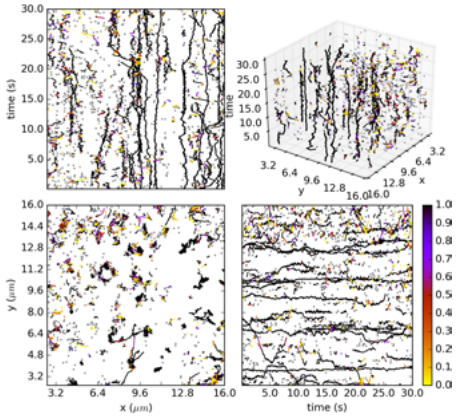

Two views on the tracking result for an SMM data set with 9761 observations. 4000 samples have been recorded. Links that appear in all samples are shown in blue. The colour of the other links indicates their frequency of occurrence as shown by the colour bar. Observations that are assigned to the clutter in all samples are shown as grey dots.

Contact: D.J. Rolfe (daniel.rolfe@stfc.ac.uk)

Miro2 tethers the ER to mitochondria to promote mitochondrial fusion in tobacco leaf epidermal cells

R.R. White, I. Leaves, J. Metz *(Biosciences, CLES, Exeter University, UK)*
C. Lin (*Department of Mathematics, Harrison Building, University of Exeter, UK; Center for Mathematical Sciences, Huazhong University of Science and Technology, Wuhan, China; Key Lab of Engineering Modeling and Scientific Computing, Huazhong University of Science and Technology, Wuhan, China)*
I.G. Castro *(Biosciences, CLES, Exeter University, UK; Department of Molecular Genetics, Weizmann Institute of Science, Rehovot 7610001, Israel)*
B.C. Bateman, S.W. Botchway, A.D. Ward *(Central Laser Facility, Research Complex at Harwell, STFC Rutherford Appleton Laboratory, Harwell Campus, Didcot, UK)*
P. Ashwin *(Department of Mathematics, Harrison Building, University of Exeter, UK)*
I. Sparkes *(Biosciences, CLES, Exeter University, UK ; School of Biological Sciences, University of Bristol, UK)*

Mitochondria are highly pleomorphic, undergoing rounds of fission and fusion. Mitochondria are essential for energy conversion, with fusion favouring higher energy demand. Unlike fission, the molecular components involved in mitochondrial fusion in plants are unknown. Here, we show a role for the GTPase Miro2 in mitochondria interaction with the ER and its impacts on mitochondria fusion and motility. Mutations in AtMiro2's GTPase domain indicate that the active variant results in larger, fewer mitochondria which are attached more readily to the ER when compared with the inactive variant. These results are contrary to those in metazoans where Miro predominantly controls mitochondrial motility, with additional GTPases affecting fusion. Synthetically controlling mitochondrial fusion rates could fundamentally change plant physiology by altering the energy status of the cell. Furthermore, altering tethering to the ER could have profound effects on subcellular communication through altering the exchange required for pathogen defence.

Reproduced from White, R.R., Lin, C., Leaves, I. et al. Miro2 tethers the ER to mitochondria to promote mitochondrial fusion in tobacco leaf epidermal cells. Commun Biol 3, 161 (2020), published by Springer Nature, under the terms of the Creative Commons Attribution 4.0 International License. doi: 10.1038/s42003-020-0872-x

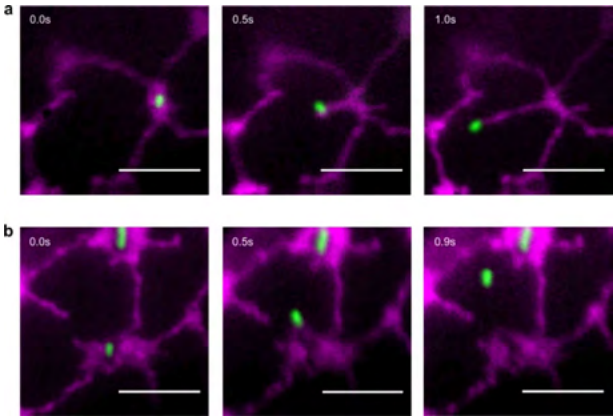

Mitochondria are physically attached to the ER. Consecutive TIRF microscopy images showing ER (magenta) either following a or separating b from a mitochondrion (mito, green) that has been optically trapped and moved using an automated routine; trapping laser power of 40 mW, moved 6 μm at 6 μms^{-1}. Scale bar indicates 5 μm, time is indicated in seconds (s). Cells were treated with latrunculin b.

Contact: I. Sparkes (i.sparkes@bristol.ac.uk)

Gemini operational statistics

S. Hawkes *(Central Laser Facility, STFC Rutherford Appleton Laboratory, Harwell Campus, Didcot, UK)*

During the reporting year, April 19 – April 20, a total of 6 complete experiments were delivered in the Astra-Gemini Target Area and 2 experiments in TA2. In total 35 high power laser experimental weeks were delivered the Gemini Target Area and 25 weeks to TA2. The delivered schedule is presented in Figure 2.

The availability of the Gemini laser system (delivery to the Gemini Target Area) was 88% during normal working hours, rising to 140% with time made up from running out of normal working hours. The reliability of the Gemini laser was 92%. An individual breakdown of the availability and reliability for the experiments conducted is presented in Figure 1.

TA2 availability was 77% during normal working hours, rising to 123% with time made up from running out of normal working hours. The reliability of the Gemini laser was 84%

The high levels of total availability were made possible by the continued unique operational model employed on Gemini, which involves running the laser late into the evening. In addition, frequent weekend operational days were made available.

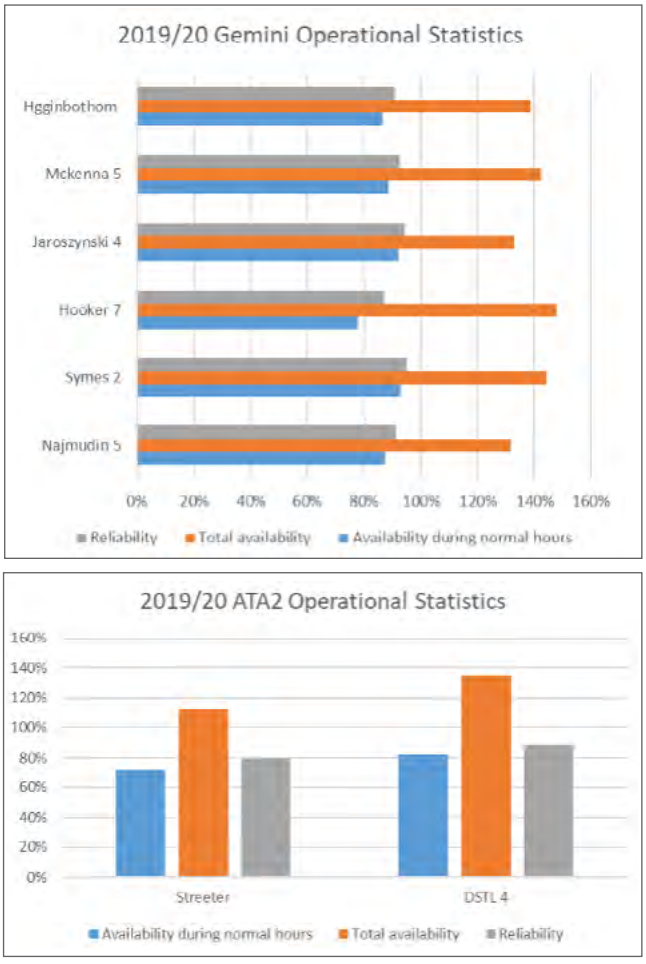

Figure 1: 2019/20 Gemini/TA2 operational statistics.

Week beginning	Gemini	TA2
01/04/2019	Set up	
08/04/2019		
15/04/2019		
22/04/2019	Najmudin 18110022	
29/04/2019		
06/05/2019		
13/05/2019		
20/05/2019	Maintenance	
27/05/2019	Symes 18210006	
03/06/2019		
10/06/2019	Set up	
17/06/2019		
24/06/2019		
01/07/2019	Hooker 18210006	Streeter 18210012
08/07/2019		
15/07/2019		
22/07/2019		
29/07/2019	Extension	Extension
05/08/2019	Maintenance	
12/08/2019		
19/08/2019	Compressor installation	
26/08/2019	Jaroszynski 18210027	Streeter 18210012
02/09/2019		
09/09/2019		
16/09/2019		
23/09/2019		Streeter 18210012
30/09/2019		
07/10/2019		
14/10/2019	Extension	
21/10/2019	Maintenance	
28/10/2019	Set up	Streeter 18210012
04/11/2019	Mckenna 18210005	
11/11/2019		
18/11/2019		Commercial access 20110014
25/11/2019		
02/12/2019		
09/12/2019		
16/12/2019	Extension	
23/12/2019	Christmas	
30/12/2019		
06/01/2020	Electrical shutdown	
13/01/2020	Maintenance	
20/01/2020	Higginbotham 19210013	Commercial access 20110014
27/01/2020		
03/02/2020		
10/02/2020		
17/02/2020		
24/02/2020	System access	System access

Figure 2: 2019/20 Gemini/TA2 operational schedule.

Contact: S. Hawkes (steve.hawkes@stfc.ac.uk)

Octopus and Ultra operational statistics

B. C. Bateman, M. Szynkiewicz, E. Gozzard, I. P. Clark, D.T. Clarke *(Central Laser Facility, STFC Rutherford Appleton Laboratory, Harwell Campus, Didcot, UK)*

Octopus facility
In the reporting period (April 2019 to March 2020), 46 unique User groups submitted a total of 57 proposals bidding for time at the Octopus facility. 37 experiments comprising 85 weeks of access time were awarded to the UK User community throughout the year. A full breakdown of number of weeks applied for versus number of weeks scheduled is shown in Figure 1, indicating an oversubscription ratio of 1.71:1. Figure 3 shows that Biology and Bio-materials formed the majority of applications.

There were a total of 24 formal reviewed publications recorded throughout the year.

Ultra facility
In the reporting period (April 2019 to March 2020), 32 unique User groups submitted a total of 40 proposals bidding for time at the Ultra facility. 26 experiments comprising 61 weeks of access time were awarded to the UK User community. A full breakdown of number of weeks applied for versus number of weeks scheduled is shown in Figure 2, indicating an oversubscription ratio of 1.52:1. Figure 4 shows that Chemistry formed the majority of applications.

There were a total of 21 formal reviewed publications recorded throughout the year.

Octopus and Ultra availability
There was a total of 282 hours downtime reported over the combined 104 weeks of delivered access during this reporting period.

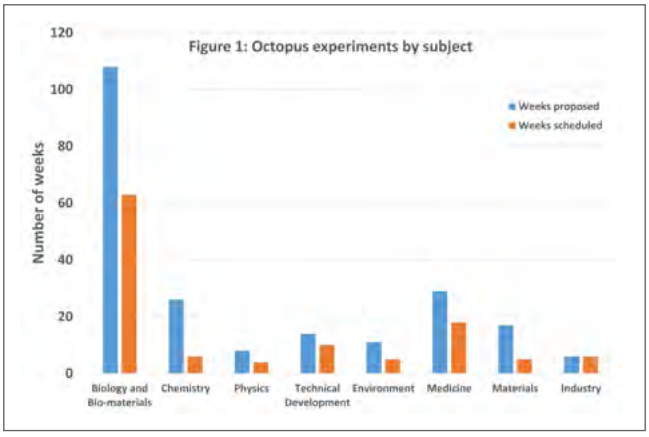

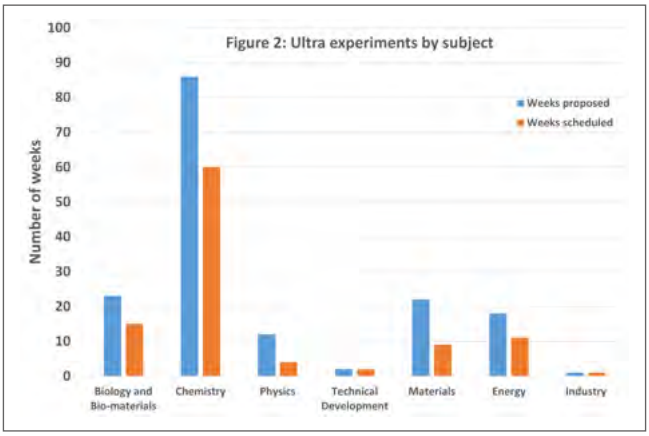

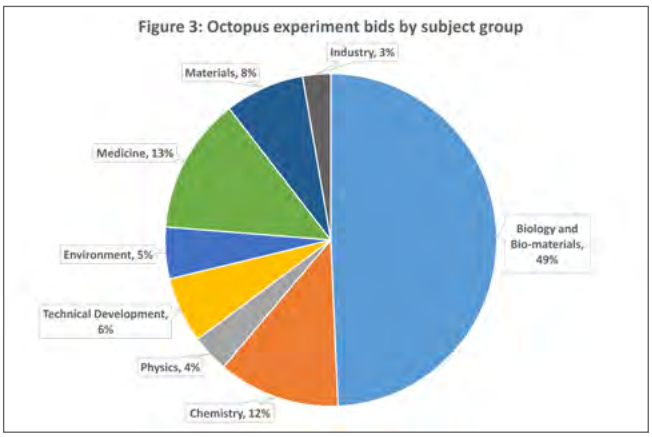

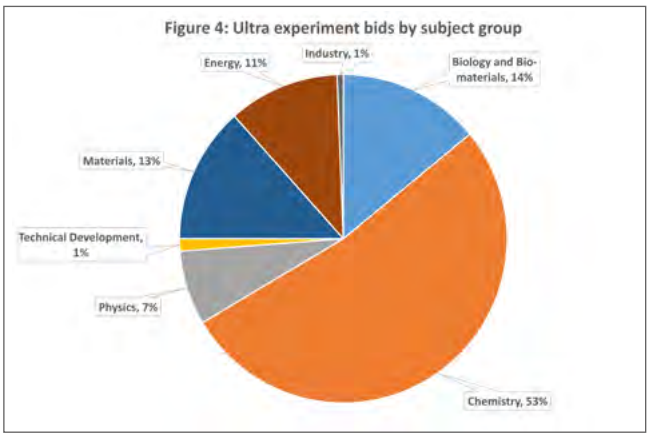

Contact: D.T. Clarke (dave.clarke@stfc.ac.uk)

Target Fabrication operational statistics

D. Haddock, C. Spindloe & M.K. Tolley *(Target Fabrication Group, Central Laser Facility, STFC Rutherford Appleton Laboratory, Harwell Campus, Didcot, UK)*

Experimental Support

This paper details Target Fabrication support given to experimental groups in the Vulcan target areas TAW and TAP, along with those in the Gemini Target Area, between April 2019 and April 2020. Target Fabrication supported five solid target Vulcan experiments and one solid target Gemini experiment, totalling 45 weeks of Vulcan access (plus training weeks) and 5 weeks of Gemini access. Additional experiments were also supported with filters and other diagnostic elements which are non-trivial but not reported on in these statistics. At 50, the total number of weeks supported is less than the previous year (60 in 2018-2019). The years previous to that were 71 weeks in 2017-2018, 56 in 2016-2017 and 57 in 2015-2016. This reporting period included the start of the national lockdown in response to the COVID-19 pandemic. Experiments scheduled for March were delayed and their analysis will be covered in subsequent reports.

The Target Fabrication Group also supports academic access experiments at AWE and internal activities run by facility staff; however, due to the low-level nature of support, it is not covered in this report.

Gemini and Vulcan target types are separated out when described in tables and graphics. Gemini targets are produced in arrays or tapes; with multiple shots available per object delivered, each position on the array or tape is referred to as an individual target. Quantifying such types alongside Vulcan single-shot targets disproportionately skews analysis. Gemini almost exclusively requires ultra-thin films which, although they are manufactured similarly to Vulcan targets, end up being used very differently in experiments.

1) Supported experiments

For the reporting year the total number of targets produced for each experiment is shown in Table 1. To better understand the amount of resources required for each experiment a classification of complexity is used:

- Class 1 Targets that require few resources and can typically be made with no specialist equipment with materials widely available from suppliers. Examples: i) micron thick foils, ii) wires glued to posts
- Class 2 Targets that require specialist manufacturing equipment and knowledge but manufacture is a well-established process in Target Fabrication. Examples: i) nanometre thick coatings, ii) multi-layered coatings
- Class 3 Targets that require long-term R&D and multiple technologies - also referred to as "high-specification targets". Examples: i) complex 3D assemblies, ii) foams, iii) structured MEMS coatings

The classification system and Table 1 show how Target Fabrication's resources were used throughout the reporting year. For example, the system can then be used to separate out experiments that use a high-number of targets requiring low amount of resource, compared with experiments that require multiple capabilities and resources to produce a few very high specification targets. The year saw a relatively even distribution of Class 3 experiments, which is in contrast to last reporting year in which two high-complexity experiments were concentrated in January and February. TAW experiments are typically complex with a higher proportion of their targets being Class 3. This is unsurprising because TAW experiments often use multiple probing beams from multiple angles, allowing 3D geometries to be investigated.

Experiment		Total Targets Produced	Class 1	Class 2	Class 3
VULCAN	0419 TAW	131	36	49	46
	0619 TAP	167	133		34
	0719 TAW*				
	0819 TAW	175	113		62
	1019 TAP	170	154		15
	1119 TAW	131	78		53
	Total	**775**	**514**	**49**	**210**
GEMINI	0419 GTA*				
	0619 GTA*				
	1119 GTA			2825	
	Total			**2825**	

Table 1: Targets produced by experiment and their relative complexity. (Class 3 targets have the highest complexity and Class 1 are the simplest targets to produce.)

**Specialist support given but no targets delivered.*

The total number of targets supplied to target areas at RAL by Target Fabrication this reporting period was 775 for Vulcan and 2825 for Gemini. The large number of targets delivered to Gemini can be explained by the 25 position mounting arrays. 113 arrays were delivered in total.

The number of high specification targets this year was 210 which is a reduction on the previous year's total of 323, but an increase on 119 in 2017-2018 and 98 in 2016-2017. The high number last year can be attributed to the particularly demanding 0319TAW experiment, which accounted for 190 high-specification targets.

2) Experimental Response

It is seen as a significant strength of Target Fabrication to be rapidly responsive to experimental results and conditions by working collaboratively with user groups. The Group responds to experimental changes during a campaign and often implements a number of modifications or redesigns to the original requests. The number of modifications and variations differs on each experiment and is dependent on the type of experiment and also on external conditions such as diagnostic and laser performance.

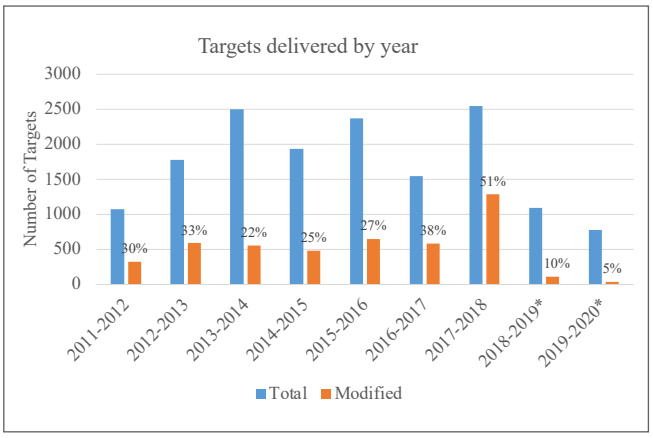

Chart 1: Total targets delivered by year showing the percentage that were modified from initial deliverables. Modified targets include any delivered targets that did not appear on the initial agreed target request.

**This reporting year and last only Vulcan targets are included. For Gemini no modifications were required to the 2825 targets delivered; thin film targets are pre-prepared and are therefore far less likely to be changed.*

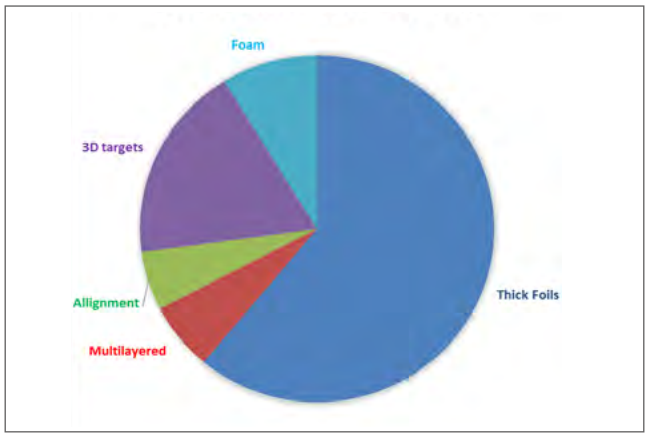

Chart 2: Target types (by number) for 2019-2020 delivered to Vulcan.

Target Fabrication's Quality Management System (QMS) ensures that there is tracking of all targets that are modified from the initial design. Modified targets include a) those that were delivered but not initially specified on the approved target list, b) modifications to approved designs, or c) completely new requests arising during campaigns. It is important to note that the capability to change designs can often ensure experimental success. For the reporting year the data on modified targets is shown in Chart 1.

Chart 1 shows that this reporting year and the previous had far fewer modified requests compared to previous years; good evidence that the experiments in this reporting year ran more-or-less in line with the target requests.

3) Target Categories

Targets can be separated into six main categories as shown in Table 2 and Chart 2.

Description of the types is as follows:

- Ultra-thin foil targets are specified as having a thickness <500 nm which require a coating capability and a skilled fabricator to process. Thick foils make up the rest of the >500nm single component foils
- Multilayer foils are stacks or layers of foils that require thin film coating capability to deposit multiple layers onto an existing foil; they are often different composition layers with different thicknesses
- Alignment targets are wires or pinholes that are used for set-up purposes
- 3D micro-structures are complex 3D geometries that combine multiple fabrication techniques with skilled assembly. Typically requires specialist micro-machining
- Foams are porous structures produced by novel chemistry techniques

Demand for high-specification 3D assemblies has been high for the past two years. This is the most challenging and time consuming target type which often incorporates multiple technologies such as micro-machining, coating and foams assembled into one object. Ultra-thin foils have been exclusively shot on Gemini this year with none requested on Vulcan which is the first time this has happened in recorded statistics.

It should be noted that Chart 2 is not a reflection of staff effort; assembly time for a single thick foil target is relatively short whereas for a batch of 3D targets R&D trials, manufacture and characterisation activities can amount to weeks of effort.

Target Category	2019-2020	2018-2019	2017-2018	2016-2017	2015-2016	2014-2015
Ultra-thin Foil	0	485	485	449	197	530
Thick Foils	472	2017	1208	743	1349	708
Multi-layered Foils	49	577	577	237	605	500
Alignment	42	2016	159	78	110	85
3D assemblies	142	73	73	38	99	82
Foams	68	2015	47	0	11	0
TOTAL	**775***	**2551**	**2551**	**1546**	**2371**	**1937**

*Table 2: Target type by year. *Only Vulcan targets are recorded in the totals. Gemini targets totalled 2825 for the year all of which were ultra-thin foils.*

Adapting to Demand

Experiments usually require similar targets with varying thickness, composition or geometry; for example, a thin foil experiment typically requests a thickness scan of a particular material. In such experiments each thickness or composition change requires a separate thin-film coating run. Experiments using 3D targets require a new assembly set up for every geometry change. Each new target thickness or geometry is designated a "unique variation". This reporting period within the 775 targets for Vulcan there were 110 unique variations which averages to nearly 7 targets per variation. Last reporting period the average number was 5 targets per variation, 7 in 2017-2018, and 7 in the two preceding reporting periods.

The number of targets per variation is a good measure of how complicated delivery is to an experiment. For example the 1019TAP experiment only required 15 different target iterations in the 170 delivered. One of those target iterations, "15um Gold foil on standard post", accounting for 152 targets. On the other hand 0419TAW required 32 iterations with 131 targets delivered. 0419TAW is a good example of an experiment that not only required a high quantity of Class 3 targets (see Table 1) but also many iterations in addition to the intrinsic target fabrication complexity. The flexibility provided by the Group to produce targets variations is a key capability of the CLF and enables the user community to fully utilize the limited time that is available during each experiment.

4) Waste Reduction

Unexpected delays or changes during an experiment often result in a number of targets that have been fabricated but that are not used by the end of an experimental campaign. Un-shot targets in this reporting period totalled 24 accounting for only 5% of the total targets made. The comparison with previous years can be seen in Chart 3. A value of 5% appears very low compared to previous years. An explanation for this could be that this reporting year saw few high-quantity low-complexity experiments. Low complexity experiments ask for more modifications because the targets are easier to change in an experiment. Also targets changes can be made if there are temporary issues with laser and diagnostic performance.

Any un-issued or returned targets are carefully sorted and high specification targets are stored under closely controlled conditions for potential use on future experiments. Where possible all spare target components and mounts are also stored for future use. The variety of mounts and components held in stock contributes to the Group's ability to adapt target designs quickly in response to experimental changes. Target Fabrication also continued to expand its 3D printing capability to manufacture the majority of target posts; both reducing costs and improving adaptability and responsiveness.

Targets that don't meet the user's requirements are recorded as non-conformities. Only 1 target was returned as non-conforming in the reporting period. The number is unlikely to be representative of the real non-conformity rate this reporting year and accurate ongoing recording

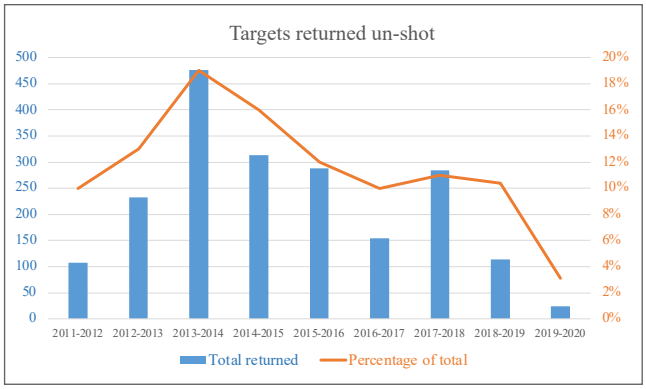

Chart 3: Total number of targets returned un-shot (in blue). The orange line shows the returned targets as a percentage of total targets delivered in that reporting year.

continues to be a challenge. In addition a number of internal non-conformities are found during the production phase which (obviously) are not issued to the user groups. It is a difficult metric to track; non-conforming targets might be recorded as "returned un-shot" or possibly targets will be un-used without notification to the Target Fabrication of the reason. Work is ongoing to ensure user groups record targets that do not meet their requirements as "non-conforming". However, the non-conformity rate is still expected to be low because Target Fabrication quality controls the targets before delivery as part of the manufacturing process. Target Fabrication update characterisation records of each target for the users to access during the experiment.

Orion Academic Access

The Target Fabrication Group has continued to support and supply targets to the Orion Academic Access campaign. In the reporting year targets were delivered to an experiment led by Queen's University Belfast investigating ion and neutron beam production. This experiment used a combination of ultra-thin foils and complex coil targets that required a large amount of fabrication time and effort. A final total of 64 complex targets were delivered and a number of targets were made during the experimental run which added resource demand. The targets required the integration of a range of complex assembly and characterisation capabilities across STFC including collaboration with the Technology Department for the manufacture of precision coils and Scitech Precision Ltd for the laser machining of target components.

External Contracts

Scitech Precision Ltd (a spinout company from the Central Laser Facility) provides high power laser targets and micro engineering solutions to the high power laser community and supplies targets, specialist coatings, laser machining services and consultancy across the world. In the reporting year 2019-2020 the company provided services to 32 individual institutions with a total number of contracts totalling 120. Of the contracts 55% were for high power

laser targets, 34% for laser micromachining, 2% for phase plates, and 9% for target delivery system contracts. The spread of contracts is similar to the previous year with approximately one-third of the business being laser machining support for the Harwell Campus (including Diamond Light Source) and a number of spin out and spin in companies. Target contracts were delivered to large scales facilities including experiments carried out on the Orion laser at AWE, LMJ in France, SG-II in China and LLE in the US.

Summary

Target Fabrication has delivered targets to six experiments in the CLF this reporting year. Two experiments scheduled for March 2020 were rescheduled due to national lockdown and will fall into the scope of next year's report.

The total number of targets delivered to Vulcan is lower this reporting year than usual, in part because of the laboratory shutdown and also because there were no TAP experiments requiring low-complexity, high-quantity targets. Instead this year saw a marked increase in the number of high-complexity experiments spread across the year.

Target Fabrication has supported nine experiments in the CLF and twelve in other international facilities in the last year, as well as providing an increasing amount of characterisation services and acting as a knowledge base for target fabrication activities throughout Europe.

References

1. *D. Haddock, C. Spindloe & M. Tolley, Target Fabrication Operational Statistics, CLF Annual Report 2018-2019*
2. *D. Haddock, C. Spindloe & M. Tolley, Target Fabrication Operational Statistics, CLF Annual Report 2017-2018, p45-48*
3. *D. Haddock, C. Spindloe & M. Tolley, Target Fabrication Operational Statistics, CLF Annual Report 2016-2017, p48-50*
4. *D. Haddock, C. Spindloe & M. Tolley, Target Fabrication Operational Statistics, CLF Annual Report 2015-2016, p49-51*
5. *D. Haddock, C. Spindloe & M. Tolley, Target Fabrication Operational Statistics, CLF Annual Report 2014-2015, p58-60*
6. *D. Haddock, C. Spindloe & M. Tolley, Target Fabrication Operational Statistics, CLF Annual Report 2013-2014, p68-70*
7. *D. Haddock, C. Spindloe & M. Tolley, Target Fabrication Operational Statistics, CLF Annual Report 2012-2013, p74-75*
8. *D. Haddock, C. Spindloe & M. Tolley, Target Fabrication Operational Statistics, CLF Annual Report 2011-2012 , p71-72*
9. *H. F. Lowe, C. Spindloe & M. Tolley, Target Fabrication Operational Statistics, CLF Annual Report 2010-2011 , p76-77*

Contact: D. Haddock (david.haddock@stfc.ac.uk)

Vulcan operational statistics

A.K. Kidd *(Central Laser Facility, STFC Rutherford Appleton Laboratory, Harwell Campus, Didcot, UK)*

Introduction

Vulcan has completed an active experimental year, with 31 full experimental weeks allocated to target areas TAW and TAP between April 2019 and March 2020; the schedule was interrupted in March 2020 due to Covid-19. Table 1 shows the operational schedule for the year, and reports the shot rate statistics for each experiment.

PERIOD	TAW	TAP
	2019	
22 Apr – 26 May	L Antonelli *High resolution phase contrast imaging of strong shock-cloud interactions* (74, 26, 64.9%) (85.3%, 104.2%) (5 weeks) 18210019	
01 Jul / 24 Jun – 28 Jul	N Woolsey *Measuring the dynamics of magnetic fields in high energy-density plasmas* (56, 9, 83.9%) (89.6%, 109.8%) (4 weeks) 18110017	M Borghesi *Irradiation of 3D cell models with high-flux, high-energy laser-driven protons* (139, 10, 92.8%) (87.6%, 103.8%) (5 weeks) 18210022
26 Aug – 06 Oct	F Keenan *Generation of high photoionization parameter plasmas to simulate accretion-powered astronomical X-ray sources* (133, 5, 96.2%) (83.0%, 113.9%) (6 weeks + 2 day overrun) 18210003	
28 Oct – 08 Dec / 01 Dec	P Norreys *Monoenergetic ion beam from collisionless shocks* (64, 18, 71.9%) (87.7%, 112.0%) (6 weeks) 18210002	M Borghesi *Sub-lethal effects of proton irradiation of cellular media at ultra-high dose rate* (187, 34, 81.8%) (86.5%, 126.6%) (5 weeks + 3½ day overrun) 19210020
	2020	
02 Mar – 05 Apr	C Palmer **Laboratory investigation of dust charging and destruction in shocked plasma** (Experiment interrupted due to Covid-19) 19210011	D Carroll *Investigation of EMP emissions for understanding the source mechanisms and the rules for tuning and employing them in high power lasers* (Experiment interrupted due to Covid-19) 19210019

Table 1: Experimental schedule for the period April 2019 – March 2020.

(Total shots fired, failed shots, reliability)
(Availability normal, additional hours)

Numbers in parentheses indicate the total number of full energy laser shots delivered to target, followed by the number of these that failed and the percentage of successful shots. The second set of numbers are the availability of the laser to target areas during normal operating hours and including outside hours operations.

The total number of full disc amplifier shots that have been fired to target this year is 653. Table 2 shows how this figure compares with that for the four previous years. 102 shots failed to meet user requirements. The overall shot success rate to target for the year is 84%, compared to 91%, 90%, 86% and 81% in the previous four years. Figure 1 shows the reliability of the Vulcan laser to all target areas over the past five years.

Year	No of shots	Failed shots	Reliability
15–16	1143	108	91%
16–17	948	93	90%
17–18	934	132	86%
18–19	607	113	81%
19–20	653	102	84%

Table 2: Shot totals and proportion of failed shots for the past five years.

The shot reliability to TAW is 82%, up 2% from the previous year. The shot reliability to TAP is 84% - down from 86% in 2018-19.

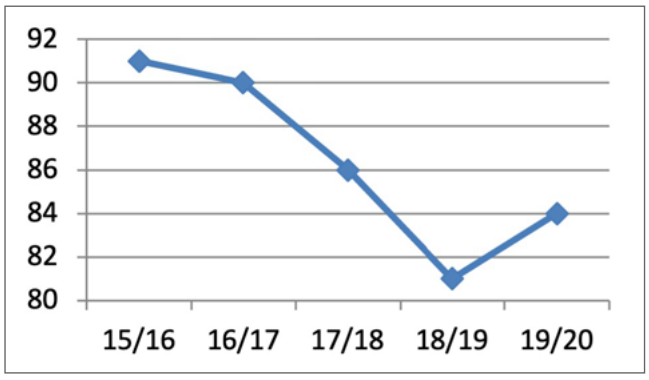

Figure 1: All areas shot reliability for each year 2015-16 to 2019-20.

Analysis of the failure modes reveals that the overriding causes of failed shots are beam alignment, front end related issues and triggering. The first two causes are manifested in low or high energy output of the rod amplifier chain (outside of +/-20% of the requested energy). Instability in the pulse energy is introduced during propagation from the front end room to the laser area> Novel methods of beam stabilization are being investigated to improve this fault mode.

There is a requirement which was originally instigated for the EPSRC FAA that the laser system be available, during the five week periods of experimental data collection, from 09:00 to 17:00 hours, Monday to Thursday, and from 09:00 to 16:00 hours on Fridays (a total of 195 hours over the five week experimental period). The laser has not always met the startup target of 9:00 am but it has been common practice to operate the laser well beyond the standard contracted finish time on several days during the week. In addition, the introduction of early start times on some experiments continues to lead to improvements in availability.

On average, Vulcan has been available for each experiment to target areas for 86.7% of the time during contracted hours, compared with 85.1% for the previous year. The overall availability to all target areas has remained constant at 112.6% compared with 112.9% in 2018-19. The time that the laser is unavailable to users is primarily the time taken for beam alignment at the start of the day.

Contact: A.K. Kidd (andy.kidd@stfc.ac.uk)

Publications

Journal Papers

ARTEMIS

P Hollebon, O Ciricosta, MP Desjarlais, C Cacho, C Spindloe, E Springate, ICE Turcu, JS Wark, SM Vinko
Ab initio simulations and measurements of the free-free opacity in aluminum
PHYSICAL REVIEW E, **100**, 43207 (2019)

K Volckaert, H Rostami, D Biswas, I Marković, F Andreatta, CE Sanders, P Majchrzak, C Cacho, RT Chapman, A Wyatt, E Springate, D Lizzit, L Bignardi, S Lizzit, SK Mahatha, M Bianchi, N Lanata, PDC King, JA Miwa, AV Balatsky, P Hofmann, S Ulstrup
Momentum-resolved linear dichroism in bilayer MoS_2
PHYSICAL REVIEW B, **100**, 241406 (2019)

EM Warne, B Downes-Ward, J Woodhouse, MA Parkes, D Bellshaw, E Springate, P Majchrzak, Y Zhang, G Karras, AS Wyatt, RT Chapman, A Kirrander, RS Minns
Photodissociation dynamics of CH3I probed via multiphoton ionisation photoelectron spectroscopy
PHYSICAL CHEMISTRY CHEMICAL PHYSICS, **21**, 11142-11149 (2019)

L Longetti, M Randulová, J Ojeda, L Mewes, L Miseikis, J Grilj, A Sanchez-Gonzalez, T Witting, T Siegel, Z Diveki, F van Mourik, R Chapman, C Cacho, S Yap, JWG Tisch, E Springate, JP Marangos, P Slavíček, CA Arrell, M Chergui
Photoemission from non-polar aromatic molecules in the gas and liquid phase
PHYSICAL CHEMISTRY CHEMICAL PHYSICS, **22**, 3965-3974 (2020)

Y Zhang, DT Payne, CL Pang, C Cacho, RT Chapman, E Springate, HH Fielding, G Thornton
State-Selective Dynamics of TiO_2 Charge-Carrier Trapping and Recombination
JOURNAL OF PHYSICAL CHEMISTRY LETTERS, **10**, 5265-5270 (2019)

R Liu, M Lin, P Chen, T Suzuki, PCJ Clark, NK Lewis, C Cacho, E Springate, C Chang, K Okazaki, W Flavell, I Matsuda, T Chiang
Symmetry-breaking and spin-blockage effects on carrier dynamics in single-layer tungsten diselenide
PHYSICAL REVIEW B, **100**, 214309 (2019)

F Andreatta, H Rostami, AG Čabo, M Bianchi, CE Sanders, D Biswas, C Cacho, AJH Jones, RT Chapman, E Springate, PDC King, JA Miwa, A Balatsky, S Ulstrup, P Hofmann
Transient hot electron dynamics in single-layer TaS_2
PHYSICAL REVIEW B, **99**, 165421 (2019)

CALTA

S Banerjee, PJ Phillips, J Nygaard, PD Mason, K Ertel, M De Vido, T Butcher, S Tomlinson, J Smith, R Allott, C Edwards, J Collier
Acoustic signature of laser shock peening for a qualitative evaluation of residual stresses
APPLIED PHYSICS A MATERIALS SCIENCE AND PROCESSING, **125**, 571 (2019)

M De Vido, A Wojtusiak, K Ertel
***High-resolution absorption measurement at the zero phonon line of Yb:YAG between 80 K and 300* K**
OPTICAL MATERIALS EXPRESS, **10**, 717-723 (2020)

RK Zhukavin, SG Pavlov, N Stavrias, K Saeedi, KA Kovalevsky, PJ Phillips, VV Tsyplenkov, NV Abrosimov, H Riemann, N Deβmann, H Hübers, VN Shastin
Influence of uniaxial stress on phonon-assisted relaxation in bismuth-doped silicon
JOURNAL OF APPLIED PHYSICS, **127**, 35706 (2020)

M Sawicka-Chyla, M Divoky, O Slezak, M De Vido, A Lucianetti, T Mocek
***Numerical Analysis of Thermal Effects in a Concept of a Cryogenically Cooled Yb:YAG Multislab 10* J/100-Hz Laser Amplifier**
IEEE JOURNAL OF QUANTUM ELECTRONICS, **55**, 1-8 (2019)

M De Vido, K Ertel, A Wojtusiak, PD Mason, PJ Phillips, S Banerjee, JM Smith, TJ Butcher, C Edwards
Optical rotatory power of quartz between 77 K and 325 K for 1030 nm wavelength
OPTICAL MATERIALS EXPRESS, **9**, 2708-2715 (2019)

M Divoky, J Pilar, M Hanus, P Navratil, M Sawicka-Chyla, M De Vido, PJ Phillips, K Ertel, T Butcher, M Fibrich, JT Green, M Koselja, J Preclikova, J Kubat, J Houzvicka, B Rus, J Collier, A Lucianetti, T Mocek
Performance comparison of Yb:YAG ceramics and crystal gain material in a large-area, high-energy, high average-power diode-pumped laser
OPTICS EXPRESS, **28**, 3636-3646 (2020)

CN Danson, C Haefner, J Bromage, T Butcher, JF Chanteloup, EA Chowdhury, A Galvanauskas, LA Gizzi, J Hein, DI Hillier, NW Hopps, Y Kato, EA Khazanov, R Kodama, G Korn, R Li, Y Li, J Limpert, J Ma, CH Nam, D Neely, D Papadopoulos, RR Penman, L Qian, JJ Rocca, AA Shaykin, CW Siders, C Spindloe, S Szatmári, RMGM Trines, J Zhu, P Zhu, JD Zuegel
Petawatt and exawatt class lasers worldwide
HIGH POWER LASER SCIENCE AND ENGINEERING, **7**, e54 (2019)

GEMINI

A McIlvenny, D Doria, L Romagnani, H Ahmed, P Martin, S Williamson, E Ditter, O Ettlinger, G Hicks, P McKenna, Z Najmudin, D Neely, S Kar, M Borghesi
Absolute calibration of microchannel plate detector for carbon ions up to 250 MeV
JOURNAL OF INSTRUMENTATION, **14**, C04002 (2019)

A McIlvenny, H Ahmed, C Scullion, D Doria, L Romagnani, P Martin, K Naughton, A Sgattoni, D Symes, A Macchi, P McKenna, M Zepf, S Kar, M Borghesi
Characteristics of ion beams generated in the interaction of ultra-short laser pulses with ultra-thin foils
PLASMA PHYSICS AND CONTROLLED FUSION, **62**, 54001 (2020)

MJ Duff, R Wilson, M King, B Gonzalez-Izquierdo, A Higginson, SDR Williamson, ZE Davidson, R Capdessus, N Booth, S Hawkes, D Neely, RJ Gray, P McKenna
High order mode structure of intense light fields generated via a laser-driven relativistic plasma aperture
SCIENTIFIC REPORTS, **10**, 105 (2020)

S Dann, C Baird, N Bourgeois, O Chekhlov, S Eardley, C Gregory, J Gruse, J Hah, D Hazra, S Hawkes, C Hooker, K Krushelnick, S Mangles, V Marshall, C Murphy, Z Najmudin, J Nees, J Osterhoff, B Parry, P Pourmoussavi, S Rahul, P Rajeev, S Rozario, J Scott, R Smith, E Springate, Y Tang, S Tata, A Thomas, C Thornton, D Symes, M Streeter
Laser wakefield acceleration with active feedback at 5 Hz
PHYSICAL REVIEW ACCELERATORS AND BEAMS, **22**, 41303 (2019)

A Alejo, GM Samarin, JR Warwick, G Sarri
Laser-Wakefield Electron Beams as Drivers of High-Quality Positron Beams and Inverse-Compton-Scattered Photon Beams
FRONTIERS IN PHYSICS, **7**, 49 (2019)

R Shalloo, C Arran, A Picksley, A von Boetticher, L Corner, J Holloway, G Hine, J Jonnerby, H Milchberg, C Thornton, R Walczak, S Hooker
Low-density hydrodynamic optical-field-ionized plasma channels generated with an axicon lens
PHYSICAL REVIEW ACCELERATORS AND BEAMS, **22**, 41302 (2019)

B Kettle, E Gerstmayr, M Streeter, F Albert, R Baggott, N Bourgeois, J Cole, S Dann, K Falk, I Gallardo González, A Hussein, N Lemos, N Lopes, O Lundh, Y Ma, S Rose, C Spindloe, D Symes, M Šmíd, A Thomas, R Watt, S Mangles
Single-Shot Multi-keV X-Ray Absorption Spectroscopy Using an Ultrashort Laser-Wakefield Accelerator Source
PHYSICAL REVIEW LETTERS, **123**, 254801 (2019)

M Mayr, L Ceurvorst, M Kasim, J Sadler, B Spiers, K Glize, A Savin, N Bourgeois, F Keeble, A Ross, D Symes, R Aboushelbaya, R Fonseca, J Holloway, N Ratan, R Trines, R Wang, R Bingham, L Silva, P Burrows, M Wing, P Rajeev, P Norreys
Wakefields in a cluster plasma
PHYSICAL REVIEW ACCELERATORS AND BEAMS, **22**, 113501 (2019)

LASER DEVELOPMENTS

M Galletti, G Archipovaite, P Oliveira, M Galimberti, I Musgrave, C Hernandez-Gomez
Broadband, picosecond two-stage optical parametrical chirped pulse amplification system at 100 Hz
PHYSICAL REVIEW ACCELERATORS AND BEAMS, **22**, 51301 (2019)

G Figueira, L Braga, S Ahmed, A Boyle, M Galimberti, M Galletti, P Oliveira
Pulse front tilt control using non-collimated beams in a single pass grating compressor
OPTICS EXPRESS, **28**, 7678-7690 (2020)

M Ahmad, M Galletti, P Oliveira, E Dilworth, DJ Robinson, M Galimberti, AJ Crawford, I Musgrave, MJD Esser
Time-resolved thermally induced aberrations in a flash-lamp pumped Nd:Glass disk amplifier using a 2 x 2 position sensitive detector array
REVIEW OF SCIENTIFIC INSTRUMENTS, **90**, 123106 (2019)

F Bisesto, M Galletti, A Curcio
Zemax ray tracing model for plasma waveguides
LASER PHYSICS LETTERS, **17**, 36001 (2020)

PLASMA PHYSICS

J Polz, APL Robinson, A Kalinin, GA Becker, RAC Fraga, M Hellwing, M Hornung, S Keppler, A Kessler, D Klöpfel, H Liebetrau, F Schorcht, J Hein, M Zepf, RE Grisenti, MC Kaluza
Efficient Laser-Driven Proton Acceleration from a Cryogenic Solid Hydrogen Target
SCIENTIFIC REPORTS, **9**, 16534 (2019)

AF Savin, AJ Ross, R Aboushelbaya, MW Mayr, B Spiers, RH Wang, PA Norreys
Energy absorption in the laser-QED regime
SCIENTIFIC REPORTS, **9**, 8956 (2019)

APL Robinson, K Tangtartharakul, K Weichman, AV Arefiev
Extreme nonlinear dynamics in vacuum laser acceleration with a crossed beam configuration
PHYSICS OF PLASMAS, **26**, 93110 (2019)

K Jana, AD Lad, M Shaikh, VR Kumar, D Sarkar, YM Ved, J Pasley, APL Robinson, GR Kumar
Generation of a strong reverse shock wave in the interaction of a high-contrast high-intensity femtosecond laser pulse with a silicon target
APPLIED PHYSICS LETTERS, **114**, 254103 (2019)

JD Sadler, Y Lu, B Spiers, MW Mayr, A Savin, RHW Wang, R Aboushelbaya, K Glize, R Bingham, H Li, KA Flippo, PA Norreys
Kinetic simulations of fusion ignition with hot-spot ablator mix
PHYSICAL REVIEW E, **100**, 33206 (2019)

K Weichman, APL Robinson, FN Beg, AV Arefiev
Laser reflection as a catalyst for direct laser acceleration in multipicosecond laser-plasma interaction
PHYSICS OF PLASMAS, **27**, 13106 (2020)

APL Robinson, AV Arefiev
Net energy gain in direct laser acceleration due to enhanced dephasing induced by an applied magnetic field
PHYSICS OF PLASMAS, **27**, 23110 (2020)

APL Robinson
Nonlinear screening in moderate-Z hot dense matter
PLASMA PHYSICS AND CONTROLLED FUSION, **61**, 65013 (2019)

R Aboushelbaya, K Glize, A Savin, M Mayr, B Spiers, R Wang, J Collier, M Marklund, R Trines, R Bingham, P Norreys
Orbital angular momentum coupling in elastic photon-photon scattering
PHYSICAL REVIEW LETTERS, **123**, 113604 (2019)

PW Hatfield, SJ Rose, RHH Scott
The blind implosion-maker: Automated inertial confinement fusion experiment design
PHYSICS OF PLASMAS, **26**, 62706 (2019)

RHH Scott, N Booth, SJ Hawkes, DR Symes, C Hooker, HW Doyle, SI Olsson-Robbie, HF Lowe, CJ Price, D Bigourd, S Patankar, K Mecseki, ET Gumbrell, RA Smith
Modeling radiative-shocks created by laser-cluster interactions
PHYSICS OF PLASMAS, **27**, 33301 (2020)

VULCAN

G Milluzzo, V Scuderi, A Alejo, AG Amico, N Booth, M Borghesi, GAP Cirrone, G Cuttone, D Doria, J Green, S Kar, G Korn, G Larosa, R Leanza, D Margarone, P Martin, P McKenna, G Petringa, J Pipek, L Romagnani, F Romano, A Russo, F Schillaci
A new energy spectrum reconstruction method for time-of-flight diagnostics of high-energy laser-driven protons
REVIEW OF SCIENTIFIC INSTRUMENTS, **90**, 83303 (2019)

CD Armstrong, CM Brenner, C Jones, DR Rusby, ZE Davidson, Y Zhang, J Wragg, S Richards, C Spindloe, P Oliveira, M Notley, R Clarke, SR Mirfayzi, S Kar, Y Li, T Scott, P McKenna, D Neely
Bremsstrahlung emission from high power laser interactions with constrained targets for industrial radiography
HIGH POWER LASER SCIENCE AND ENGINEERING, **7**, e24 (2019)

M Sedov, A Faenov, A Andreev, I Skobelev, S Ryazantsev, T Pikuz, P Durey, L Doehl, D Farley, C Baird, K Lancaster, C Murphy, N Booth, C Spindloe, K Platonov, P McKenna, R Kodama, N Woolsey, S Pikuz
Features of the generation of fast particles from microstructured targets irradiated by high intensity, picosecond laser pulses
LASER AND PARTICLE BEAMS, **37**, 176-183 (2019)

CAJ Palmer, PT Campbell, Y Ma, L Antonelli, AFA Bott, G Gregori, J Halliday, Y Katzir, P Kordell, K Krushelnick, SV Lebedev, E Montgomery, M Notley, DC Carroll, CP Ridgers, AA Schekochihin, MJV Streeter, AGR Thomas, ER Tubman, N Woolsey, L Willingale
Field reconstruction from proton radiography of intense laser driven magnetic reconnection
PHYSICS OF PLASMAS, **26**, 83109 (2019)

F Consoli, R De Angelis, TS Robinson, S Giltrap, GS Hicks, EJ Ditter, OC Ettlinger, Z Najmudin, M Notley, RA Smith
Generation of intense quasi-electrostatic fields due to deposition of particles accelerated by petawatt-range laser-matter interactions
SCIENTIFIC REPORTS, **9**, 8551 (2019)

G Liao, Y Li
Review of Intense Terahertz Radiation from Relativistic Laser-Produced Plasmas
IEEE TRANSACTIONS ON PLASMA SCIENCE, 47, 3002-3008 (2019)

TG White, MT Oliver, P Mabey, M Kühn-Kauffeldt, AFA Bott, LNK Döhl, AR Bell, R Bingham, R Clarke, J Foster, G Giacinti, P Graham, R Heathcote, M Koenig, Y Kuramitsu, DQ Lamb, J Meinecke, T Michel, F Miniati, M Notley, B Reville, D Ryu, S Sarkar, Y Sakawa, MP Selwood, J Squire, RHH Scott, P Tzeferacos, N Woolsey, AA Schekochihin, G Gregori
Supersonic plasma turbulence in the laboratory
NATURE COMMUNICATIONS, **10**, 1758 (2019)

S Passalidis, OC Ettlinger, GS Hicks, NP Dover, Z Najmudin, EP Benis, E Kaselouris, NA Papadogiannis, M Tatarakis, V Dimitriou
Hydrodynamic computational modelling and simulations of collisional shock waves in gas jet targets
HIGH POWER LASER SCIENCE AND ENGINEERING, **8**, e7 (2020)

ULTRA

S Hume, GM Greetham, PM Donaldson, M Towrie, AW Parker, MJ Baker, NT Hunt
2D-Infrared Spectroscopy of Proteins in Water: Using the Solvent Thermal Response as an Internal Standard
ANALYTICAL CHEMISTRY, **92**, 3463-3469 (2020)

E Benazzi, GH Summers, FA Black, IV Sazanovich, IP Clark, EA Gibson
Assembly, charge-transfer and solar cell performance with porphyrin-C_{60} on NiO for p-type dye-sensitized solar cells
PHILOSOPHICAL TRANSACTIONS OF THE ROYAL SOCIETY A: MATHEMATICAL PHYSICAL AND ENGINEERING SCIENCES, **377**, 20180338 (2019)

N-H Yin, AW Parker, P Matousek, HL Birch
Can Raman spectroscopy detect age-related changes in tendon matrix?
INTERNATIONAL JOURNAL OF EXPERIMENTAL PATHOLOGY, **100**, A43 (2019)

G Greetham, IP Clark, B Young, R Fritzsch, L Minnes, N Hunt, M Towrie
EXPRESS: Time-Resolved Temperature-Jump Infrared Spectroscopy at a High Repetition Rate
APPLIED SPECTROSCOPY, **74**, 720-727 (2020)

K Karadi, SM Kapetanaki, K Raics, I Pecsi, R Kapronczai, Z Fekete, JN Iuliano, JT Collado, AA Gil, J Orban, M Nyitrai, GM Greetham, MH Vos, PJ Tonge, SR Meech, A Lukacs
Functional dynamics of a single tryptophan residue in a BLUF protein revealed by fluorescence spectroscopy
SCIENTIFIC REPORTS, **10**, 2061 (2020)

AM Beale, M Agote-Arán, RE Fletcher, M Briceno, AB Kroner, IV Sazanovich, B Slater, ME Rivas, AW Smith, P Collier, I Lezcano-González
Implications of the Molybdenum Coordination Environment in MFI Zeolites on Methane Dehydroaromatisation Performance
CHEMCATCHEM, **12**, 294-304 (2019)

BJ Aucott, JB Eastwood, L Anders Hammarback, IP Clark, IV Sazanovich, M Towrie, IJS Fairlamb, JM Lynam
Insight into the mechanism of CO-release from trypto-CORM using ultra-fast spectroscopy and computational chemistry
DALTON TRANSACTIONS, **48**, 16426-16436 (2019)

L Cabo-Fernandez, AR Neale, F Braga, IV Sazanovich, R Kostecki, LJ Hardwick
Kerr gated Raman spectroscopy of LiPF6 salt and LiPF6-based organic carbonate electrolyte for Li-ion batteries
PHYSICAL CHEMISTRY CHEMICAL PHYSICS, **21**, 23833-23842 (2019)

BJ Aucott, A Duhme-Klair, BE Moulton, IP Clark, IV Sazanovich, M Towrie, LA Hammarback, IJS Fairlamb, JM Lynam
Manganese Carbonyl Compounds Reveal Ultrafast Metal-Solvent Interactions
ORGANOMETALLICS, **38**, 2391-2401 (2019)

S Hume, G Hithell, GM Greetham, P Donaldson, M Towrie, AW Parker, MJ Baker, N Hunt
Measuring proteins in H_2O with 2D-IR spectroscopy
CHEMICAL SCIENCE, **10**, 6448-6456 (2019)

WJ Kendrick, M Jirásek, MD Peeks, GM Greetham, IV Sazanovich, PM Donaldson, M Towrie, AW Parker, HL Anderson
Mechanisms of IR amplification in radical cation polarons
CHEMICAL SCIENCE, **11**, 2112-2120 (2020)

R Fritzsch, GM Greetham, IP Clark, L Minnes, M Towrie, AW Parker, NT Hunt
Monitoring Base Specific Dynamics during Melting of DNA-Ligand Complexes Using Temperature-Jump Time-Resolved Infrared Spectroscopy
JOURNAL OF PHYSICAL CHEMISTRY B, **123**, 6188-6199 (2019)

SA Bartlett, NA Besley, AJ Dent, S Diaz-Moreno, J Evans, ML Hamilton, MWD Hanson-Heine, R Horvath, V Manici, X Sun, M Towrie, L Wu, X Zhang, MW George
Monitoring the Formation and Reactivity of Organometallic Alkane and Fluoroalkane Complexes with Silanes and Xe Using Time-Resolved X-ray Absorption Fine Structure Spectroscopy
JOURNAL OF THE AMERICAN CHEMICAL SOCIETY, **141**, 11471-11480 (2019)

JC Manton, FJR Cerpentier, EC Harvey, IP Clark, GM Greetham, C Long, MT Pryce
Photochemical or electrochemical bond breaking - exploring the chemistry of (μ_2-alkyne)$Co_2(CO)_6$ complexes using time-resolved infrared spectroscopy, spectro-electrochemical and density functional methods
DALTON TRANSACTIONS, **48**, 14642-14652 (2019)

A Bhattacherjee, M Sneha, L Lewis-Borrell, O Tau, IP Clark, AJ Orr-Ewing
Picosecond to millisecond tracking of a photocatalytic decarboxylation reaction provides direct mechanistic insights
NATURE COMMUNICATIONS, **10**, 5152 (2019)

CR Hall, J Tolentino Collado, JN Iuliano, K Adamczyk, A Lukacs, GM Greetham, IV Sazanovich, PJ Tonge, SR Meech
Site Specific Protein Dynamics Probed by Ultrafast Infrared Spectroscopy of a Noncanonical Amino Acid
JOURNAL OF PHYSICAL CHEMISTRY B, **123**, 9592-9597 (2019)

X Wu, Z Liu, TS Murphy, XZ Sun, MWD Hanson-Heine, M Towrie, JN Harvey, MW George
The effect of coordination of alkanes, Xe and CO_2 (η^1-OCO) on changes in spin state and reactivity in organometallic chemistry: a combined experimental and theoretical study of the photochemistry of $CpMn(CO)_3$
FARADAY DISCUSSIONS, **220**, 86-104 (2019)

NJ Cheetham, M Ortiz, A Perevedentsev, L Dion-Bertrand, GM Greetham, IV Sazanovich, M Towrie, AW Parker, J Nelson, C Silva, DD Bradley, SC Hayes, PN Stavrinou
The importance of microstructure in determining polaron generation yield in poly(9,9-dioctylfluorene)
CHEMISTRY OF MATERIALS, **31**, 6787-6797 (2019)

JH van Wonderen, CR Hall, X Jiang, K Adamczyk, A Carof, I Heisler, SEH Piper, TA Clarke, NJ Watmough, IV Sazanovich, M Towrie, SR Meech, J Blumberger, JN Butt
Ultrafast Light-Driven Electron Transfer in a Ru(II) tris(bipyridine)-Labeled Multiheme Cytochrome
JOURNAL OF THE AMERICAN CHEMICAL SOCIETY, **141**, 15190-15200 (2019)

L Minnes, GM Greetham, DJ Shaw, IP Clark, R Fritzsch, M Towrie, AW Parker, AJ Henry, RJ Taylor, NT Hunt
Uncovering the Early Stages of Domain Melting in Calmodulin with Ultrafast Temperature-Jump Infrared Spectroscopy
JOURNAL OF PHYSICAL CHEMISTRY B, **123**, 8733-8739 (2019)

N Omori, AG Greenaway, M Sarwar, P Collier, G Valentini, AM Beale, A Candeo
Understanding the Dynamics of Fluorescence Emission during Zeolite Detemplation Using Time Resolved Photoluminescence Spectroscopy
JOURNAL OF PHYSICAL CHEMISTRY C, **124**, 531-543 (2019)

OCTOPUS

Raza, SA Archer, SD Fairbanks, KL Smitten, SW Botchway, JA Thomas, S MacNeil, JW Haycock
A Dinuclear Ruthenium(II) Complex Excited by Near-Infrared Light through Two-Photon Absorption Induces Phototoxicity Deep within Hypoxic Regions of Melanoma Cancer Spheroids
JOURNAL OF THE AMERICAN CHEMICAL SOCIETY, **142**, 4639-4647 (2020)

M Hirsch, R Wareham, JW Yoon, DJ Rolfe, LC Zanetti Domingues, MP Hobson, PJ Parker, ML Martin-Fernandez, SS Singh
A global sampler of single particle tracking solutions for single molecule microscopy
PLOS ONE, **14**, e0221865 (2019)

J Periz, M Del Rosario, A McStea, S Gras, C Loney, L Wang, ML Martin-Fernandez, M Meissner
A highly dynamic F-actin network regulates transport and recycling of micronemes in Toxoplasma gondii vacuoles
NATURE COMMUNICATIONS, **10**, 4183 (2019)

J Schoberer, J König, C Veit, U Vavra, E Liebminger, SW Botchway, F Altmann, V Kriechbaumer, C Hawes, R Strasser
A signal motif retains Arabidopsis ER-alpha-mannosidase I in the cis-Golgi and prevents enhanced glycoprotein ERAD
NATURE COMMUNICATIONS, **10**, 3701 (2019)

J Ho, X Yang, S Nikou, N Kichik, A Donkin, NO Ponde, JP Richardson, RL Gratacap, LS Archambault, CP Zwirner, C Murciano, R Henley-Smith, S Thavaraj, CJ Tynan, SL Gaffen, B Hube, RT Wheeler, DL Moyes, JR Naglik
Candidalysin activates innate epithelial immune responses via epidermal growth factor receptor
NATURE COMMUNICATIONS, **10**, 2297 (2019)

N Fili, Y Hari-Gupta, B Aston, Á dos Santos, RE Gough, B Alamad, L Wang, ML Martin-Fernandez, CP Toseland
Competition between two high- and low-affinity protein-binding sites in myosin VI controls its cellular function.
JOURNAL OF BIOLOGICAL CHEMISTRY, **295**, 337-347 (2019)

B Mao, F Cortezon-Tamarit, H Ge, N Kuganathan, V Mirabello, FJ Palomares, G Kociok-Köhn, SW Botchway, DG Calatayud, SI Pascu
Directed Molecular Stacking for Engineered Fluorescent Three-Dimensional Reduced Graphene Oxide and Coronene Frameworks
CHEMISTRYOPEN, **8**, 1383-1398 (2019)

HK Saeed, S Sreedharan, PJ Jarman, SA Archer, SD Fairbanks, SP Foxon, AJ Auty, D Chekulaev, T Keane, AJHM Meijer, JA Weinstein, CGW Smythe, J Bernardino de la Serna, JA Thomas
Making the Right Link to Theranostics: The Photophysical and Biological Properties of Dinuclear Ru^{II}–Re^{I} dppz Complexes Depend on Their Tether
JOURNAL OF THE AMERICAN CHEMICAL SOCIETY, **142**, 1101-1111 (2019)

OEC Gould, SJ Box, CE Boott, AD Ward, MA Winnik, MJ Miles, I Manners
Manipulation and Deposition of Complex, Functional Block Copolymer Nanostructures Using Optical Tweezers
ACS NANO, **13**, 3858-3866 (2019)

H Ge, F Cortezon-Tamarit, H Wang, AC Sedgwick, RL Arrowsmith, V Mirabello, SW Botchway, TD James, SI Pascu
Multiphoton fluorescence lifetime imaging microscopy (FLIM) and super-resolution fluorescence imaging with a supramolecular biopolymer for the controlled tagging of polysaccharides
NANOSCALE, **11**, 9498-9507 (2019)

SA Belhout, FR Baptista, SJ Devereux, AW Parker, AD Ward, SJ Quinn
Preparation of polymer gold nanoparticle composites with tunable plasmon coupling and their application as SERS substrates
NANOSCALE, **11**, 19884-19894 (2019)

KL Smitten, SD Fairbanks, CC Robertson, J Bernardino de la Serna, SJ Foster, JA Thomas
Ruthenium based antimicrobial theranostics - using nanoscopy to identify therapeutic targets and resistance mechanisms in Staphylococcus aureus
CHEMICAL SCIENCE, **11**, 70-79 (2020)

ML Martin-Fernandez, DT Clarke, SK Roberts, LC Zanetti Domingues, FL Gervasio
Structure and Dynamics of the EGF Receptor as Revealed by Experiments and Simulations and Its Relevance to Non-Small Cell Lung Cancer
CELLS, **8**, 316 (2019)

B Bateman, L Zanetti Domingues, A Moores, S Needham, D Rolfe, L Wang, D Clarke, M Martin-Fernandez
Super-resolution Microscopy at Cryogenic Temperatures Using Solid Immersion Lenses
BIO-PROTOCOL, **9**, e3426 (2019)

J Ihli, DC Green, C Lynch, MA Holden, PA Lee, S Zhang, IK Robinson, SED Webb, FC Meldrum
Super-Resolution Microscopy Reveals Shape and Distribution of Dislocations in Single-Crystal Nanocomposites
ANGEWANDTE CHEMIE INTERNATIONAL EDITION, **58**, 17328-17334 (2019)

SC Salvage, JS Rees, A McStea, M Hirsch, L Wang, CJ Tynan, MW Reed, JR Irons, R Butler, AJ Thompson, ML Martin-Fernandez, CL Huang, AP Jackson
Supramolecular clustering of the cardiac sodium channel Nav1.5 in HEK293F cells, with and without the auxiliary β3-subunit
THE FASEB JOURNAL, **34**, 3537-3553 (2020)

JF McKenna, DJ Rolfe, SED Webb, AF Tolmie, SW Botchway, ML Martin-Fernandez, C Hawes, J Runions
The cell wall regulates dynamics and size of plasma-membrane nanodomains in Arabidopsis
PROCEEDINGS OF THE NATIONAL ACADEMY OF SCIENCES USA, **116**, 12857-12862 (2019)

AD Graham, R Pandey, VS Tsancheva, A Candeo, SW Botchway, AJ Allan, L Teboul, K Madi, TS Babra, LAK Zolkiewski, X Xue, L Bentley, J Gannon, SN Olof, RD Cox
The development of a high throughput drug-responsive model of white adipose tissue comprising adipogenic 3T3-L1 cells in a 3D matrix
BIOFABRICATION, **12(1)**, 15018 (2019)

J Schoberer, E Liebminger, U Vavra, C Veit, C Grünwald-Gruber, F Altmann, SW Botchway, R Strasser
The Golgi Localization of GnTI Requires a Polar Amino Acid Residue within Its Transmembrane Domain
PLANT PHYSIOLOGY, **180**, 859-873 (2019)

A Elbediwy, Y Zhang, M Cobbaut, P Riou, RS Tan, SK Roberts, C Tynan, R George, S Kjaer, ML Martin-Fernandez, BJ Thompson, NQ McDonald, PJ Parker
The Rho family GEF FARP2 is activated by aPKCι to control tight junction formation and polarity
JOURNAL OF CELL SCIENCE, **132**, jcs223743 (2019)

KL Smitten, HM Southam, J Bernardino de la Serna, MR Gill, PJ Jarman, CGW Smythe, RK Poole, JA Thomas
Using Nanoscopy To Probe the Biological Activity of Antimicrobial Leads That Display Potent Activity against Pathogenic, Multidrug Resistant, Gram-Negative Bacteria
ACS NANO, **13**, 5133-5146 (2019)

INDIVIDUAL CONTRIBUTIONS AND COLLABORATIVE SCIENCE

YA El-Neaj, C Alpigiani, S Amairi-Pyka, H Araújo, A Balaž, A Bassi, L Bathe-Peters, B Battelier, A Belić, E Bentine, J Bernabeu, A Bertoldi, R Bingham, D Blas, V Bolpasi, K Bongs, S Bose, P Bouyer, T Bowcock, W Bowden, O Buchmueller, C Burrage, X Calmet, B Canuel, L Caramete, A Carroll, G Cella, V Charmandaris, S Chattopadhyay, X Chen, ML Chiofalo, J Coleman, J Cotter, Y Cui, A Derevianko, A De Roeck, GS Djordjevic, P Dornan, M Doser, I Drougkakis, J Dunningham, I Dutan, S Easo, G Elertas, J Ellis, M El Sawy, F Fassi, D Felea, C Feng, R Flack, C Foot, I Fuentes, N Gaaloul, A Gauguet, R Geiger, V Gibson, G Giudice, J Goldwin, O Grachov, PW Graham, D Grasso, M van der Grinten, M Gündogan, MG Haehnelt, T Harte, A Hees, R Hobson, J Hogan, B Holst, M Holynski, M Kasevich, BJ Kavanagh, W von Klitzing, T Kovachy, B Krikler, M Krutzik, M Lewicki, Y Lien, M Liu, GG Luciano, A Magnon, MA Mahmoud, S Malik, C McCabe, J Mitchell, J Pahl, D Pal, S Pandey, D Papazoglou, M Paternostro, B Penning, A Peters, M Prevedelli, V Puthiya-Veettil, J Quenby, E Rasel, S Ravenhall, J Ringwood, A Roura, D Sabulsky, M Sameed, B Sauer, SA Schäffer, S Schiller, V Schkolnik, D Schlippert, C Schubert, HR Sfar, A Shayeghi, I Shipsey, C Signorini, Y Singh, M Soares-Santos, F Sorrentino, T Sumner, K Tassis, S Tentindo, GM Tino, JN Tinsley, J Unwin, T Valenzuela-Salazar, G Vasilakis, V Vaskonen, C Vogt, A Webber-Date, A Wenzlawski, P Windpassinger, M Woltmann, E Yazgan, M Zhan, X Zou, J Zupan
AEDGE: Atomic Experiment for Dark Matter and Gravity Exploration in Space
EPJ QUANTUM TECHNOLOGY, **7**, 6 (2020)

H Beyer, G Rohde, A Grubišić Čabo, A Stange, T Jacobsen, L Bignardi, D Lizzit, P Lacovig, C Sanders, S Lizzit, K Rossnagel, P Hofmann, M Bauer
80% Valley Polarization of Free Carriers in Singly Oriented Single-Layer WS_2 on Au(111)
PHYSICAL REVIEW LETTERS, **123**, 236802 (2019)

SS Grønborg, K Thorarinsdottir, L Kyhl, J Rodriguez-Fernández, CE Sanders, M Bianchi, P Hofmann, JA Miwa, S Ulstrup, JV Lauritsen
Basal plane oxygen exchange of epitaxial MoS_2 without edge oxidation
2D MATERIALS, **6**, 45013 (2019)

R Stan, SK Mahatha, M Bianchi, CE Sanders, D Curcio, P Hofmann, JA Miwa
Epitaxial single-layer NbS_2 on Au(111): Synthesis, structure, and electronic properties
PHYSICAL REVIEW MATERIALS, **3**, 044003 (2019)

H Rostami, K Volckaert, N Lanata, SK Mahatha, CE Sanders, M Bianchi, D Lizzit, L Bignardi, S Lizzit, JA Miwa, AV Balatsky, P Hofmann, S Ulstrup
Layer and orbital interference effects in photoemission from transition metal dichalcogenides
PHYSICAL REVIEW B, **100**, 235423 (2019)

S Ulstrup, CE Giusca, JA Miwa, CE Sanders, A Browning, P Dudin, C Cacho, O Kazakova, DK Gaskill, RL Myers-Ward, T Zhang, M Terrones, P Hofmann
Nanoscale mapping of quasiparticle band alignment
NATURE COMMUNICATIONS, **10**, 3283 (2019)

D Kutnyakhov, RP Xian, M Dendzik, M Heber, F Pressacco, SY Agustsson, L Wenthaus, H Meyer, S Gieschen, G Mercurio, A Benz, K Bühlman, S Däster, R Gort, D Curcio, K Volckaert, M Bianchi, C Sanders, JA Miwa, S Ulstrup, A Oelsner, C Tusche, Y Chen, D Vasilyev, K Medjanik, G Brenner, S Dziarzhytski, H Redlin, B Manschwetus, S Dong, J Hauer, L Rettig, F Diekmann, K Rossnagel, J Demsar, H Elmers, P Hofmann, R Ernstorfer, G Schönhense, Y Acremann, W Wurth
Time- and momentum-resolved photoemission studies using time-of-flight momentum microscopy at a free-electron laser
REVIEW OF SCIENTIFIC INSTRUMENTS, **91**, 013109 (2020)

F Bisesto, M Galletti, MP Anania, M Ferrario, R Pompili, M Botton, E Schleifer, A Zigler
Review on TNSA diagnostics and recent developments at SPARC_LAB
HIGH POWER LASER SCIENCE AND ENGINEERING, 7, e56 (2019)

F Bisesto, M Galletti, MP Anania, M Ferrario, R Pompili, M Botton, A Zigler, F Consoli, M Salvadori, P Andreoli, C Verona
Single-shot electrons and protons time-resolved detection from high-intensity laser-solid matter interactions at SPARC_LAB
HIGH POWER LASER SCIENCE AND ENGINEERING, **7**, e53 (2019)

JH Churchwell, K Sowoidnich, O Chan, AE Goodship, AW Parker, P Matousek
Adaptive band target entropy minimization: Optimization for the decomposition of spatially offset Raman spectra of bone
JOURNAL OF RAMAN SPECTROSCOPY, **51**, 66-78 (2019)

K Sowoidnich, M Towrie, M Maiwald, B Sumpf, P Matousek
Shifted Excitation Raman Difference Spectroscopy with Charge-Shifting Charge-Coupled Device (CCD) Lock-In Detection
APPLIED SPECTROSCOPY, **73**, 1265-1276 (2019)

S Mosca, P Dey, TA Tabish, F Palombo, N Stone, P Matousek
Determination of inclusion depth in ex vivo animal tissues using surface enhanced deep Raman spectroscopy
JOURNAL OF BIOPHOTONICS, **13**, e201960092 (2019)

B Gardner, P Matousek, N Stone
Direct monitoring of light mediated hyperthermia induced within mammalian tissues using surface enhanced spatially offset Raman spectroscopy (T-SESORS)
ANALYST, **144**, 3552-3555 (2019)

S Mosca, P Lanka, N Stone, S Konugolu Venkata Sekar, P Matousek, G Valentini, A Pifferi
Optical characterization of porcine tissues from various organs in the 650-1100nm range using time-domain diffuse spectroscopy
BIOMEDICAL OPTICS EXPRESS, **11**, 1697-1706 (2020)

P Dey, TA Tabish, S Mosca, F Palombo, P Matousek, N Stone
Plasmonic Nanoassemblies: Tentacles Beat Satellites for Boosting Broadband NIR Plasmon Coupling Providing a Novel Candidate for SERS and Photothermal Therapy
SMALL, **16**, 1906780 (2020)

S Mosca, P Dey, TA Tabish, F Palombo, N Stone, P Matousek
Spatially Offset and Transmission Raman Spectroscopy for Determination of Depth of Inclusion in Turbid Matrix
ANALYTICAL CHEMISTRY, **91**, 8994-9000 (2019)

B Gardner, P Matousek, N Stone
Sub-surface Chemically Specific Measurement of pH Levels in Biological Tissues using Combined Surface Enhanced and Deep Raman Spectroscopy
ANALYTICAL CHEMISTRY, **91**, 10984-10987 (2019)

C Conti, A Botteon, C Colombo, D Pinna, M Realini, P Matousek
Advances in Raman spectroscopy for the non-destructive subsurface analysis of artworks: Micro-SORS
JOURNAL OF CULTURAL HERITAGE, **43**, 319-328 (2019)

C Conti, A Botteon, C Colombo, M Realini, P Matousek
Application of Micro-spatially Offset Raman Spectroscopy to Street Art Paintings
RAMAN SPECTROSCOPY IN ARCHAEOLOGY AND ART HISTORY: VOLUME 2, P. Vandenabeele and H. Edwards, Eds (The Royal Society of Chemistry, Cambridge) **Chapter 12**, p174-183 (2019)

B Gardner, N Stone, P Matousek
Noninvasive simultaneous monitoring of pH and depth using surface-enhanced deep Raman spectroscopy
JOURNAL OF RAMAN SPECTROSCOPY, **51**, 1078-1082 (2020)

N Yin, AW Parker, P Matousek, HL Birch
Detection of Age-Related Changes in Tendon Molecular Composition by Raman Spectroscopy-Potential for Rapid, Non-Invasive Assessment of Susceptibility to Injury
INTERNATIONAL JOURNAL OF MOLECULAR SCIENCES, **21**, 2150 (2020)

DR Rusby, CD Armstrong, GG Scott, M King, P McKenna, D Neely
Effect of rear surface fields on hot, refluxing and escaping electron populations via numerical simulations
HIGH POWER LASER SCIENCE AND ENGINEERING, **7**, e45 (2019)

Y Zhang, W Wang, Y Li, Z Zhang, P McKenna, D Neely, J Zhang
Effects of internal target structures on laser-driven neutron production
NUCLEAR FUSION, **59**, 76032 (2019)

D Mariscal, T Ma, SC Wilks, AJ Kemp, GJ Williams, P Michel, H Chen, PK Patel, BA Remington, M Bowers, L Pelz, MR Hermann, W Hsing, D Martinez, R Sigurdsson, M Prantil, A Conder, J Lawson, M Hamamoto, P Di Nicola, C Widmayer, D Homoelle, R Lowe-Webb, S Herriot, W Williams, D Alessi, D Kalantar, R Zacharias, C Haefner, N Thompson, T Zobrist, D Lord, N Hash, A Pak, N Lemos, M Tabak, C McGuffey, J Kim, FN Beg, MS Wei, P Norreys, A Morace, N Iwata, Y Sentoku, D Neely, GG Scott, K Flippo
First demonstration of ARC-accelerated proton beams at the National Ignition Facility
PHYSICS OF PLASMAS, **26**, 43110 (2019)

B Hidding, A Beaton, L Boulton, S Corde, A Doepp, FA Habib, T Heinemann, A Irman, S Karsch, G Kirwan, A Knetsch, GG Manahan, A Martinez de la Ossa, A Nutter, P Scherkl, U Schramm, D Ullmann
Fundamentals and Applications of Hybrid LWFA-PWFA
APPLIED SCIENCES, **9**, 2626 (2019)

J Tu, XB Chen, XZ Ruan, YF Zhao, HF Xu, ZD Chen, XQ Zhang, XW Zhang, J Wu, L He, Y Zhang, R Zhang, YB Xu
Direct observation of hidden spin polarization in 2H-$MoTe_2$
PHYSICAL REVIEW B, **101**, 35102 (2020)

Conference Proceedings

CALTA

J Preclíková, K Bartoš, J Polak, J Kubát, J Pilar, P Navrátil, M Hanuš, M Divoký, A Lucianetti, M Fibrich, M Košelja, JT Green, K Ertel, J Phillips, M De Vido, B Rus, T Mocek, J Houžvicka
Monocrystalline materials for high-power ultrafast lasers
PROCEEDINGS OF SPIE, **11033**, 1103306 (2019)

INDIVIDUAL CONTRIBUTIONS AND COLLABORATIVE SCIENCE

A Ward, M McGrory, M King
Spectroscopic studies of optically trapped aerosol at elevated temperatures
PROCEEDINGS OF SPIE, **11083**, 1108323 (2019)

K Sowoidnich, M Maiwald, B Sumpf, M Towrie, P Matousek
Charge-shifting optical lock-in detection with shifted excitation Raman difference spectroscopy for the analysis of fluorescent heterogeneous samples
PROCEEDINGS OF SPIE, **11236**, 112360K (2020)

GEMINI

R Spesyvtsev, E Brunetti, G Vieux, M Shahzad, A Maitrallain, SR Yoffe, B Ersfeld, A Kornaszewski, M Streeter, O Finlay, Y Ma, B Kettle, SJD Dann, F Albert, N Bourgeois, S Cipiccia, JM Cole, E Gerstmayr, IG Gonzales, A Higginbotham, AE Hussein, K Falk, K Krushelnick, N Lemos, NC Lopes, C Lumsdon, O Lundh, SPD Mangles, Z Najmudin, PP Rajeev, M Smid, DR Symes, AGR Thomas, DA Jaroszynski, DA Jaroszynski, M Hur
Generation of electron high energy beams with a ring-like structure by a dual stage laser wakefield accelerator
PROCEEDINGS OF SPIE, **11036**, 110360F (2019)

Theses

GEMINI

Samarin, G.M.
Experimental studies of radiation reaction and photon-photon collisions in ultrahigh intensity regimes
PhD Thesis, Queen's University Belfast (2019)

Warwick, J.
Experimental Studies of the dynamics of neutral electron-positron beams
PhD Thesis, Queen's University Belfast (2019)

Duff, M.
Radiation generation and high-field physics phenomena in ultra-intense laser-solid interactions
PhD Thesis, University of Strathclyde (2019)

Rozario, S.
Novel injection and targetry in laser wakefield acceleration
PhD Thesis, Imperial College London (2019)

VULCAN

Savin, A.
Modelling Laser-Plasma Interactions for the Next Generation of High Power Laser Experiments
PhD Thesis, University of Oxford (2019)

Doehl, L.
High-contrast, ultra-intense laser-solid interaction physics with engineered targets
PhD Thesis, University of York (2019)

Armstrong, C.
Bremsstrahlung radiation and fast electron transport in laser-plasma interactions
PhD Thesis, University of Strathclyde (2019)

Ditter, E.J.
Optical diagnostics of ultra-thin target laser-plasma interactions
PhD Thesis, Imperial College London (2019)

Eardley, S.
Optimising secondary particle and radiation sources in high-intensity laser interaction experiments
PhD Thesis, Imperial College London (2019)

ULTRA

Hammarback, L.A.
A Mechanistic Investigation into Mn(I)-Catalysed C-H Bond Functionalisation: from Pre-Catalyst Activation to Substrate Coordination and Transformation
PhD Thesis, University of York (2019)

O'Reilly, L.
Synthesis, Characterisation, Time-Resolved and Photocatalytic Studies of Inorganic Assemblies for Hydrogen Generation
PhD Thesis, Dublin College University (2019)

Deverux, S.
Biological application of surface functionalised carbon nanomaterials
PhD Thesis, University College Dublin (2019)

Minnes, L.
Creating an automated analysis toolbox for ultrafast 2D-IR spectroscopy
PhD Thesis, University of Strathclyde (2020)

Reynolds, K.
Probing the photochemistry and photophysics of organic and inorganic chromophores
PhD Thesis, University of Nottingham (2020)

Kendrick, W.
Synthesis and Ultrafast Spectroscopy of Porphyrin Molecular Wires
PhD Thesis, University of Oxford (2020)

Jirasek, M.
Exploring Electronic Delocalization in Porphyrin Oligomers
PhD Thesis, University of Oxford (2020)

Taylor, J.
Advancing Spectroelectrochemistry in Coordination Chemistry, Laser Spectroscopy and Green Electrochemistry
PhD Thesis, University of Reading (2020)

OCTOPUS

Perico, C.
Molecular factors controlling plant organelle movement and positioning
PhD Thesis, University of Bristol (2020)

Panel membership and CLF structure

Laser for Science Facility Access Panel 2019/20

REVIEWERS

Professor P. Kukura (Chair)
Department of Chemistry
University of Oxford

Dr S. Ameer-Beg
School of Cancer and Pharmaceutical Sciences
King's College London

Professor A. Beale
Department of Chemistry
University College London

Dr J. Bernadino de la Serna
Faculty of Medicine
Imperial College London

Professor J. Bredenbeck
Johann Wolfgang Goethe-Universität

Dr A. Cowan
Department of Chemistry
University of Liverpool

Dr S. Cox
Faculty of Life Sciences and Medicine
King's College London

Dr I. Dobbie
Department of Biochemistry
University of Oxford

Dr M. Frogley
Diamond Light Source

Dr E. Gibson
School of Natural and Environmental Sciences
University of Newcastle

Dr M. Kuimova
Department of Chemistry
Imperial College London

Dr S. Leveque-Fort
Institut des Sciences Moléculaires d'Orsay

Professor G. McConnell
Centre for Biophotonics
University of Strathclyde

Professor J. Moger
University of Exeter

Professor S. Pascu
Department of Chemistry
University of Bath

Professor J. Weinstein
Department of Chemistry
University of Sheffield

RESEARCH COUNCIL REPRESENTATIVES

A. McGavigan
MRC

A. Chapman
EPSRC

J. Swarbrick
BBSRC

M. Simons
STFC

L. Garratt
NERC

SCIENCE & TECHNOLOGY FACILITIES COUNCIL REPRESENTATIVES

Dr D. T. Clarke (Head of Laser for Science Facility)
Central Laser Facility
Science & Technology Facilities Council

Prof J.L Collier (Director)
Central Laser Facility
Science & Technology Facilities Council

Professor M. Towrie (ULTRA Group Leader)
Central Laser Facility
Science & Technology Facilities Council

Dr M. Martin-Fernandez (OCTOPUS Group Leader)
Central Laser Facility
Science & Technology Facilities Council

Dr A. Kaye
ISIS & CLF User Office
Science & Technology Facilities Council

Professor D. Payne (Director)
Research Complex at Harwell

Professor L. Chapon (Physical Sciences Director)
Diamond Light Source

Dr E. Gozzard
Central Laser Facility
Science & Technology Facilities Council

Artemis Facility Access Panel 2019/20

REVIEWERS

Professor M. Vrakking (Panel Chairman)
Max Born Institute, Berlin

Professor M. Aeschlimann
University of Kaiserslautern, Germany

Dr J. Stahler
Fritz Haber Institute, Germany

Professor H. Fielding
Department of Chemistry, Christopher Ingold Laboratories
University College London

Professor J. Tisch
Department of Physics, Blackett Laboratory
Imperial College London

Professor L. Perfetti
Laboratoire des Solides Irradies, Ecole Polytechnique
Palaiseau Cedex

Professor A. Taleb-Ibrahimi
Synchrotron SOLEIL, L'Orme des Merisiers, France

Dr P. King
School of Physics and Astronomy
University of St. Andrews

SCIENCE & TECHNOLOGY FACILITIES COUNCIL REPRESENTATIVES

Professor J.L. Collier (Director)
Central Laser Facility
Science & Technology Facilities Council

Ms C. Hernandez-Gomez (Head, High Power Laser Programme)
Central Laser Facility
Science & Technology Facilities Council

Dr E. Springate (Artemis Group Leader)
Central Laser Facility
Science & Technology Facilities Council

Dr R.T. Chapman (Artemis, AMO and Imaging)
Central Laser Facility
Science & Technology Facilities Council

Dr D.T Clarke (Head of Laser for Science Facility)
Central Laser Facility
Science & Technology Facilities Council

Professor M. Towrie (Molecular and Structural Dynamics)
Central Laser Facility
Science & Technology Facilities Council

Vulcan, Astra TA2 & Gemini Facility Access Panel 2019/20

REVIEWERS

Professor N. Woolsey (Panel Chair)
York Plasma Institute
University of York

Professor B. Dromey
Department of Pure and Applied Physics
Queen's University of Belfast

Professor G. Gregori
Clarendon Laboratory
University of Oxford

Dr S. Mangles
Blackett Laboratory
Imperial College London

Dr J. Pasley
York Plasma Institute
University of York

Professor B. Hidding
Department of Physics
University of Strathclyde

Professor T. Arber
Department of Physics
University of Warwick

Dr R. Kingham
Blackett Laboratory
Imperial College London

Dr A. Klisnick
Institut des Sciences Moléculaires d'Orsay
Université Paris-Saclay

Dr B. Cros
Laboratory of Gas Physics and Plasmas
Université Paris-Sud

RESEARCH COUNCIL REPRESENTATIVES

Mr C. Danson
AWE

SCIENCE & TECHNOLOGY FACILITIES COUNCIL REPRESENTATIVES

Professor J.L. Collier (Director)
Central Laser Facility
Science & Technology Facilities Council

Ms C. Hernandez-Gomez (Head, High Power Laser Programme)
Central Laser Facility
Science & Technology Facilities Council

Dr I.O. Musgrave (Vulcan Group Leader)
Central Laser Facility
Science & Technology Facilities Council

Mr R.J. Clarke (Experimental Science Group Leader)
Central Laser Facility
Science & Technology Facilities Council

Dr R. Pattathil (Gemini Group Leader)
Central Laser Facility
Science & Technology Facilities Council

Dr D. Symes (Gemini Target Area Section Leader)
Central Laser Facility
Science & Technology Facilities Council

Dr D. Carroll (Panel Secretary)
Central Laser Facility
Science & Technology Facilities Council

Mr C. Spindloe
Scitech Precision

Dr A. Kaye
ISIS Neutron & Muon Source
Science & Technology Facilities Council

Central Laser Facility Structure

Director

Professor John Collier
john.collier@stfc.ac.uk

Research Complex Division

Dr Dave Clarke
dave.clarke@stfc.ac.uk

CALTA Division

Dr Chris Edwards
chris.edwards@stfc.ac.uk

High Power Lasers Division

Ms Cristina Hernandez-Gomez
cristina.hernandez-gomez@stfc.ac.uk

Engineering & Technology Division

Mr Brian Wyborn
brian.wyborn@stfc.ac.uk

Ultra

Prof Mike Towrie
mike.towrie@stfc.ac.uk

Octopus

Dr Marisa Martin-Fernandez
marisa.martin-fernandez@stfc.ac.uk

Gemini

Dr Rajeev Pattathil
rajeev.pattathil@stfc.ac.uk

Artemis

Dr Emma Springate
emma.springate@stfc.ac.uk

Experimental Science

Mr Rob Clarke
rob.clarke@stfc.ac.uk

Target Fabrication

Mr Martin Tolley
martin.tolley@stfc.ac.uk

Vulcan

Dr Ian Musgrave
ian.musgrave@stfc.ac.uk

Plasma Physics

Dr Alex Robinson
alex.robinson@stfc.ac.uk

Mechanical

Mr Steve Blake
steve.blake@stfc.ac.uk

Electrical

Vacancy
vacancy@stfc.ac.uk

UKRI Science and Technology Facilities Council